In this work, the author's present an in-depth look at the gas-particle partitioning of a handful of important, highly oxygenated compounds. Uncertainty in the partitioning of these compounds, and the potential of salting-in to describe observed discrepancies is an important unanswered question that is of interest to readers of this journal. Overall, this work is technically sound and should be published. Some minor concerns and comments are described below:

Response:
    Thanks for the reviewer's comments, and we'll reply these point by point.

General comments:

1. The approach to modeling partitioning nicely accounts for partitioning between phases, but a lot of the information to understand their approach is split between the SI and the main text. Some of the SI I think should maybe be brought into the main text (probably at least Eq. S1 and/or S2, and Figure S2)

Response:

    Thanks. We have moved those equations and Figure S2 (now Figure 1) into the main text. To clarify the approach used for the exploration of gas-particle partitioning of polyol tracers, three partitioning cases were defined in the revised manuscript.

Pages 10-13, lines 238-295
"**Calculations of partitioning coefficients**. Here, we defined three partitioning cases to explore the influence of dissolution in aerosol liquid water on gas-particle partitioning of polyol tracers in the atmosphere. *Case 1* presumes instantaneous equilibrium between the gas phase and particulate OM based on the equilibrium absorptive partitioning theory. In this case, particulate OM is assumed to be the only absorbing phase and behave as an ideal solution. Then the absorptive gas-particle partitioning coefficients ($K_{p,OM}$, $m^3\,\mu g^{-1}$) were calculated from measurements ($K^m_{p,OM}$) and predicted theoretically ($K^t_{p,OM}$) as follows

$$K^m_{p,OM} = \frac{F/M_{OM}}{A} \qquad (2)$$

$$K^t_{p,OM} = \frac{RT}{10^6 \overline{MW}_{OM} \zeta_{OM} p^o_L} \qquad (3)$$

where M_{OM} denotes the mass concentration of absorptive organic matter (OM = OC × 1.6; Turpin and Lim, 2001); F ($ng\,m^{-3}$) and A ($ng\,m^{-3}$) are particulate and gaseous concentrations of individual polyols, respectively. In eq 3, R ($m^3\,atm\,K^{-1}\,mol^{-1}$) and T (K) are the ideal gas constant and ambient temperature; $\overline{MW}_{OM}$, average molecular weight of absorptive OM, is set at 200 g mol^{-1} for all samples (Barsanti and Pankow, 2004; Williams et al., 2010); ζ_{OM} denotes the mole fraction scale activity coefficient, and is presumed to be unity for all species in each sample; p^o_L (atm) is the vapor pressure of each pure compound, and is predicted with several estimation tools and adjusted for each sampling interval based on the average temperature (Text S3 and Table S4).
    Due to the influence of mixing state and water content in aerosols, several studies modeled the gas-particle partitioning of oxygenated organic compounds by defining a liquid-liquid phase separation (LLPS) in the aerosol (Zuend and Seinfeld, 2012; Pye

et al., 2018). The organic-inorganic interactions and changes of activity coefficients in aqueous mixtures were fully considered as well. In this study, we proposed a simplified LLPS partitioning mechanism (*Case 2*) in Figure 1. First, aerosol water and water-insoluble OM (WIOM = OM – WSOC × 1.6) exist in two separate liquid phases, and WSOC and inorganic ions are totally dissolved in the aqueous phase. The distribution of polyol tracers between aqueous (F_W, ng m^{-3}) and WIOM (F_{WIOM}, ng m^{-3}) phases is simply depicted by their octanol-water partition coefficients (K_{OW})

$$K_{OW} = \frac{F_{WIOM}/V_{WSIOM}}{F_w/V_w} = \frac{c_{WIOM}}{c_w} \qquad (4)$$

where V_{WIOM} and V_w are volumes (m^3) of WIOM and water in aerosols per cubic meter air; c_{WIOM} and c_w are solution concentrations (ng m^{-3}) of polyols concentrations in organic and aqueous phases; log K_{OW} values of target polyols were estimated using the Estimation Programs Interface (EPI) Suite developed by the US Environmental Protection Agency and Syracuse Research Corporation (Table S4; US EPA, 2012). The density of organic matter and water (ρ_w) in aerosols are set at 1.4 and 1.0 g cm^{-3}, respectively (Isaacman-VanWertz et al., 2016; Taylor et al., 2017). Second, gas-phase polyol tracers are in equilibrium with hydrophobic OM and the aqueous phase, respectively

$$K_{p,WIOM}^m = \frac{F_{WIOM}/M_{WIOM}}{A} \qquad (5)$$

$$K_{H,e}^m = \frac{\frac{F_w}{M_i}}{\frac{A}{M_i}\times R\times T\times \frac{c_{ALW}}{\rho_w}} = \frac{\rho_w \times F_w}{A\times R\times T\times c_{ALW}} \qquad (6)$$

where $K_{H,e}^m$ (mol m^{-3} atm^{-1}) is the measurement-based effective Henry's law coefficient; M_{WIOM} represents the mass concentration (μg m^{-3}) of WIOM; M_i (g mol^{-1}) is the molecular weight of specific compound; c_{ALW} (μg m^{-3}) is the mass concentration of aerosol liquid water predicted using ISORROPIA II model. *Case 3* is generally the same as *Case 2*, and the only difference is that water-soluble OM (WSOM) and WIOM exist in a single organic phase. Here total particulate OM was used instead of WIOM to assess the distribution of polyol tracers between aqueous and organic phases, and calculate partitioning coefficients of gas vs. particulate organic ($K_{p,OM}^m$) and aqueous ($K_{H,e}^m$) phases. Note that the polarity of particulate OM phase in *Case 3* was expected to increase, then using K_{OW} to calculate the distribution of polyols between organic and aqueous phases might lead to underestimated $K_{p,OM}^m$ and overestimated $K_{H,e}^m$. For comparison purposes, the Henry's law coefficient in pure water at 25 ^{o}C ($K_{H,w}^*$) was estimated using EPI and SPARC (Hilal et al., 2008; http://archemcalc.com/sparc-web/calc), respectively (Table S4), and was adjusted for each sampling interval due to the changes in ambient temperature using van 't Hoff equation (Text S4). "

2. A critical question in this work, I think, what is the uncertainty on F%? Uncertainty on these measurements is not really discussed. This parameter is calculated as the ratio of two measurements, each of which likely have at least 10-15% uncertainty (typical of GC), so there is some uncertainty on F% for any given point (though that may decrease as you get to the extreme cases of being mostly in the particle phase as in this case). That doesn't account for the uncertainty on the breakthrough which is significant (e.g., methyltetrols breakthrough is ~20+/-10%, so the correction factor for breakthrough is between a factor of roughly 1.1 and 1.3). Random error on each point should be reduced in the average (i.e., the average F% is known better than any one point), but the averages could be susceptible to systemic errors like uncertainty in

breakthrough that could create bias. I do notice that during the periods of high particle concentrations for e.g., 2-MTs, F% does sometimes reach 100%, so perhaps bias is minimal, but it would be nice to get some estimates of uncertainties, or additional discussion and analysis of potential error. For instance, couldn't the divergence in Figure 2 of the isoprene tracers from the line be due to some bias like uncertainty in breakthrough?

Response:

Thanks. The measurement uncertainties will not only impact the calculation results of particle phase fractions ($F\%$) of polyol tracers, but also the partitioning coefficients of gas vs. particulate organic ($K^{m}_{p,OM}$) and aqueous ($K^{m}_{H,e}$) phases.
The uncertainty estimation for measurements and partitioning coefficients were added in the revised manuscript and supplementary information, respectively.

Page 13, lines 296 – 303 of the main text:
"***Uncertainty estimation.*** To obtain the uncertainty associated with the calculation of $F\%$ and partitioning coefficients ($K^{m}_{p,OM}$ and $K^{m}_{H,e}$), measurement uncertainties of polyol tracers in filter and PUF samples were estimated from their recoveries and breakthrough for gaseous sampling. The root sum of squares (RSS) method was applied to propagate uncertainties of gas and particle-phase concentrations for $F\%$, $K^{m}_{p,OM}$, and $K^{m}_{H,e}$ calculations. Details of the uncertainty estimation and propagation methods were provided in Text S5, and the average relative uncertainties were summarized in Table S5."

Text S5 in supplementary information:
"***Text S5. Uncertainty estimation methods***
In this work, the measurement results of some polyol tracers in filter and PUF samples are subject to substantial uncertainties due to their low and variable recoveries (Table S2) and excessive breakthrough (Figure S2). A general equation was derived to estimate measurement uncertainties of individual polyols in filter and PUF samples

$$\Delta C = \sqrt{(\text{error fraction} \times \text{concentration})^2 + (0.5 \times \text{detection limit})^2} \qquad (5)$$

where ΔC is the uncertainty of target species in filter (ΔQ_f and ΔQ_b, ng m^{-3}) or PUF (ΔPUF, ng m^{-3}) samples. The error fraction (%) of filter sample analysis was defined as half of the difference between maximum and minimum recoveries scaled by the average (Table S2), which was divided by (1 - average breakthrough) for PUF analysis (Figure S2). The average breakthrough of meso-erythritol (23.8%), mannose (38.1%), xylitol (36.4%), and arabitol (36.4%) were set as those of C5-alkene triols, glucose, and mannitol, respectively. According to the gas-particle separation method in this work, ΔQ_f was used to represent the uncertainty of particle-phase concentration (ΔF, ng m^{-3}), and the uncertainty of gas-phase concentration (ΔA, ng m^{-3}) was propagated by

$$\Delta A = \sqrt{\Delta Q_b{}^2 + \Delta\text{PUF}^2} \qquad (6)$$

Then the uncertainty of total concentration (ΔS, ng m^{-3}) was calculated as

$$\Delta S = \sqrt{\Delta F^2 + \Delta A^2} \qquad (7)$$

The uncertainties of particle-phase fractions ($\Delta F\%$) and partitioning coefficients ($K^{m}_{p,OM}$ and $K^{m}_{p,WIOM}$, m^3 ug^{-1}; $K^{m}_{H,e}$, mol m^{-3} atm^{-1}) were estimated by propagating

ΔF, ΔS, and ΔA using a simplified root sum of squares (RSS) method (Dutton et al., 2009)

$$\Delta F\% = \sqrt{(\frac{\partial F\%}{\partial F}\Delta F)^2 + (\frac{\partial F\%}{\partial S}\Delta S)^2} \times 100\% \qquad (8)$$

$$\Delta K = \sqrt{(\frac{\partial K}{\partial F'}\Delta F')^2 + (\frac{\partial K}{\partial A}\Delta A)^2} \qquad (9)$$

where ΔK is the uncertainty of $K^m_{p,OM}$, $K^m_{p,WIOM}$, or $K^m_{H,e}$; F' could be F, concentrations of polyols in WIOM (F_{WIOM}) or aqueous (F_w) phases, depending on the partitioning scheme (*Cases 1–3*) and partitioning coefficient for calculation. ΔF was split into ΔF_w and ΔF_{WIOM} (or ΔF_{OM}) based on their ratios in eq. 4 of the main text. In Table S5, the estimated uncertainties are summarized and expressed in average ratios. As $K^m_{p,OM}$ and $K^m_{H,e}$ are all directly related to the ratio of particle- (F, ng m^{-3}) and gas-phase (A, ng m^{-3}) concentrations (eqs. 2, 4, 5, and 6 in the main text), their average $\Delta K/K$ values are the same (Table S5)."

Moreover, Figure 2 (now Figure 3 in the revised manuscript, shown below) has been changed by including the uncertainty of $F\%$ and one standard deviation of log $p^{o,*}_L$ derived from different estimation tools (Table S4). Because monosaccharides (e.g., fructose) and sugar alcohols (e.g., mannitol) had low and variable recoveries (Table S2) and excessive breakthrough for gaseous sampling (Figure S2), their average $F\%$ uncertainties (6.16–31.2%) are much larger than those of isoprene SOA tracers and levoglucosan (3.33–7.24%). As shown in the figure below, more than 95% of polyols with extremely low vapor pressures (< ~10^{-10} atm) are distributed into the particle phase, so their prominent uncertainties in $F\%$ are not physically meaningful. Considering the uncertainties in $F\%$ and log $p^{o,*}_L$ and high average $F\%$ (> 85%) of polyol tracers, a dependence of $F\%$ on the vapor pressure could not be determined.
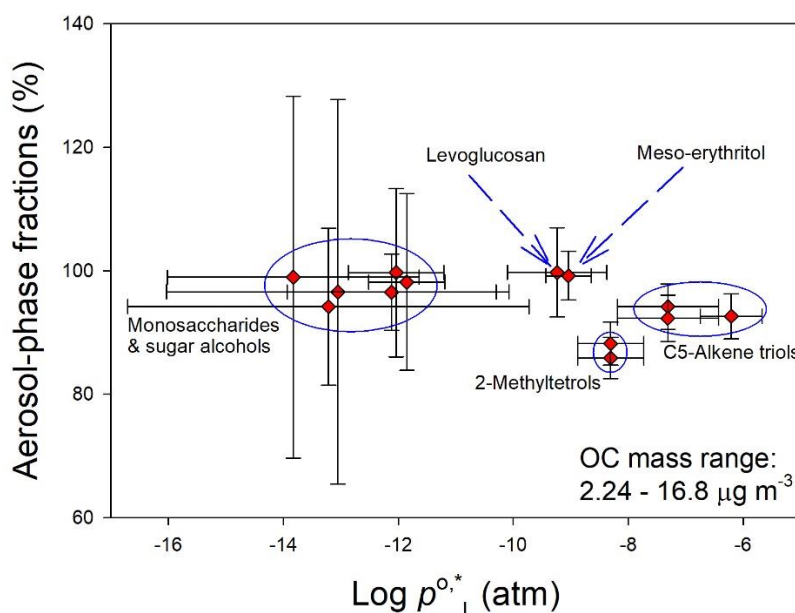

Figure 3. Average particle-phase fractions and log $p^{o,*}_L$ of individual polyol tracers. Whiskers represent uncertainties of $F\%$ and one standard deviation of log $p^{o,*}_L$ derived from different estimation tools.

In the revised manuscript, we added the above discussions on uncertainties of $F\%$ (Pages 17-18, lines 410–419).

"In Figure 3, The average $F\%$ uncertainties (6.16–31.2%) of monosaccharides (e.g., fructose) and sugar alcohols (e.g., mannitol) were larger than those of isoprene SOA tracers and levoglucosan (3.33–7.24%) due to their low and variable recoveries (Table S2) and excessive breakthrough (Figure S2). However, the estimated uncertainties of $F\%$ for less volatile polyols ($p^{o,*}_L < \sim 10^{-10}$ atm) were not physically meaningful, as more than 95% of these compounds existed in the particle phase. Considering the uncertainties in $F\%$ and log $p^{o,*}_L$ and high average $F\%$ (> 85%) of target polyol tracers, a dependence of $F\%$ on the vapor pressure could not be determined, and the seasonality and day-night difference ($p > 0.05$) of $F\%$ were obscured."

3. Some of these results might be impacted by uncertainty in theoretical partitioning coefficients and by poorly constrained empirically determined coefficients.
All of the tracers shown here have values close to 100%, so there is not much dynamic range in the data and it might be susceptible to biases.
Calculation of partitioning coefficients in particular could be sensitive to uncertainties because of this (as you approach 100% in one phase, small changes in partitioning might imply large changes in K). For this reason, I'm not sure the discussion of comparison between theoretical and measured K is always that meaningful. As an extreme example, levoglucosan looks like it is always at ~100% except for maybe one point. Under these conditions, how can any meaningful K be measured, since a partitioning coefficient of 10^3 and 10^100 would both produce the same effect?
On the other hand, there is substantial error in the theoretical values as well, with uncertainty in vapor pressure likely on the order of 1-2 orders of magnitude for most of these compounds (and some evidence that EPI has a tendency to overestimate compared, see Barley and McFiggans 2010).
While I agree that the time-dependent comparisons between measured and expected K against things like sulfate (e.g., Figure 3) provide insight, comments like that on line 345 comparing measured to theoretical K quantitatively aren't that meaningful.
Similarly, if you account for these sources of uncertainty, it's not clear to me that the lines in Figure 3 necessarily have a negative intercept as described. Some discussion of these uncertainties and biases might help clarify what we do know (e.g., these tracers are mostly particle phase, theoretical vapor pressures are wrong, and correlations with absorptive theory are poor), with the quantitative aspects we don't know as well (e.g., how wrong are the vapor pressures, how strong is the dependence on salt).

Response:

In our replies to the previous two comments, we have clarified the three partitioning cases defined in this work and uncertainty estimation methods for measurements and measurement-based partitioning coefficients. To address the uncertainty of vapor pressure estimated using EPI, a variety of estimation tools were deployed to provide a reasonable vapor pressure range for each polyol tracer. Referring to Table S4 of the revised supplementary information, we can find that the vapor pressure ranges of isoprene SOA tracers, levoglucosan, and meso-erythritol are within two orders of magnitude, while those for monosaccharides and mannitol are larger (> 10^3).

The target for comparing measured and predicted partitioning coefficients is to demonstrate that particulate OM is not the only absorbing phase, and the aerosol liquid water also plays a significant role in influencing the gas-particle partitioning of polyol tracers. In Table S5 of the revised supplementary information, the average relative uncertainties of measurement-based partitioning coefficients range from a few percent to ~50%, which will result in an uncertainty of less than ± 0.3 for logarithms of partitioning coefficients. In revised Table 1, the measurement-based $K_{p,OM}$ ($K^m_{p,OM}$) of isoprene SOA tracers, levoglucosan, and meso-erythritol for *Case 1* were more than 10 times greater than most theoretical predictions ($K^t_{p,OM}$). When the dissolution in aerosol liquid water was considered, their average log $K^m_{p,OM}$ became much closer to or even lay within the range (e.g., levoglucosan) of log $K^t_{p,OM}$, whenever water-soluble and water-insoluble organic matter (OM) partitioned into separate (*Cases 2*) or single (*Case 3*) liquid phases. These results support that the partitioning between gas and aerosol liquid water should not be ignored for water-soluble organic compounds like polyol tracers.

In other words, if particulate OM is the only absorbing phase in aerosols, log $K^m_{p,OM}$ values of *Case 1* will be closer to log $K^t_{p,OM}$ ranges, and the expected $F\%$ of isoprene SOA tracers, levoglucosan, and meso-erythritol should be much lower than measured in this work. To make the comparison between measured and predicted $K_{p,OM}$ meaningful, we predefined three partitioning cases and estimate vapor pressures of polyol tracers using several tools, and compared average log $K^m_{p,OM}$ of different partitioning cases with log $K^t_{p,OM}$ ranges. Moreover, the $K^m_{p,OM}$ uncertainty derived from measurements was estimated and would not impact the main conclusion.

The negative intercepts shown in Figures 4 and S5 of the revised manuscript and supplements are not likely ascribed to the small relative uncertainties of partitioning coefficients (Table S5). Shen et al. (2018) also identified negative intercepts of linear regressions between log ($K_{H,w}/K_{H,e}$) and $c_{sulfate}$ for glyoxal and methylglyoxal in the ambient atmosphere, and attributed this to unknown gas-particle partitioning mechanisms. By performing chamber experiments and comparing to existing laboratory studies, Kampf et al. (2013) found that the exponential increase of gas vs. aqueous phase partitioning coefficient ($K_{H,e}$, mol m^{-3} atm^{-1}) with sulfate concentration only occurred at $c_{sulfate} < 12$ mol kg^{-1} ALWC. In Figures 4 and S5, the log ($K_{H,w}/K_{H,e}$) values of most polyols increase faster as $c_{sulfate}$ approaches 0, supporting that the enhanced uptake at low sulfate concentrations could be partly parameterized by the equation defining "salting-in" effects. However, the "salting-in" effect is a known phenomenon that is not likely linked with a specific physical or chemical mechanism. In previous studies, the increased partitioning of polar organic compounds to the particle phase was often attributed to organic-inorganic interactions, including reactive uptake, aqueous phase chemistry, etc.

In addition to the changes mentioned in previous two responses, we reorganized and rewrote the discussions on partitioning coefficients of gas versus organic and aqueous phases (*Sections 3.4 and 3.5*), considering the uncertainties in both measurements and predictions.

Pages 18-24, lines 420-560

"*3.4 Partitioning coefficients of gas versus organic phases*
To understand if particulate OM is the only absorbing phase in aerosols for polyol tracers in Nanjing, the absorptive partitioning coefficients of gas vs. organic phases were calculated based on measurement results ($K^m_{p,OM}$) for predefined *Cases*

1-3 and predicted theoretically ($K^t_{p,OM}$) using eq. 3 and vapor pressures listed in Table S4. In Table 1, $K^t_{p,OM}$ ranges of isoprene SOA tracers, levoglucosan, and meso-erythritol are within two orders of magnitude, while those of monosaccharides and mannitol are larger (> 10^3).When particulate OM was assumed as the only absorbing phase (*Case 1*), the average $K^m_{p,OM}$ of isoprene SOA tracers, levolgucosan, and meso-erythritol were more than 10 times greater than most of their $K^t_{p,OM}$ (Table 1), and this difference was not likely susceptible to measurement uncertainties. As shown in Table S5, the average relative uncertainties of measurement-based partitioning coefficients are all <50%, leading to an uncertainty of log $K^m_{p,OM}$ less than ± 0.30. Comparable or even greater (up to 10^5) gap between $K^m_{p,OM}$ and $K^t_{p,OM}$ has been observed for carbonyls in a number of laboratory and field studies (Healy et al., 2008; Zhao et al., 2013; Shen et al., 2018), which could be ascribed to reactive uptake (e.g., hydration, oligomerization, and esterification) of organic gases onto condensed phase (Galloway et al., 2009). Oligomers, sulfate and nitrate esters of 2-methyltetrols can be formed in the aerosol phase (Surratt et al., 2010; Lin et al., 2014), and their decomposition and hydrolysis during filter analysis will lead to an overestimation of particle-phase concentrations (Lin et al., 2013; Cui et al., 2018). However, the occurrence of oligomers, sulfate or nitrate esters of levoglucosan was not ever reported in ambient aerosols, although it can be readily oxidized by •OH in the aqueous phase of atmospheric particles (Hennigan et al., 2010; Hoffmann et al., 2010).

When solubility in aerosol liquid water was considered by assuming a LLPS in ambient aerosols, and whenever WSOM and WIOM partitioned into separate (*Case 2*) or single (*Case 3*) liquid phases, the average log $K^m_{p,OM}$ of the above mentioned compounds became much closer to or even lay within the range (e.g., levoglucosan) of log $K^t_{p,OM}$ (Table 1). These results indicated that the aerosol liquid water (21.3 ± 24.2 µg m^{-3}; Table S1) is also an important absorbing phase of ambient polyol tracers in Nanjing. Similarly, the measured average *F*% of isoprene SOA tracers in southeastern US and central Amazonia were higher than predictions by assuming instantaneous equilibrium between the gas phase and particulate OM only, and the agreement was improved when parameterization of solubility was included for predictions (Isaacman-VanWertz et al., 2016). But none of these two studies could reasonably predict the temporal variability of *F*% or log $K^m_{p,OM}$. One possible explanation is that the activity coefficients of isoprene SOA tracers and levoglucosan deviate from unity (0.42–2.04; Pye et al., 2018) and vary with PM composition. Pye et al. (2018) re-analyzed the measurement data from Isaacman-VanWertz et al. (2016) using a thermodynamic equilibrium gas-particle partitioning model in two LLPS modes, which involved organic-inorganic interactions and estimations of activity coefficients as a function of liquid PM mixture composition. The resulting predictions captured both the average and diurnal variations of measured *F*% for polyol tracers, suggesting a necessity in obtaining time-resolved activity coefficients for the implementation of absorptive equilibrium partitioning model.

…………………………………………………………………………..

3.5 Partitioning coefficients of gas versus aqueous phases

The predicted Henery's law coefficients in pure water ($K^t_{H,w}$, mol m^{-3} atm^{-1}) from EPI and SPARC estimates differed by several orders of magnitude, but literature values of isoprene SOA and levoglucosan were closer to EPI estimates (Table S4). If SPARC $K^*_{H,w}$ values were used, the average log $K^m_{H,e}$ of most polyol tracers would be lower than their average log $K^t_{H,w}$ (Table 2), indicating that the aqueous phase of ambient aerosol is less hospital to polyol tracers than pure water. This is in conflict with the fact that the interactions of organic compounds, water, and inorganic ions in

aerosols will increase the partitioning of highly oxygenated compounds (O:C≥0.6; e.g., isoprene SOA tracers and levoglucosan) into the particle phase (Pye et al., 2018). Several studies identified a close relationship between salt concentrations of aerosol water and enhanced uptake of very polar compounds (Almeida et al., 1983; Kroll et al., 2005; Ip et al., 2009; Kampf et al., 2013; Shen et al., 2018). Thus, log $K^t_{H,w}$ values of EPI estimates were used for further data analysis.

In Table 2, the $K^t_{H,w}$ values of isoprene SOA tracers, levoglucosan, and meso-erythritols based on EPI estimations were 10^2 to 10^6 lower than their corresponding $K^m_{H,e}$. Log $K^m_{H,e}$ values of *Cases 2* and *3* had ignorable difference and were not presented separately. Other polyol compounds exhibited less difference between log $K^m_{H,e}$ and log $K^t_{H,w}$, which was very likely caused by the overestimation of their gas-phase concentrations. The average $K^m_{H,e}$ values of polyol tracers (10^{13}–10^{15} mol m^{-3} atm^{-1}) in this study were several orders of magnitude larger than those of carbonyls derived from ambient measurements (10^{10}–10^{12} mol m^{-3} atm^{-1}; Shen et al., 2018) and chamber simulations (~10^{11} mol m^{-3} atm^{-1}; Kroll et al., 2005; Volkamer et al., 2006; Galloway et al., 2009). This is because low molecular weight carbonyls (e.g., glyoxal) are much more volatile ($p^{o,*}_L > 10^{-2}$ atm) than our target polyols (Table S4). According to existing studies, the minimum concentrations of gas-phase glyoxal and methylglyoxal in Chinese cities (~0.1 μg m^{-3}) are magnitudes higher than the averages of polyol tracers in this work, while their particle-phase concentrations are of the same magnitude (Shen et al., 2018; Liu et al., 2020).

A number of previous studies observed enhanced $K_{H,e}$ of carbonyls with salt concentrations in aqueous solution (Ip et al., 2009; Kampf et al., 2013; Waxman et al., 2015; Shen et al., 2018), and described this "salting-in" effect using

$$\text{Log}\left(\frac{K_{H,w}}{K_{H,e}}\right) = K_s c_{salt} \qquad (7)$$

where K_s (kg mol^{-1}) is the salting constant, and c_{salt} is the aqueous-phase concentration of salt in mol kg^{-1} ALWC. This equation is originally defined in Setschenow (1889) by plotting log ($K_{H,w}/K_{H,e}$) versus the total salt concentration (mol L^{-1}).

As sulfate has been identified as the major factor influencing the salting effect of carbonyl species (Kroll et al., 2005; Ip et al., 2009), Figure 4 shows modified Setschenow plots for C5-alkene triols, 2-methyltetrols, and levoglucosan, where log ($K^t_{H,w}/K^m_{H,e}$) values were regressed to the molality of sulfate ion in aerosol liquid water ($c_{sulfate}$, mol kg^{-1} ALWC). The log ($K^t_{H,w}/K^m_{H,e}$) data increased faster when $c_{sulfate}$ approached 0, and deviated from their expected behavior with increased $c_{sulfate}$. Kampf et al. (2013) selected a threshold $c_{sulfate}$ of 12 mol kg^{-1} ALWC to illustrate the deviation for chamber experiments, and attributed it to elevated viscosity and slow particle-phase reactions at high $c_{sulfate}$. In Figure 4, negative correlations ($p < 0.01$) are observed at $c_{sulfate} < 12$ mol kg^{-1} ALWC, and Figure S5 exhibits significant negative correlations ($p < 0.01$) between log ($K^t_{H,w}/K^m_{H,e}$) and $c_{sulfate}$ for individual polyols even without excluding the deviations at high $c_{sulfate}$. The K_s values of polyol tracers from Figures 4 and S5 (-0.17 – -0.037 kg mol^{-1}) are in a similar range as that of glyoxal (-0.24 – -0.04 kg mol^{-1}; Kampf et al., 2013; Shen et al., 2018; Waxman et al., 2015). These results indicated that the shifting of gas-particle equilibrium toward the condensed phase might be partly parameterized by the equation defining "salting-in" effects.

However, the "salting-in" effect is a known phenomenon that is not likely linked with a specific physical or chemical mechanism. Quantum chemical calculation results indicated negative Gibbs free energy of water displacement for interactions between SO$_4^{2-}$ and glyoxal monohydrate (Waxman et al., 2015). The net "salting-in"

effect of 1-nitro-2-naphthol in NaF solution was interpreted by postulating hydrogen bonding (Almeida et al., 1983). A direct binding of cations to ether oxygens was proposed to be responsible for the increased solubility of water-soluble polymers (Sadeghi and Jahani, 2012). Due to the moderate correlations and negative intercepts in Figures 4 and S5, the gap between $K^t_{H,e}$ and $K^m_{H,w}$ cannot be closed by the "salting-in" effect alone. Shen et al. (2018) also obtained negative intercepts when plotting log ($K^t_{H,w}/K^m_{H,e}$) over $c_{sulfate}$ for glyoxal and methylglyoxal in ambient atmosphere, and attributed this to unknown gas-particle partitioning mechanisms. Evidences showing that the thermal degradation of less volatile oligomers and organosulfates can lead to an overestimation of 2-methyltetrols by 60–188% when using a conventional GC/EI-MS method (Cui et al., 2018). To fit the gas-particle distribution of 2-methyltetrols in southeastern US, 50% of particulate 2-methyltetrols was presumed to exist in chemical forms with much lower vapor pressures by Pye et al. (2018). So, the reactive uptake and aqueous phase chemistry could be explanations for the enhanced uptake of isoprene SOA tracers. Moreover, log ($K^t_{H,w}/K^m_{H,e}$) values of polyol tracers also negatively correlated with the aqueous-phase concentrations of WSOC (c_{WSOC}, Figure S6), but not NH_4^+ or NO_3^-. This dependence might be associated with the "like-dissolves-like" rule, or indicate the importance of aqueous-phase heterogeneous reactions (Hennigan et al., 2009; Volkamer et al., 2009). Although several studies have estimated Henry's law constants for a variety of polar organic compounds in pure water (e.g., polyols and polyacids; Compernolle and Müller, 2014a, b), more work is warranted to decrease the estimation uncertainty and explain their increased partitioning toward aerosol liquid water explicitly."

Specific comments:

4. Line 57: Typo, "Filed" should say "Field"

Response:

It has been revised as suggested. (Page 4, line 80)

5. Line 85: Probably also worth mentioning that Yatavelli et al. (2014, 10.5194/acp-14-1527-2014) and Isaacman-VanWertz et al. (2016) also found good agreement with theory for alkanoic acids

Response:

The two references were added, and the original expression has been changed into

"Unlike non-polar species (e.g., *n*-alkanes, polycyclic aromatic hydrocarbons) and alkanoic acids that are well simulated (Simcik et al., 1998; Xie et al., 2014a; Yatavelli et al., 2014; Isaacman-VanWertz et al., 2016), particle-phase concentrations of carbonyls were underestimated by several orders of magnitude when particulate OM is presumed as the only absorbing phase in ideal condition (Healy et al., 2008; Kampf et al., 2013; Shen et al., 2018)." (Page 5, 109-114)

6. Line 90: Typo, "every" should say "very"

Response:

It has been revised as suggested. (Page 5, line 117)

7. Line 176: When quantifying the isoprene tracers using meso-erythritol, I assume the effect of fragmentation on the quant ion was accounted for, but that is not clear here or in the supplmental. In other words, while m/z 219 is used for the 2-MTs, something different, likely m/z 217, is used for meso-erythritol, and the fraction of total signal that is the quant ion could be different - if this was corrected for it should be stated at least in the SI, if not it should be justified.

Response:

In the current work, we did not consider the effect of fragmentation on the quant ion due to the following reasons:
(1) Meso-erythritol and isoprene tracers (C5-alkene triols and 2-methyltetrols) should have different total ion signal intensity for the same amount, so the calibration curve of meso-erythritol is expected to differ from isoprene tracers. Even if the effect of fragmentation on the quant ion was accounted for, the quantification accuracy might not be improved. A number of previous studies used meso-erythritol as surrogate for isoprene tracers without considering the effect of fragmentation (Claeys et al., 2004; Hu et al., 2008; Ding et al., 2008, 2012; Lin et al., 2013; Xie et al., 2014). It should also be noted that ketopenic acid was used to quantify all SOA tracers by Kleindienst et al. (2007).
(2) The present study focused on the gas-particle partitioning of polyol tracers. Their particle-phase fractions, measurement-based partitioning coefficients of gas versus organic ($K^m_{p,OM}$) and aqueous ($K^m_{H,e}$) phases were all directly related to the ratio of particle- to gas-phase concentrations, which is not impacted by the effect of fragmentation.
(3) The total ion peaks corresponding to isoprene tracers in ambient air samples usually combined with other compounds, thus the quant ions (m/z 219) fractions of 2-methyltetrols in total ion signal (0.14 ± 0.035, 0.20 ± 0.015) had larger variability than that of meso-erythritol (0.12 ± 0.0039), then the correction for fragmentation effect might introduce new uncertainty.

In the revised supplementary information, we added some justifications for not correcting the fragmentation effect.
"Meso-erythritol and isoprene SOA tracers were expected to have different total ion intensity for the same amount, and the total ion signals of isoprene tracers in ambient air sample often co-eluted with other compounds, so the fragmentation difference between quantification ions of meso-erythritol (m/z 217) and isoprene SOA tracers (m/z 219) was not adjusted in this work. It should be noted that meso-erythritol was used as the surrogate for isoprene tracers without considering the fragmentation effect in a number of previous studies (Claeys et al., 2004; Hu et al., 2008; Ding et al., 2008, 2012; Lin et al., 2013; Xie et al., 2014)."

8. Line 197: If gas-phase mass is being taken as Qb plus PUF, what is the purpose of the Qb measurement at all? Why not just do Qf backed by a PUF?

Response:

The backup quartz fiber filter was typically used to assess positive sampling artifact of particulate OC due to gaseous adsorption (Chow et al., 2010; Subramanian et al., 2004). In a companion study to this work, concentrations of bulk species in PM$_{2.5}$ were determined by subtracting measurement results of Q$_b$ from Q$_f$ (Yang et al., 2021). This has been mentioned in section 2.2 of the manuscript (Pages 8, lines 176-178).

Concentrations of polyol tracers detected on Q$_b$ reflected filter-based sampling artifacts, which is ascribed to gaseous adsorption ("positive artifact") and evaporation loss from particles on Q$_f$ ("negative artifact"). If polyol tracers on Q$_b$ account for significant fractions of their total concentrations, then the separation of their particle- and gas-phase concentrations will depend largely on sampling artifact corrections. In the current work, polyol tracers were predominantly observed on Q$_f$ with averages 1-3 orders of magnitude higher than those on Q$_b$ and PUF, and it would be safe to assume that Q$_b$ values were equally contributed by positive and negative artifacts. So, Q$_b$ measurement is necessary in determining the magnitude of sampling artifacts.

The original expressions have been revised (Pages 9-10, lines 218-229).
"Polyol tracers detected in Q$_b$ samples are contributed by both gaseous adsorption ("positive artifact") and particle-phase evaporation from Q$_f$ samples ("negative artifact"), but their relative contributions are unknown. Xie et al. (2014b) adjusted particle- and gas-phase concentrations of levoglucosan and 2-methyltetrol based on Q$_b$ measurements in two different ways. One assumed that Q$_b$ values were completely attributed to gaseous adsorption; the other presumed equal contributions from gaseous adsorption and Q$_f$ evaporation. However, negligible difference in gas-particle distribution was observed due to the small Q$_b$ values. In Table S3, concentrations of polyol tracers on Q$_b$ are far below those on Q$_f$, and it would be safe to presume equal positive and negative artifacts. In this study, particle-phase concentrations of polyols were represented by Q$_f$ values, and the gas phase was calculated as the sum of Q$_b$ and PUF measurements."

9. Line 220-225: I'm not completely clear on the partitioning approach. The Kow is used to partition the particle fraction between condensed phases - is this information then used in the gase-particle partitioning? For instance, is K_OM used for the organic component, and K_H used for the aqueous? I guess I'm just not clear on how Kow fits into the scheme.

Response:

Yes, the K_{OW} is used to calculate concentrations of polyol tracers in two separate aerosol phases (organic and aqueous). $K_{p,OM}$ and K_H represent gas-particle partitioning coefficients of gas versus organic and aqueous phases, respectively.

To make it clear, we defined three partitioning cases, and elucidate the calculation methods for the two partitioning coefficients in the revised manuscript.

Pages 10-13, lines 238-295 (See responses to *Comment 1*, eqs 4, 5, and 6)

10. Line 297-298: Isaacman-VanWertz et al. (2016) also show hourly diurnal profiles with a daytime high, it is interesting to see in this work that the difference between daytime and nighttime values was not significant. As noted later in the manuscript, in the summer when there are actually strong concentrations of these compounds, there is a strong diurnal, so I'm not sure it really makes sense to claim here there is no diurnal.

Response:

Similar to the observations by Fu and Kawamura (2011) at a forest site in Hokkaido, Japan, concentrations of isoprene SOA tracers in southeastern US and central Amazonia also exhibited peak concentrations from late afternoon to mid night. In the current work, daytime and nighttime samples were collected during 8:00 AM – 7:00 PM and 7:00 PM – 7:00 AM (next day), respectively. Neither the daytime or nighttime sample covered the whole period when isoprene SOA had peak concentrations. This explains why the strong diurnal variations of isoprene SOA tracers were not captured in this work.

The original expression was changed into
"Previous field studies observed strong diurnal variations of isoprene SOA tracers with peak concentrations from afternoon till midnight (Fu and Kawamura, 2011; Isaacman-VanWertz et al., 2016). Although no IEPOX will be generated from the oxidation of isoprene by •OH and HO_2• after sunset, the formations of C5-alkene triols and 2-methyltetrols might continue until pre-existing IEPOX is exhausted. In this work, neither the daytime (8:00 AM–7:00 PM) or night-time (7:00 AM–7:00 AM next day) sample covered the whole period when isoprene SOA tracers had peak concentrations, and the strong diurnal variations of C5-alkene triols and 2-methyltetrols were not captured." (Page 16, 367-375)

11. Line 336: This is the first place F% is given any error or range, though I assume here the uncertainty is the standard deviation.

Response:

We clarified in the revised manuscript that the numbers here represented ranges of average ± standard deviation. (Page 17, lines 405)
Moreover, measurement uncertainties and their influences on *F*% and partitioning coefficients were estimated in the revised manuscript. (Text S5 and Figure 3, see responses to *Comment 2*; Table S5, shown below)

Table S5. Average relative uncertainties of measurements and calculated parameters.

Species	$\Delta F/F$ [a]	$\Delta A/A$ [b]	$\Delta S/S$ [c]	$\Delta F\%/F\%$ [d]	$\Delta K/K$ [e]
Isoprene SOA tracers					
C5-alkene triol 1	0.028	0.032	0.027	0.037	0.043
C5-alkene triol 2	0.028	0.054	0.033	0.036	0.059
C5-alkene triol 3	0.028	0.077	0.034	0.038	0.084
2-Methylthreitol	0.028	0.051	0.028	0.033	0.059
2-Methylerythritol	0.028	0.066	0.030	0.035	0.072
Biomass burning tracer					
Levoglucosan	0.051	0.16	0.054	0.072	0.17
Sugars ang sugar alcohols					
Meso-erythritol	0.028	0.11	0.028	0.040	0.12
Fructose	0.23	0.27	0.26	0.31	0.36
Mannose	0.045	0.27	0.049	0.062	0.28
Glucose	0.094	0.28	0.10	0.18	0.31
Xylitol	0.10	0.12	0.10	0.14	0.16
Arabitol	0.097	0.26	0.099	0.14	0.28
Mannitol	0.21	0.42	0.21	0.29	0.47

[a] Particle-phase concentration; [b] gas-phase concentration; [c] total concentration; [d] particle-phase fraction; [e] partitioning coefficients of gas vs. organic and aqueous phases.

12. Line 370: This could also be due to some systematic bias in how EPI estimates vapor pressures. This might be reconcile by testing other vapor pressure estimation methods. For example EVAPORATION agrees with EPI on the vapor pressure of erythritol (log vp (atm) = ~ -8.2-8.5) but EPI estimates mannose to be two orders of magnitude more volatile (log vp (atm) = -9.5) than EVAPORATION estimates (log vp (atm) = -11.5). This also highlights the uncertainty of using comparisons against theoretical K to draw conclusions.

Response:

To address the concern on uncertainties of vapor pressures, other estimation tools were tested (Table S4). The revised Table 1 (shown below) compared measurement-based log $K_{p,OM}$ of predefined *Cases 1-3* and theoretical predictions based on different vapor pressure estimation methods. Then the discussions on comparisons between measured and predicted $K_{p,OM}$ were revised accordingly (Section 3.4, see responses to *Comment 3*; pages 18-20, lines 420-480).

As shown in Table 1, when the solubility in aerosol liquid water is considered (*Cases 2* and *3*), the agreement between log $K^m_{p,OM}$ and log $K^t_{p,OM}$ for isoprene SOA tracers and levoglucosan has been improved substantially. While the deviations of log $K^m_{p,OM}$ versus log $K^t_{p,OM}$ for monosaccharides and sugar alcohols became larger. This is expected to be caused by the overestimations of their gas phase concentrations due to sampling artifacts, since the vapor pressures of sugar polyols were orders of magnitude lower than isoprene SOA tracers and levoglucosan.

Table 1. Comparisons of measurement-based log $K_{p,OM}$ (m^3 μg^{-1}) at three proposed cases and predicted values.

Species	No. of obs.	Log $K^m_{p,OM}$ [a]			Log $K_{p,OM}$ [b]			
		Case 1	Case 2	Case 3	EPI	EVAPORATION	SPARC	SIMPOL
Isoprene SOA tracers								
C5-alkene triol 1	53	0.33 ± 0.71	-0.79 ± 0.86	-0.82 ± 0.85	-3.09	-2.84	-1.19	-2.88
C5-alkene triol 2	63	0.15 ± 0.55	-1.02 ± 0.74	-1.05 ± 0.73	-3.62	-3.67	-4.14	-2.85
C5-alkene triol 3	83	0.35 ± 0.68	-0.83 ± 0.86	-0.86 ± 0.85	-2.90	-2.65	-1.00	-2.69
2-Methylthreitol	101	-0.12 ± 0.48	-2.09 ± 0.71	-2.09 ± 0.70	-1.87	-1.30	-1.18	-0.47
2-Methylerythritol	95	-0.011 ± 0.58	-1.96 ± 0.71	-1.96 ± 0.71	-1.90	-1.34	-1.22	-0.50
Biomass burning tracer								
Levoglucosan	65	2.23 ± 0.72	0.63 ± 0.90	0.62 ± 0.90	-0.04	-0.81	1.04	-0.76
Sugars ang sugar alcohols								
Meso-erythritol	31	0.87 ± 0.53	-1.43 ± 0.60	-1.43 ± 0.60	-0.65	-1.21	-0.45	
Fructose	85	0.65 ± 0.73	-1.20 ± 0.83	-1.20 ± 0.89	1.17	2.76	6.94	
Mannose	74	0.62 ± 0.71	-2.12 ± 0.95	-2.12 ± 0.95	1.28	2.13	4.77	
Glucose	88	0.42 ± 0.67	-2.77 ± 0.93	-2.77 ± 0.93	0.34	3.75	7.32	
Xylitol	22	0.24 ± 0.54	-2.61 ± 0.72	-2.61 ± 0.72	3.37	2.34	3.57	
Arabitol	30	1.46 ± 0.89	-1.35 ± 1.24	-1.35 ± 1.24	3.25	1.67	2.90	
Manitol	65	1.08 ± 0.63	-2.24 ± 0.95	-2.24 ± 0.95	2.33	4.16	6.68	

[a] Average ± standard deviation; [b] temperature range: -4~36 °C.

13. Line 391: Here and throughout, why use K_H,e and K_H,w for measured and predicted, respectively, for Henry's law, but K_p^m and K_p^t or measured and predicted, respectively, for absorptive partitioning. I think the discussion would be more clear if notation were more consistent (e.g, K_H^m and K_H^t

Response:

Thanks. To make it more clear and consistent, $K_{H,e}$ and $K_{H,w}$ were changed into $K^m_{H,e}$ and $K^t_{H,w}$ if necessary throughout the manuscript.

14. Line 407: out of curiosity, why did the authors choose to switch to molality instead of molarity?

Response:

The switch from molarity to molality will not influence the correlation between log $(K_{H,w}/K_{H,e})$ and sulfate concentrations. It also makes it easier to compare the salting constant (K_s) with previous studies (Kampf et al., 2013; Waxman et al., 2015; Shen et al., 2018).

References

Chow, J. C., Watson, J. G., Chen, L. W. A., Rice, J., and Frank, N. H.: Quantification of PM2.5 organic carbon sampling artifacts in US networks, Atmos. Chem. Phys., 10, 5223-5239, 10.5194/acp-10-5223-2010, 2010.

Claeys, M., Graham, B., Vas, G., Wang, W., Vermeylen, R., Pashynska, V., Cafmeyer, J., Guyon, P., Andreae, M. O., Artaxo, P., and Maenhaut, W.: Formation of secondary organic aerosols through photooxidation of isoprene, Science, 303, 1173-1176, 10.1126/science.1092805, 2004.

Ding, X., Zheng, M., Yu, L., Zhang, X., Weber, R. J., Yan, B., Russell, A. G., Edgerton, E. S., and Wang, X.: Spatial and seasonal trends in biogenic secondary organic aerosol tracers and water-soluble organic carbon in the Southeastern United States, Environ. Sci. Technol., 42, 5171-5176, 10.1021/es7032636, 2008.

Ding, X., Wang, X.-M., Gao, B., Fu, X.-X., He, Q.-F., Zhao, X.-Y., Yu, J.-Z., and Zheng, M.: Tracer-based estimation of secondary organic carbon in the Pearl River Delta, south China, J. Geophys. Res. Atmos., 117, D05313, 10.1029/2011jd016596, 2012.

Hu, D., Bian, Q., Li, T. W. Y., Lau, A. K. H., and Yu, J. Z.: Contributions of isoprene, monoterpenes, β-caryophyllene, and toluene to secondary organic aerosols in Hong Kong during the summer of 2006, J. Geophys. Res. Atmos., 113, D22206, 10.1029/2008jd010437, 2008.

Kleindienst, T. E., Jaoui, M., Lewandowski, M., Offenberg, J. H., Lewis, C. W., Bhave, P. V., and Edney, E. O.: Estimates of the contributions of biogenic and anthropogenic hydrocarbons to secondary organic aerosol at a southeastern US location, Atmos. Environ., 41, 8288-8300, 10.1016/j.atmosenv.2007.06.045, 2007.

Kampf, C. J., Waxman, E. M., Slowik, J. G., Dommen, J., Pfaffenberger, L., Praplan, A. P., Prévôt, A. S. H., Baltensperger, U., Hoffmann, T., and Volkamer, R.: Effective Henry's law partitioning and the salting constant of glyoxal in aerosols containing sulfate, Environ. Sci. Technol., 47, 4236-4244, 10.1021/es400083d, 2013.

Lin, Y. H., Knipping, E. M., Edgerton, E. S., Shaw, S. L., and Surratt, J. D.: Investigating the influences of SO2 and NH3 levels on isoprene-derived secondary organic aerosol formation using conditional sampling approaches, Atmos. Chem. Phys., 13, 8457-8470, 10.5194/acp-13-8457-2013, 2013.

Shen, H., Chen, Z., Li, H., Qian, X., Qin, X., and Shi, W.: Gas-particle partitioning of carbonyl compounds in the ambient atmosphere, Environ. Sci. Technol., 52, 10997-11006, 10.1021/acs.est.8b01882, 2018.

Subramanian, R., Khlystov, A. Y., Cabada, J. C., and Robinson, A. L.: Positive and negative artifacts in particulate organic carbon measurements with denuded and undenuded sampler configurations special issue of aerosol science and technology on findings from the fine particulate matter supersites program, Aerosol Sci. Tech., 38, 27-48, 10.1080/02786820390229354, 2004.

Waxman, E. M., Elm, J., Kurtén, T., Mikkelsen, K. V., Ziemann, P. J., and Volkamer, R.: Glyoxal and methylglyoxal Setschenow salting constants in sulfate, nitrate, and chloride solutions: Measurements and Gibbs energies, Environ. Sci. Technol., 49, 11500-11508, 10.1021/acs.est.5b02782, 2015.

Xie, M., Hannigan, M. P., and Barsanti, K. C.: Gas/particle partitioning of 2-methyltetrols and levoglucosan at an urban site in Denver, Environ. Sci. Technol., 48, 2835-2842, 10.1021/es405356n, 2014.

Yang, L., Shang, Y., Hannigan, M. P., Zhu, R., Wang, Q. g., Qin, C., and Xie, M.: Collocated speciation of PM2.5 using tandem quartz filters in northern nanjing, China: Sampling artifacts and measurement uncertainty, Atmos. Environ., 246, 118066, https://doi.org/10.1016/j.atmosenv.2020.118066, 2021.

This study presents the results of simultaneous gas- and particle-phase measurements of oxygenated organic compounds in Nanjing, China. Due to some potential measurement artifacts with some compounds, the results focus on C5-alkene triols, 2-methyltetrols, and levoglucosan. The major finding is that the particle-phase fraction of these compounds were on average orders of magnitude higher than can be explained by either absorptive partitioning theory or Henry's law. There is moderate evidence that sulfate caused a "salting in" effect, though more discussion and/or data are needed to support this point (comment detailed below). The writing and organization are generally good, and the topic is of interest to a broad audience. I recommend the manuscript for publication after the following comments are addressed.

Response:

Thanks for the reviewer's comments, and we will reply these point by point in the reviewers' specific comments.

Specific Comments

1. How much does measurement uncertainty affect the partitioning coefficients? The stated acceptable threshold for breakthrough (< 33%) seems relatively high. How do the observed levels of breakthrough contribute to the uncertainty in the partitioning coefficients? Further, did breakthrough vary as a function of ambient temperature, OA loading, etc? Discussion of these points is needed.

Response:

The estimation of measurement uncertainties and their influences on partitioning coefficients were added in the revised manuscript. In general, measurement uncertainties of polyol tracers in filter samples were estimated from averages and ranges of their recoveries and method detection limits. Breakthrough of gaseous sampling was additionally considered for measurement uncertainties of PUF samples. Uncertainties associated with the calculations of particle-phase fractions and partitioning coefficients were estimated using a simplified root sum of squares (RSS) method by propagating measurement uncertainties of gas- and particle-phase concentrations. Details of the method were provided in Text S5 in supplementary information and mentioned in the main text.

Text S5 in supplementary information:
"***Text S5. Uncertainty estimation methods***

In this work, the measurement results of some polyol tracers in filter and PUF samples are subject to substantial uncertainties due to their low and variable recoveries (Table S2) and excessive breakthrough (Figure S2). A general equation was derived to estimate measurement uncertainties of individual polyols in filter and PUF samples

$$\Delta C = \sqrt{(\text{error fraction} \times \text{concentration})^2 + (0.5 \times \text{detection limit})^2} \qquad (5)$$

where ΔC is the uncertainty of target species in filter (ΔQ_f and ΔQ_b, ng m^{-3}) or PUF (ΔPUF, ng m^{-3}) samples. The error fraction (%) of filter sample analysis was defined as half of the difference between maximum and minimum recoveries scaled by the average (Table S2), which was divided by (1 - average breakthrough) for PUF analysis (Figure S2). The average breakthrough of meso-erythritol (23.8%), mannose (38.1%), xylitol (36.4%), and arabitol (36.4%) were set as those of C5-alkene triols, glucose, and

1

mannitol, respectively. According to the gas-particle separation method in this work, ΔQ_f was used to represent the uncertainty of particle-phase concentration (ΔF, ng m^{-3}), and the uncertainty of gas-phase concentration (ΔA, ng m^{-3}) was propagated by

$$\Delta A = \sqrt{\Delta Q_b{}^2 + \Delta PUF^2} \qquad (6)$$

Then the uncertainty of total concentration (ΔS, ng m^{-3}) was calculated as

$$\Delta S = \sqrt{\Delta F^2 + \Delta A^2} \qquad (7)$$

The uncertainties of particle-phase fractions ($\Delta F\%$) and partitioning coefficients ($K^m_{p,OM}$ and $K^m_{p,WIOM}$, m^3 ug^{-1}; $K^m_{H,e}$, mol m^{-3} atm^{-1}) were estimated by propagating ΔF, ΔS, and ΔA using a simplified root sum of squares (RSS) method (Dutton et al., 2009)

$$\Delta F\% = \sqrt{\left(\frac{\partial F\%}{\partial F}\Delta F\right)^2 + \left(\frac{\partial F\%}{\partial S}\Delta S\right)^2} \times 100\% \qquad (8)$$

$$\Delta K = \sqrt{\left(\frac{\partial K}{\partial F'}\Delta F'\right)^2 + \left(\frac{\partial K}{\partial A}\Delta A\right)^2} \qquad (9)$$

where ΔK is the uncertainty of $K^m_{p,OM}$, $K^m_{p,WIOM}$, or $K^m_{H,e}$; F' could be F, concentrations of polyols in WIOM (F_{WIOM}) or aqueous (F_w) phases, depending on the partitioning scheme (*Cases 1–3*) and partitioning coefficient for calculation. ΔF was split into ΔF_w and ΔF_{WIOM} (or ΔF_{OM}) based on their ratios in eq. 4 of the main text. In Table S5, the estimated uncertainties are summarized and expressed in average ratios. As $K^m_{p,OM}$ and $K^m_{H,e}$ are all directly related to the ratio of particle- (F, ng m^{-3}) and gas-phase (A, ng m^{-3}) concentrations (eqs. 2, 4, 5, and 6 in the main text), their average $\Delta K/K$ values are the same (Table S5). ”

Page 13, lines 296 – 303 of the main text:
“***Uncertainty estimation.*** To obtain the uncertainty associated with the calculation of $F\%$ and partitioning coefficients ($K^m_{p,OM}$ and $K^m_{H,e}$), measurement uncertainties of polyol tracers in filter and PUF samples were estimated from their recoveries and breakthrough for gaseous sampling. The root sum of squares (RSS) method was applied to propagate uncertainties of gas and particle-phase concentrations for $F\%$, $K^m_{p,OM}$, and $K^m_{H,e}$ calculations. Details of the uncertainty estimation and propagation methods were provided in Text S5, and the average relative uncertainties were summarized in Table S5.”

According to the equation for breakthrough calculation, a value of 33% means that the amount of a certain compound in backup PUF samples is half of that in front PUF samples. It was used as an indicator of excessive breakthrough in several previous studies (Peters et al., 2000; Ahrens et al., 2011; Xie et al., 2014a, b). However, the breakthrough value was rarely used to correct measurement results.

In the revised manuscript, the breakthrough of gaseous sampling was included for the estimation of measurement uncertainties and their influences on partitioning coefficients, but its individual contributions cannot be separated. In Table S5 (shown below), uncertainties of gas- and particle-phase concentrations, particle-phase fractions, and partitioning coefficients are expressed in average relative abundance.

Due to the limit in sample number for breakthrough tests and low detection rates, we can hardly evaluate the dependence of breakthrough on ambient temperature or OA loadings. The breakthrough of an ideal sampling method is expected to be extremely low (e.g., <10%) and have no dependence on ambient temperature or OA loadings. These statements were added in the revised manuscript (Pages 14-15, 337–341).

Table S5. Average relative uncertainties of measurements and calculated parameters.

Species	$\Delta F/F$[a]	$\Delta A/A$[b]	$\Delta S/S$[c]	$\Delta F\%/F\%$[d]	$\Delta K/K$[e]
Isoprene SOA tracers					
C5-alkene triol 1	0.028	0.032	0.027	0.037	0.043
C5-alkene triol 2	0.028	0.054	0.033	0.036	0.059
C5-alkene triol 3	0.028	0.077	0.034	0.038	0.084
2-Methylthreitol	0.028	0.051	0.028	0.033	0.059
2-Methylerythritol	0.028	0.066	0.030	0.035	0.072
Biomass burning tracer					
Levoglucosan	0.051	0.16	0.054	0.072	0.17
Sugars ang sugar alcohols					
Meso-erythritol	0.028	0.11	0.028	0.040	0.12
Fructose	0.23	0.27	0.26	0.31	0.36
Mannose	0.045	0.27	0.049	0.062	0.28
Glucose	0.094	0.28	0.10	0.18	0.31
Xylitol	0.10	0.12	0.10	0.14	0.16
Arabitol	0.097	0.26	0.099	0.14	0.28
Mannitol	0.21	0.42	0.21	0.29	0.47

[a] Particle-phase concentration; [b] gas-phase concentration; [c] total concentration; [d] particle-phase fraction; [e] partitioning coefficients of gas vs. organic and aqueous phases.

2. The assumption of LLPS should be discussed. Other studies, for example Pye et al. (2018), could be included in this discussion.

Response:

Thanks. We discussed the assumption of LLPS by citing two existing studies (Zuend and Seinfeld, 2012; Pye et al., 2018) in the revised manuscript. Pye et al. (2018) was included in discussions on the agreement between measurement-based and predicted partitioning coefficients.

Page 11, lines 258-262

"Due to the influence of mixing state and water content in aerosols, several studies modeled the gas-particle partitioning of oxygenated organic compounds by defining a liquid-liquid phase separation (LLPS) in the aerosol (Zuend and Seinfeld, 2012; Pye et al., 2018). The organic-inorganic interactions and changes of activity coefficients in aqueous mixtures were fully considered as well."

Pages 19-20, lines 444-464

"When solubility in aerosol liquid water was considered by assuming a LLPS in ambient aerosols, and whenever WSOM and WIOM partitioned into separate (*Case 2*) or single (*Case 3*) liquid phases, the average log $K^m_{p,OM}$ of the above mentioned compounds became much closer to or even lay within the range (e.g., levoglucosan) of log $K^t_{p,OM}$ (Table 1). These results indicated that the aerosol liquid water (21.3 ± 24.2 µg m^{-3}; Table S1) is also an important absorbing phase of ambient polyol tracers in Nanjing. Similarly, the measured average $F\%$ of isoprene SOA tracers in southeastern US and central Amazonia were higher than predictions by assuming instantaneous equilibrium between the gas phase and particulate OM only, and the agreement was improved when parameterization of solubility was included for predictions (Isaacman-

VanWertz et al., 2016). But none of these two studies could reasonably predict the temporal variability of F% or log $K^m_{p,OM}$. One possible explanation is that the activity coefficients of isoprene SOA tracers and levoglucosan deviate from unity (0.42–2.04; Pye et al., 2018) and vary with PM composition. Pye et al. (2018) re-analyzed the measurement data from Isaacman-VanWertz et al. (2016) using a thermodynamic equilibrium gas-particle partitioning model in two LLPS modes, which involved organic-inorganic interactions and estimations of activity coefficients as a function of liquid PM mixture composition. The resulting predictions captured both the average and diurnal variations of measured F% for polyol tracers, suggesting a necessity in obtaining time-resolved activity coefficients for the implementation of absorptive equilibrium partitioning model."

Page 21, lines 487-490
     "This is in conflict with the fact that the interactions of organic compounds, water, and inorganic ions in aerosols will increase the partitioning of highly oxygenated compounds (O:C$\geqslant$0.6; e.g., isoprene SOA tracers and levoglucosan) into the particle phase (Pye et al., 2018)."

3. I think that the title is somewhat misleading because the answer to the question is actually "neither" for most of the organic markers investigated. I suggest revising the title to reflect this.

Response:

     In the revised manuscript, it was shown that the solubility of polyol tracers in aerosol liquid water should not be ignored. Comparisons of measurement-based effective Henry's law constants versus predicted values in pure water indicated increased partitioning toward the particle phase.
     Then the title has been changed into
     "Gas-particle partitioning of polyol tracers at a suburban site in Nanjing, east China: Increased partitioning to the particle phase"

4. The comparisons to Denver, CO seem completely random given that meteorology, OA loadings, inorganic composition, and ALWC are quite different between the two locations. I understand that this research group made measurements in both locations, but some additional discussion is warranted to better connect the two locations.

Response:

     The observation study in Denver, CO (Xie et al., 2014b) did not measure inorganic composition or estimate ALWC. In that study, evidences showing that gas-particle partitioning of 2-methyltetrol and levoglucosan depended on variations in ambient temperature and absorbing OM mass. Then the influence of aerosol liquid water on partitioning coefficients could not be compared between these two studies. Thus, in the revised manuscript, we only kept the comparisons of measured gas- and particle-phase concentrations. The partitioning coefficients obtained here were discussed by referring to other studies (e.g., Isaacman-VanWertz et al., 2016; Pye et al., 2018)

Pages 19-20, lines 444-464

"When solubility in aerosol liquid water was considered by assuming a LLPS in ambient aerosols, and whenever WSOM and WIOM partitioned into separate (*Case 2*) or single (*Case 3*) liquid phases, the average log $K^{\mathrm{m}}_{\mathrm{p,OM}}$ of the above mentioned compounds became much closer to or even lay within the range (e.g., levoglucosan) of log $K^{\mathrm{t}}_{\mathrm{p,OM}}$ (Table 1). These results indicated that the aerosol liquid water (21.3 ± 24.2 µg m^{-3}; Table S1) is also an important absorbing phase of ambient polyol tracers in Nanjing. Similarly, the measured average *F*% of isoprene SOA tracers in southeastern US and central Amazonia were higher than predictions by assuming instantaneous equilibrium between the gas phase and particulate OM only, and the agreement was improved when parameterization of solubility was included for predictions (Isaacman-VanWertz et al., 2016). But none of these two studies could reasonably predict the temporal variability of *F*% or log $K^{\mathrm{m}}_{\mathrm{p,OM}}$. One possible explanation is that the activity coefficients of isoprene SOA tracers and levoglucosan deviate from unity (0.42–2.04; Pye et al., 2018) and vary with PM composition. Pye et al. (2018) re-analyzed the measurement data from Isaacman-VanWertz et al. (2016) using a thermodynamic equilibrium gas-particle partitioning model in two LLPS modes, which involved organic-inorganic interactions and estimations of activity coefficients as a function of liquid PM mixture composition. The resulting predictions captured both the average and diurnal variations of measured *F*% for polyol tracers, suggesting a necessity in obtaining time-resolved activity coefficients for the implementation of absorptive equilibrium partitioning model."

5. Several points in the manuscript, including in the 1st sentence of the abstract, the discussion links gas-particle partitioning to source apportionment. However, gas-particle partitioning has importance in the atmosphere that extends way beyond source apportionment (e.g., it affects the PM mass concentration, the lifetime and distribution of organics in the atmosphere, among others). The study thus has broader relevance than is discussed in the manuscript.

Response:

Gas/particle partitioning is important in predicting the formation, transport, and life time of organic aerosols in the atmosphere, which are mostly involved in atmospheric transport models (e.g., CMAQ).

Tracer-based source apportionment is a different research method highly dependent on the identification of source-specific tracers. As mentioned in the introduction, the target polyols in this work are firstly known as tracers liked with specific emission sources. But their gas-particle partitioning was poorly characterized. Several measurement studies on gas-particle partitioning of polar organic tracers also emphasized its importance in both modeling and tracer-based source apportionment of organic aerosols (e.g., Zhao et al., 2013; Isaacman-VanWertz et al., 2016). That's the reason gas-particle partitioning of polyol tracers was also linked to source apportionment in some places of the manuscript.

In the abstract, the first sentence has been changed into

"Gas-particle partitioning of water-soluble organic compounds plays a significant role in influencing the formation, transport, and lifetime of organic aerosols in the atmosphere, but is poorly characterized." (Page 2, lines 31-33)

Technical Corrections

(1) Line 55: "documented" is not the right word here

Response:

Here, "documented for" was replaced by "in". (Page 4, line 78)

(2) Line 65-66: include "GC-MS" in parentheses after introducing the terms

Response:

It was revised as suggested. (Page 4, line 89)

(3) Line 80-83: I do not follow the logic of this sentence, please clarify

Response:

The original expression has been changed into
"In addition to absorptive partitioning to particulate OM after the formation of oxygenated organic compounds in gas phase, other formation pathways (e.g., reactive uptake) have been identified and are responsible for the large discrepancy between modeled and observed SOA loadings (Jang et al., 2002; Kroll et al., 2005; Perraud et al., 2012)." (Page 5, 104-108)

(4) Line 90: typo in this line

Response:

Thanks, "every" should be "very". (Page 5, line 117)

(5) Line 93: suggest changing "depict" to "describe"

Response:

It has been changed as suggested. (Page 5, line 120)

(6) Line 101: delete "termed"

Response:

It was deleted as suggested.

(7) Line 116: "unveils" is not the right word here

Response:

It was replaced by "tends to explain". (Page 6, line 145)

(8) Line 118-120: suggest deleting this sentence

Response:

It was deleted as suggested.

(9) Line 134: change "was" to "were"

Response:

It was changed as suggested. (Page 7, line 163)

(10) Line 153: change "involving" to "using" or similar

Response:

Here, "involving" was replaced by "using". (Page 7, line 179)

(11) Line 221-222: specify that this is theoretical

Response:

The whole sentence has been deleted in the revised manuscript.

(12) Line 244: edit sentence for grammar

Response:

The original expression has been changed into
"It is therefore suitable to collect gaseous 2-methylterols and levoglucosan using PUF materials only." (Page 13, lines 312-313)

(13) Line 317: edit sentence for grammar

Response:

The original expression has been changed into
"………which might be attributed to high levels of vegetation during growing seasons and autumn decomposition (Burshtein et al., 2011)." (Page 17, lines 390-491)

(14) Line 331: delete "data"

Response:

It was deleted and the whole paragraph has been rewritten. (Pages 17-18, lines 397-419)

(15) Line 333: suggest deleting "majorly" and revising the sentence accordingly

Response:

The sentence has been changed into

"Gas-phase C5-alkene triols and 2-methyltetrols had maximum concentrations in summer and significant ($p < 0.05$) day-night variations (Figure S4)............."
(Pages 17, lines 402-403)

(16) Line 360: "prediction" should be plural

Response:

It was changed as suggested. (Page 19, line 451)

(17) Line 380: change "less stable" to "lower"

Response:

We added "lower and" in that sentence. (Page 20, line 478)

(18) Line 386-388: it is quite difficult to follow the discussion here

Response:

Here, the comparisons were reorganized and most of the discussions on $K_{p,OM}$ were rewritten.

"When solubility in aerosol liquid water was considered by assuming a LLPS in ambient aerosols, and whenever WSOM and WIOM partitioned into separate (*Case 2*) or single (*Case 3*) liquid phases, the average log $K^m_{p,OM}$ of the above mentioned compounds became much closer to or even lay within the range (e.g., levoglucosan) of log $K^t_{p,OM}$ (Table 1). These results indicated that the aerosol liquid water (21.3 ± 24.2 µg m^{-3}; Table S1) is also an important absorbing phase of ambient polyol tracers in Nanjing." (Page 19, lines 444-450)

(19) Line 412: efflorescence RH is more relevant than DRH in this scenario

Response:

Here, we deleted the original explanation, and changed the original expression into

"The log ($K^t_{H,w}/K^m_{H,e}$) data increased faster when $c_{sulfate}$ approached 0, and deviated from their expected behavior with increased $c_{sulfate}$. Kampf et al. (2013) selected a threshold $c_{sulfate}$ of 12 mol kg^{-1} ALWC to illustrate the deviation for chamber experiments, and attributed it to elevated viscosity and slow particle-phase reactions at high $c_{sulfate}$." (Pages 22, lines 521-525)

(20) Line 462-463: delete "barely" and revise sentence accordingly

Response:

The original expression was changed into

"Then gas-particle partitioning of polyol tracers should have little influence on source apportionment based on particle-phase data in Nanjing." (Page 24, lines 564-566)

(21) Line 465: not sure what exactly is a "concern"? clarification needed

Response:

The whole sentence was deleted.

(22) Line 478: delete "pre-"

Response:

It was deleted as suggested. (Page 25, line 579)

References

Ahrens, L., Shoeib, M., Harner, T., Lane, D. A., Guo, R., and Reiner, E. J.: Comparison of annular diffusion denuder and high volume air samplers for measuring per- and polyfluoroalkyl substances in the atmosphere, Anal. Chem., 83, 9622-9628, 10.1021/ac202414w, 2011.

Isaacman-VanWertz, G., Yee, L. D., Kreisberg, N. M., Wernis, R., Moss, J. A., Hering, S. V., de Sá, S. S., Martin, S. T., Alexander, M. L., Palm, B. B., Hu, W., Campuzano-Jost, P., Day, D. A., Jimenez, J. L., Riva, M., Surratt, J. D., Viegas, J., Manzi, A., Edgerton, E., Baumann, K., Souza, R., Artaxo, P., and Goldstein, A. H.: Ambient gas-particle partitioning of tracers for biogenic oxidation, Environ. Sci. Technol., 50, 9952-9962, 10.1021/acs.est.6b01674, 2016.

Peters, A. J., Lane, D. A., Gundel, L. A., Northcott, G. L., and Jones, K. C.: A comparison of high volume and diffusion denuder samplers for measuring semivolatile organic compounds in the atmosphere, Environ. Sci. Technol., 34, 5001-5006, 10.1021/es000056t, 2000.

Pye, H. O. T., Zuend, A., Fry, J. L., Isaacman-VanWertz, G., Capps, S. L., Appel, K. W., Foroutan, H., Xu, L., Ng, N. L., and Goldstein, A. H.: Coupling of organic and inorganic aerosol systems and the effect on gas–particle partitioning in the southeastern US, Atmos. Chem. Phys., 18, 357-370, 10.5194/acp-18-357-2018, 2018.

Xie, M., Hannigan, M. P., and Barsanti, K. C.: Gas/particle partitioning of n-alkanes, PAHs and oxygenated PAHs in urban Denver, Atmos. Environ., 95, 355-362, http://dx.doi.org/10.1016/j.atmosenv.2014.06.056, 2014a.

Xie, M., Hannigan, M. P., and Barsanti, K. C.: Gas/particle partitioning of 2-methyltetrols and levoglucosan at an urban site in Denver, Environ. Sci. Technol., 48, 2835-2842, 10.1021/es405356n, 2014b.

Zhao, Y., Kreisberg, N. M., Worton, D. R., Isaacman, G., Weber, R. J., Liu, S., Day, D. A., Russell, L. M., Markovic, M. Z., VandenBoer, T. C., Murphy, J. G., Hering, S. V., and Goldstein, A. H.: Insights into secondary organic aerosol formation mechanisms from measured gas/particle partitioning of specific organic tracer compounds, Environ. Sci. Technol., 47, 3781-3787, 10.1021/es304587x, 2013.

Zuend, A., and Seinfeld, J. H.: Modeling the gas-particle partitioning of secondary organic aerosol: the importance of liquid-liquid phase separation, Atmos. Chem. Phys., 12, 3857-3882, 10.5194/acp-12-3857-2012, 2012.

This study by Chao Qin et al. reports on filter-based measurements of the gas–particle partitioning of a selection of semi-volatile isoprene oxidation products, levoglucosan and polyols in Nanjing, China. Detailed simultaneous gas and particle phase measurements and assessments of the gas–particle partitioning and influence of aerosol liquid water are relatively scarce. Therefore, this manuscript and the measured data are certainly of interest to the atmospheric chemistry and physics community.

Overall, the manuscript is well written, of adequate lengths and with useful tables and figures. The field sampling and chemical quantification conducted over an extended time span are valuable. The comparison to different predictions by equilibrium gas–particle partitioning models/assumptions is of interest, but it also reveals several issues that need to be addressed.

My main concern is with the provided level of detail on the **uncertainties of the measurements and the theoretical predictions,** as outlined in the general and specific comments below. This manuscript should be (and can be) substantially improved by adding a better discussion and quantification of uncertainties and potential systematic biases as well as clarifications about partitioning mechanisms and involved assumptions. In the present manuscript, the partitioning model discussion is rather confusing, since the title and text suggest a fundamental difference between "absorptive partitioning" and Henry's law partitioning, not recognizing that Henry's law is a way of expressing equilibrium (absorptive) gas–liquid partitioning.

Response:
    Thanks for the reviewer's comments, and we will reply these point by point in the reviewers' specific comments.

General comments
    The discussion of the presented mismatch between measured and predicted partitioning of several organic tracers in this manuscript would strongly benefit from a more thorough, quantitative uncertainty analysis of the filter measurements and of the assumptions made with the "theoretical" predictions of partitioning coefficients. This would likely lead to relatively wide error bounds on the median and average partitioning coefficients listed in the tables. At present, the study suggests that there is poor agreement with absorptive (Raoult's law) partitioning as well as with solubility-based physical Henry's law partitioning. However, there seem to be substantial uncertainties in the predictions applied and assumptions involved (see the specific comments below).

    A comparison to other studies involving the same or similar compounds should be included. The work by Pye et al. (2018) focuses on measurements and conditions in the southeastern United States and includes field measurements and equilibrium partitioning calculations for several polyols and organic acids in common with this study by Qin et al. Pye et al. (2018) also assessed partitioning of 2-methyltetrol, C5 alkene triol, levoglucosan, pinonic acid and other semivolatile compounds. The Pye et al. work includes predicted or assumed liquid–liquid phase separation cases that differ in phase composition from the assumptions made in this study. Importantly, their results show generally a much better agreement between predicted and measured particle phase fractions. Therefore, it is recommended that the authors compare their findings with those from the Pye et al. study and discuss potential reasons for discrepancies in the

partitioning coefficients and their predictability (or that of particle phase fractions).

 Response:

    In the revised manuscript, we defined three gas-particle partitioning cases. *Case 1* assumed that the particulate OM was the only absorbing material in aerosols based on the equilibrium absorptive partitioning theory. Solubility of polyol tracers in an aqueous phase was included in *Cases 2 and 3*, where water-soluble and water-insoluble OM partitioned into different liquid phases and a single OM phase, respectively. Moreover, measurement uncertainties and their influences on partitioning coefficients of gas versus organic/aqueous phases in aerosols were estimated. It was shown that the average relative uncertainties of measurements and calculated partitioning coefficients ranged from a few percent to ~50%, which corresponded to an uncertainty of less than ± 0.30 for their logarithm values. Although the variability of theoretical partitioning coefficients was large, we still obtained an improved agreement between measurement-based and predicted gas-organic partitioning coefficient ($K_{p,OM}$) for *Cases 2* and *3*. So, aerosol liquid water should have substantial influences on gas-particle partitioning of target polyol tracers in this work.

    The interactions of organic and inorganic compounds in the aqueous phase were expected to increase the partitioning of highly water-soluble compounds into the condensed phase (Kroll et al., 2005; Ip et al., 2009; Kampf et al., 2013; Pye et al., 2018). Then the effective Henry's law constants ($K_{H,e}$, mol m^{-3} atm^{-1}) of target polyol compounds in aerosols should be greater than those in pure water ($K_{H,w}$). In the revised manuscript, predicted $K_{H,w}$ values from EPI and SPARC estimates varied by several orders of magnitude. Literature $K_{H,w}$ values were closer to those of 2-methyltetrols and levoglucosan estimated by EPI, while the predicted $K_{H,w}$ with SPARC was unreasonably larger than $K_{H,e}$. So, $K_{H,w}$ values based on EPI estimates were used for further data analysis. Because the "salting-in" effect is a known phenomenon that is not likely linked with a specific physical or chemical mechanism, we made some possible explanations (e.g., reactive uptake) for the enhanced uptake of polyol tracers in aerosol liquid water.

    Pye et al. (2018) re-evaluated the measurement data of gas- and particle-phase oxygenated compounds in southeastern US using a thermodynamic equilibrium gas-particle partitioning model in two LLPS modes. The modeling work was based on the AIOMFAC model and programed inorganic-organic interactions and variations of activity coefficients as a function of liquid PM mixture composition. The resulting predictions captured both the average and diurnal variability of measured *F*% for polyol tracers, suggesting a necessity in obtaining time-resolved activity coefficients for the implementation of absorptive equilibrium partitioning model. In this study, partitioning coefficients of polyol tracers were calculated and predicted empirically assuming equilibrium between gas phase and organic/aqueous phases in aerosols. Moreover, particulate OM phase was presumed as an ideal solution in which the activity coefficient ζ_{OM} was equal to 1, and no organic-inorganic interactions were considered. So, the temporal variability of $K_{p,OM}$ was poorly predicted in this work, and the gap between $K_{H,e}$ and $K_{H,w}$ could not be explicitly interpreted. Details of the changes were provided in the revised manuscript and responses to specific comments below.

Specific comments

1. Lines 83 – 87: It is stated that an absorptive partitioning model (which one?) underestimated particle-phase concentrations of carbonyls by several orders of magnitude. Is the argument made by the authors here (from the given phrasing) that absorptive partitioning is an incorrect partitioning mechanism? If so, should it be adsorptive partitioning or what kind? This statement requires further clarification/discussion.

 For context, do you mean to say that (1) absorptive partitioning does not take place or (2) that the experiments are not measuring partitioning under equilibrium conditions or that (3) inadequate vapor pressures were used in the partitioning model or (4) something else? For example, could reactive uptake be at play (e.g. mentioned in the cited study by Healy et al., 2008). If the measurement/prediction mismatch is due to reactive uptake, it is questionable to blame absorptive partitioning for this, since that theory may still apply to the parent compound that is partitioning, but further reactions in the particle phase, like hydration of glyoxal, complex formation in presence of sulfate ions or reversible oligomerization may distort the understanding of what species and in what amount is partitioning. It may well be that absorptive equilibrium gas–particle partitioning applies to each of the individual species formed but cannot simply be assumed to be represented by the parent compound considered in the gas phase. Introducing an "effective" Henry's law coefficient can be used to account for the measured partitioning; however, that formulation is then simply a parameterization and not directly elucidating a physical or chemical mechanism.

Response:

 Thanks. Here we did not intend to state that the absorptive partitioning is an incorrect partitioning mechanism. The mismatch between measurement and prediction could be associated with inappropriate assumptions on absorbing phase (e.g., particulate OM only) and formation pathways (e.g., gas-phase oxidation).

 To make it clear, we changed the original expression into
 "In addition to absorptive partitioning to particulate OM after the formation of oxygenated organic compounds in gas phase, other formation pathways (e.g., reactive uptake) have been identified and are responsible for the large discrepancy between modeled and observed SOA loadings (Jang et al., 2002; Kroll et al., 2005; Perraud et al., 2012). Unlike non-polar species (e.g., *n*-alkanes, polycyclic aromatic hydrocarbons) and alkanoic acids that are well simulated (Simcik et al., 1998; Xie et al., 2014a; Yatavelli et al., 2014; Isaacman-VanWertz et al., 2016), particle-phase concentrations of carbonyls were underestimated by several orders of magnitude when particulate OM is presumed as the only absorbing phase in ideal condition (Healy et al., 2008; Kampf et al., 2013; Shen et al., 2018)." (Page 5, lines 104-114)
 In the original manuscript, the absorptive partitioning means partitioning between gas phase and particulate OM in aerosols; Henry's law partitioning corresponds to the equilibrium between gas phase and aerosol liquid water. We have clarified this throughout the manuscript.

2. Line 89: "favored the formation of pinonaldehyde"; do you mean "partitioning" instead of "formation"? The formation of pinonaldehyde (in the gas phase) is likely independent from aerosol water content.

3

Response:

Zhao et al. (2013) stated that the aerosol water plays a role in the formation of particle-phase pinonaldehyde in the atmosphere. This might be related to the water uptake. So, here we replaced "favored" with "played a role in". (Page 5, lines 116)

3. Line 100: The work by Volkamer et al. (2009) on effective Henry's law partitioning and aqueous phase chemistry could also be cited here and perhaps discussed in context of the findings from this study later in the article.

Response:

The work by Volkamer et al. (2009) has been cited here.

"An effective Henry's law coefficient ($K_{H,e}$, mol m^{-3} atm^{-1}) can be used to account for the measured partitioning between the gas phase and aerosol liquid water (Volkamer et al., 2009)." (Page 5-6, lines 124-126).

Volkamer et al. (2009) focused on the effect of seed chemical composition and photochemistry on SOA yields. They found that the WSOC photochemical reactions can cause increased SOA yield. So, this work was also cited later in the manuscript.

"Moreover, log ($K^{t}_{H,w}/K^{m}_{H,e}$) values of polyol tracers also negatively correlated with the aqueous-phase concentrations of WSOC (c_{WSOC}, Figure S6), but not NH_4^+ or NO_3^-. This dependence might be associated with the "like-dissolves-like" rule, or indicate the importance of aqueous-phase heterogeneous reactions (Hennigan et al., 2009; Volkamer et al., 2009)." (Pages 23-24, lines 552-556)

4. Line 133 – 135: From this description of the gas and aerosol measurements using filters in series, it is not clear how much the uptake of gaseous (semivolatile) organic compounds on accumulated aerosol mass loading of filter 1 (Qf) will contribute to the total concentration on the particle filter. Based on absorptive equilibrium partitioning theory, the accumulated condensed-phase aerosol mass on the first filter may shift the actual gas–particle partitioning in the ambient air to favor additional partitioning from the gas phase to the condensed phase on the filter while the sampling flow passes through the filter, thus possibly leading to a systematic particle phase mass concentration bias. Given the long sampling times, this may constitute a substantial bias. Were such potential issues quantified in controlled experiments? Please discuss.

Response:

Based on absorptive equilibrium partitioning theory, the partitioning coefficient of a certain compound between gas and particulate OM phases ($K_{p,OM}$, m^3 ug^{-1}) is defined as

$$K_{p,OM} = \frac{F/M_{OM}}{A} \qquad (1)$$

where F and A are (ng m^{-3}) are particle- and gas-phase concentrations, and M_{OM} (µg m^{-3}) is the mass concentration of particulate OM. It is assumed that the quantity F/M_{OM} (ng µg^{-1}) represents the equilibrium concentration in the particulate matter (Pankow and Bidleman, 1992; Liang et al., 1997).

4

In previous studies, $K_{p,OM}$ values based on offline measurements were typically obtained using sampling periods of many hours (e.g., 8, 12, or 24 h). When ambient concentrations (F, A, or M_{OM}) or temperature change within a sampling interval, the particulate OM initially collected on the filter will tend to re-equilibrate with the A value though evaporation or absorption. Then whether the accumulated aerosol mass will uptake or release gaseous organic compounds depends on how changes in F, A, M_{OM}, and ambient temperature take place. Measured values of F, A, and M_{OM} will be averages over the whole sampling period, not reflecting real-time atmospheric concentrations. Therefore, the situation raised in the comment seems not applicable to this study.

5. Line 152 – 154: "Concentrations of aerosol liquid water were predicted by ISORROPIA II model"; this prediction will only account for water uptake by inorganic ions but neglect any water uptake by hygroscopic organic compounds (such as some WSOC), right? It may therefore lead to an underestimation of the WSOC effect on organic partitioning. The authors could use a simple estimation based on typical organic hygroscopicity parameters (kappa) and the median or actual RH values to estimate the organic-contributed water content by the WSOC mass fraction in particles.

Response:

According to Isaacman-VanWertz et al. (2016), the water uptake by WSOC (W_O, μg m^{-3}) could be estimated as

$$W_O = \frac{V_{WSOC} \times [\kappa \times (O:C)]}{(\frac{100}{RH\%} - 1)} \qquad (2)$$

where V_{WSOC} represents WSOC volume, and is calculated as the organic mass (WSOC ×1.6) divided by its density (1.4 g cm^{-3}). The hygroscopicity parameter (κ) and oxygen to carbon ratio (O:C) of WSOC were assumed as 0.10 and 0.5, respectively, based on field and laboratory studies (Taylor et al., 2017; Cai et al., 2020). The resulting W_O had an average of 0.47 ± 1.14 μg m^{-3}, far below the amount caused by inorganic ions (21.3 ± 24.2 μg m^{-3}). Taylor et al. (2017) predicted a growth factor range of 1.00–1.20 with κ varying from 60 to ~100%, which lead to a comparable average W_O (0.42 ± 0.70 μg m^{-3}) in this work. Thus, the water content contributed by WSOC was not accounted for in this work.

We have clarified this in the revised manuscript and supplementary information. (Page 8, lines 180-182)

"The estimated water content contributed by hygroscopic WSOC was relatively small (< 1 μg m^{-3}) and not accounted for in this work (Text S1 of supplementary information)."

6. Line 209: I suggest adding these equations to the main text.

Response:

We have defined three partitioning cases and included these equations in the revised manuscript. (Pages 10 -13, lines 238-295)

"Here, we defined three partitioning cases to explore the influence of dissolution in aerosol liquid water on gas-particle partitioning of polyol tracers in the atmosphere. *Case 1* presumes instantaneous equilibrium between the gas phase and particulate OM

based on the equilibrium absorptive partitioning theory. In this case, particulate OM is assumed to be the only absorbing phase and behave as an ideal solution. Then the absorptive gas-particle partitioning coefficients ($K_{p,OM}$, m³ µg⁻¹) were calculated from measurements ($K^m_{p,OM}$) and predicted theoretically ($K^t_{p,OM}$) as follows

$$K^m_{p,OM} = \frac{F/M_{OM}}{A} \qquad (2)$$

$$K^t_{p,OM} = \frac{RT}{10^6 \overline{MW}_{OM} \zeta_{OM} p^o_L} \qquad (3)$$

where M_{OM} denotes the mass concentration of absorptive organic matter (OM = OC × 1.6; Turpin and Lim, 2001); F (ng m⁻³) and A (ng m⁻³) are particulate and gaseous concentrations of individual polyols, respectively. In eq 2, R (m³ atm K⁻¹ mol⁻¹) and T (K) are the ideal gas constant and ambient temperature; $\overline{MW}_{OM}$, average molecular weight of absorptive OM, is set at 200 g mol⁻¹ for all samples (Barsanti and Pankow, 2004; Williams et al., 2010); ζ_{OM} denotes the mole fraction scale activity coefficient, and is presumed to be unity for all species in each sample; p^o_L (atm) is the vapor pressure of each pure compound, and is predicted with several estimation tools and adjusted for each sampling interval based on the average temperature (Text S3 and Table S4).

Due to the influence of mixing state and water content in aerosols, several studies modeled the gas-particle partitioning of oxygenated organic compounds by defining a liquid-liquid phase separation (LLPS) in the aerosol (Zuend and Seinfeld, 2012; Pye et al., 2018). The organic-inorganic interactions and changes of activity coefficients in aqueous mixtures were fully considered as well. In this study, we proposed a simplified LLPS partitioning mechanism (*Case 2*) in Figure 1. First, aerosol water and water-insoluble OM (WIOM = OM – WSOC × 1.6) exist in two separate liquid phases, and WSOC and inorganic ions are totally dissolved in the aqueous phase. The distribution of polyol tracers between aqueous (F_W, ng m⁻³) and WIOM (F_{WIOM}, ng m⁻³) phases is simply depicted by their octanol-water partition coefficients (K_{OW})

$$K_{OW} = \frac{F_{WIOM}/V_{WSIOM}}{F_W/V_W} = \frac{c_{WIOM}}{c_W} \qquad (4)$$

where V_{WIOM} and V_W are volumes (m³) of WIOM and water in aerosols per cubic meter air; c_{WIOM} and c_W are solution concentrations (ng m⁻³) of polyols concentrations in organic and aqueous phases; log K_{OW} values of target polyols were estimated using the Estimation Programs Interface (EPI) Suite developed by the US Environmental Protection Agency and Syracuse Research Corporation (Table S4; US EPA, 2012). The density of organic matter and water (ρ_w) in aerosols are set at 1.4 and 1.0 g cm⁻³, respectively (Isaacman-VanWertz et al., 2016; Taylor et al., 2017). Second, gas-phase polyol tracers are in equilibrium with hydrophobic OM and the aqueous phase, respectively

$$K^m_{p,WIOM} = \frac{F_{WIOM}/M_{WIOM}}{A} \qquad (5)$$

$$K^m_{H,e} = \frac{\frac{F_W}{M_i}}{\frac{A}{M_i} \times R \times T \times \frac{c_{ALW}}{\rho_w}} = \frac{\rho_w \times F_W}{A \times R \times T \times c_{ALW}} \qquad (6)$$

where $K^m_{H,e}$ (mol m⁻³ atm⁻¹) is the measurement-based effective Henry's law coefficient; M_{WIOM} represents the mass concentration (µg m⁻³) of WIOM; M_i (g mol⁻¹) is the molecular weight of specific compound; c_{ALW} (µg m⁻³) is the mass concentration of aerosol liquid water predicted using ISORROPIA II model. *Case 3* is generally the same as *Case 2*, and the only difference is that water-soluble OM (WSOM) and WIOM exist in a single organic phase. Here total particulate OM was used instead of WIOM to assess the distribution of polyol tracers between aqueous and organic phases, and

calculate partitioning coefficients of gas vs. particulate organic ($K^m_{p,OM}$) and aqueous ($K^m_{H,e}$) phases. Note that the polarity of particulate OM phase in *Case 3* was expected to increase, then using K_{OW} to calculate the distribution of polyols between organic and aqueous phases might lead to underestimated $K^m_{p,OM}$ and overestimated $K^m_{H,e}$. For comparison purposes, the Henry's law coefficient in pure water at 25 °C ($K^*_{H,w}$) was estimated using EPI and SPARC (Hilal et al., 2008; http://archemcalc.com/sparc-web/calc), respectively (Table S4), and was adjusted for each sampling interval due to the changes in ambient temperature using van 't Hoff equation (Text S4)."

7. Line 212: If I understand your procedure, the ISORROPIA-derived aerosol water content is not accounting for water associated with WSOC, which could be substantial at high RH and when the WSOC represent a significant mass fraction of aerosol. Also, actual interactions among organics and ions within particle phases may affect the partitioning (both between liquid phases and gas/particle), which I assume is ignored in this work. Furthermore, WSOC, while water-extractable by definition, can be of relatively moderate polarity and may preferably partition to the WIOM organic-rich phase in presence of dissolved salts in an aqueous phase (see e.g. Zuend et al., 2012; You et al., 2014; Pye et al. 2018). Hence, it would be useful to estimate errors from such effects on the determined K_{OW}. It may also be adequate to consider other liquid–liquid phase separation scenarios, such as assuming that all WIOM and WSOC organics partitioned to one aqueous organic phase and all inorganic salts to a separate aqueous inorganic phase (compare to Fig. 3 of Pye et al., 2018).

Response:

 As mentioned in responses to *Comment 5*, the estimated contribution of WSOC to aerosol liquid water is relatively small. In this study, gas-particle partitioning coefficients of polyol tracers were calculated and predicted empirically by assuming equilibrium between gas phase and organic/aqueous phases in aerosols, and the organic-inorganic interactions were not considered. This might be an important reason for the gap between measurement-based $K_{H,e}$ and predicted $K_{H,w}$. Pye et al. (2018) re-analyzed the measurement data from Isaacman-VanWertz et al. (2016) using a thermodynamic equilibrium gas-particle partitioning model in two LLPS modes, which involved inorganic-organic interactions and estimations of activity coefficients as a function of liquid PM mixture composition. The resulting predictions captured both the average and diurnal variations of measured *F*% for polyol tracers, suggesting a necessity in obtaining time-resolved activity coefficients for the implementation of absorptive equilibrium partitioning model. These discussions have been added in the revised manuscript. (Pages 19-20, lines 457-464)
 As suggested by the reviewer, we defined a third partitioning case assuming all WIOM and WSOC organics partitioned to a single organic phase (*Case 3*, see responses to *Comment 6*). However, the measurement-based partitioning coefficients of polyol tracers in *Case 3* are very close to those in *Case 2*, where WIOM and WSOC were assumed to partition into separate liquid phases. In the revised manuscript, we defined three gas-particle partitioning cases and re-analyzed the difference between measured and predicted partitioning coefficients. (Pages 10-13, lines 238-295, see responses to *Comment 6*; Sections 3.4 and 3.5 in the revised manuscript, Tables 1 and 2 below).

Table 1. Comparisons of measurement-based log $K_{p,OM}$ (m³ μg⁻¹) at three proposed cases and predicted values.

Species	No. of obs.	Log $K^m_{p,OM}$ [a]			Log $K_{p,OM}$ [b]			
		Case 1	Case 2	Case 3	EPI	EVAPORATION	SPARC	SIMPOL
Isoprene SOA tracers								
C5-alkene triol 1	53	0.33 ± 0.71	-0.79 ± 0.86	-0.82 ± 0.85	-3.09	-2.84	-1.19	-2.88
C5-alkene triol 2	63	0.15 ± 0.55	-1.02 ± 0.74	-1.05 ± 0.73	-3.62	-3.67	-4.14	-2.85
C5-alkene triol 3	83	0.35 ± 0.68	-0.83 ± 0.86	-0.86 ± 0.85	-2.90	-2.65	-1.00	-2.69
2-Methylthreitol	101	-0.12 ± 0.48	-2.09 ± 0.71	-2.09 ± 0.70	-1.87	-1.30	-1.18	-0.47
2-Methylerythritol	95	-0.011 ± 0.58	-1.96 ± 0.71	-1.96 ± 0.71	-1.90	-1.34	-1.22	-0.50
Biomass burning tracer								
Levoglucosan	65	2.23 ± 0.72	0.63 ± 0.90	0.62 ± 0.90	-0.04	-0.81	1.04	-0.76
Sugars ang sugar alcohols								
Meso-erythritol	31	0.87 ± 0.53	-1.43 ± 0.60	-1.43 ± 0.60	-0.65	-1.21	-0.45	
Fructose	85	0.65 ± 0.73	-1.20 ± 0.83	-1.20 ± 0.89	1.17	2.76	6.94	
Mannose	74	0.62 ± 0.71	-2.12 ± 0.95	-2.12 ± 0.95	1.28	2.13	4.77	
Glucose	88	0.42 ± 0.67	-2.77 ± 0.93	-2.77 ± 0.93	0.34	3.75	7.32	
Xylitol	22	0.24 ± 0.54	-2.61 ± 0.72	-2.61 ± 0.72	3.37	2.34	3.57	
Arabitol	30	1.46 ± 0.89	-1.35 ± 1.24	-1.35 ± 1.24	3.25	1.67	2.90	
Manitol	65	1.08 ± 0.63	-2.24 ± 0.95	-2.24 ± 0.95	2.33	4.16	6.68	

[a] Average ± standard deviation; [b] temperature range: -4~36 °C.

Table 2. Comparisons of measurement-based log $K_{H,e}$ (mol m⁻³ atm⁻¹) and predicted log $K_{H,w}$ of individual polyol tracers.

Species	No. of obs.	Log $K^m_{H,e}$ (Cases 2) [a]			Log $K_{H,w}$ [b]	
		Median	Average	Range	EPI	SPARC
Isoprene SOA tracers						
C5-alkene triol 1	53	14.0	13.9 ± 0.86	11.5 – 16.4	7.22	11.7
C5-alkene triol 2	63	13.7	13.6 ± 0.73	11.2 – 16.1	7.34	7.66
C5-alkene triol 3	83	13.9	13.8 ± 0.85	10.6 – 16.1	7.43	11.9
2-Methylthreitol	101	13.4	13.3 ± 0.70	10.9 – 14.8	10.0	14.1
2-Methylerythritol	95	13.5	13.5 ± 0.71	11.6 – 15.6	9.95	14.1
Biomass burning tracer						
Levoglucosan	65	15.7	15.7 ± 0.90	13.2 – 17.3	13.4	16.1
Sugars ang sugar alcohols						
Meso-erythritol	31	14.5	14.4 ± 0.60	12.8 – 15.6	9.65	13.8
Fructose	85	14.2	14.1 ± 0.89	11.9 – 16.5	14.7	19.9
Mannose	74	14.0	14.1 ± 0.94	12.1 – 16.8	10.9	18.8
Glucose	88	13.9	13.9 ± 0.93	11.3 – 16.3	14.7	20.9
Xylitol	22	13.8	13.7 ± 0.72	12.6 – 15.0	12.1	18.1
Arabitol	30	15.1	15.0 ± 1.23	13.0 – 18.2	11.3	17.4
Mannitol	65	14.6	14.5 ± 0.94	12.1 – 16.4	12.9	20.8

[a] Log $K^m_{H,e}$ values of *Case 3* had ignorable difference, and were not exhibited separately; [b] temperature range: -4~36 °C.

8. Lines 221 – 222: The rather low octanol–water partitioning coefficients indicate not only better solubility in water but also that the polyols of moderate to high polarity have low solubility in octanol; this is because octanol is a rather low polarity medium as choice for representing organic aerosol. SOA-rich phases may be of substantially higher polarity than octanol yet still form a separate phase from an aqueous salt-rich phase (e.g. You et al., 2014). This should be acknowledged, and consequences of partitioning assumptions considered in the uncertainty analysis.

Response:

As we mentioned in responses to the general comment and specific comment 6, three partitioning cases were proposed in the revised manuscript. In the newly defined *Case 3* where WIOM and WSOC organics partitioned to a single organic phase, the solubility of polyol tracers in the organic phase was expected to increase, and using K_{OW} to calculate the distribution between organic and aqueous phases in aerosols would lead to an underestimation of $K_{p,OM}$, which might not be reasonably adjusted. This was acknowledged in the revised manuscript.

Pages 12-13, lines 288-291.

"Note that the polarity of particulate OM phase in *Case 3* was expected to increase, then using K_{OW} to calculate the distribution of polyols between organic and aqueous phases might lead to underestimated $K^m_{p,OM}$ and overestimated $K^m_{H,e}$."

9. Line 224 and SI Eq. (2), Text S2: In the SI, it is stated that for the absorptive partitioning prediction an average organic molar mass MWOMof 200 g/mol was used. This seems to be a common and reasonable assumption, but only for a water-free organic absorbing phase. However, for the partitioning of WSOC compounds when assumed to prefer the aqueous phase, one should account for the low molar mass of water present in substantial amounts in that phase, which would lower the weighted mean molar mass significantly (Liu et al., 2021; Gorkowski et al. 2019). Please consider this and, where applicable, correct the estimated partitioning coefficients.

Response:

Among the three proposed partitioning cases in the revised manuscript, *Case 1* assumed that the particulate OM was the only absorbing material in aerosols, ignoring the influence of aerosol liquid water. While in *Cases 2* and *3*, particulate OM and aerosol liquid water were assumed to exist in separate liquid phases, and there was no phase distribution of water. By comparing measurement-based and predicted partitioning coefficients for different cases, we inferred that the aerosol liquid water should play a significant role in influencing gas-particle partitioning of polyol tracers (Table 1, see responses to *Comment 7*). An enhanced uptake of polyol tracers was also identified, which should be closely associated with the organic-inorganic interactions.

In this study, the particulate organic phase was assumed to contain no water, and partitioning of gaseous polyols to organic and aqueous phases in aerosols were assessed separately. So, the influence of water content on molecular weight of particulate organic matter (MW_{OM}) was not considered.

10. Line 233: Use of the EPI suite estimations should be considered uncertain by about one order of magnitude (or more in certain cases) for predictions involving multifunctional semivolatile compounds. A comparison to other estimation methods for physical Henry's law constants (and their estimated uncertainties) may provide some information on the reliability of this method.

Response:

Thanks. We also obtained Henry's law constants of polyols in pure water at 25 ºC

($K^*_{H,w}$) from SPARC (Hilal et al., 2008; http://archemcalc.com/sparc-web/calc) estimates and literatures (Table S4).

   Although the $K^*_{H,w}$ (mol m^{-3} atm^{-1}) from EPI and SPARC differed by several orders of magnitude, literature values of isoprene SOA and levoglucosan were closer to the estimates of EPI (Table S4). If SPARC $K^*_{H,w}$ values were used, the average log $K^m_{H,e}$ of most polyol tracers would be lower than predictions (log $K^t_{H,w}$, Table 2; see responses to *Comment 7*), indicating that the aqueous phase of ambient aerosol is less hospital to polyol tracers than pure water. This is in conflict with the fact that the interactions of organic compounds, water, and inorganic ions in aerosols will increase the partitioning of highly oxygenated compounds (O:C $\geqslant$ 0.6; e.g., isoprene SOA tracers and levoglucosan) into the particle phase (Pye et al., 2018). Several studies identified a close relationship between salt concentrations of aerosol water and enhanced uptake of very polar compounds (Kroll et al., 2005; Ip et al., 2009; Kampf et al., 2013). Thus, log $K^t_{H,w}$ values of EPI estimates were used for further data analysis. (Pages 20-21, lines 482-494)

11. Line 328 – 332: Why was a linear regression/relationship used? Partitioning theory would suggest that it should be a sigmoidal relationship (if applicable), e.g. O'Meara at al (2014); Donahue et al. (2009). However, the partitioning of a specific compound will also depend on the condensed phase absorbing mass concentration (in organic or aqueous phase, as appropriate) and on non-ideality, such as presence of phase separation. Given that only particle phase fraction data above ~80% were determined from the measurements, the expected sigmoidal relationship is perhaps not clear from the data alone.

Response:

   Thanks. The original Figure 2 (now Figure 3) and associated discussions was changed considering the uncertainties in measurements
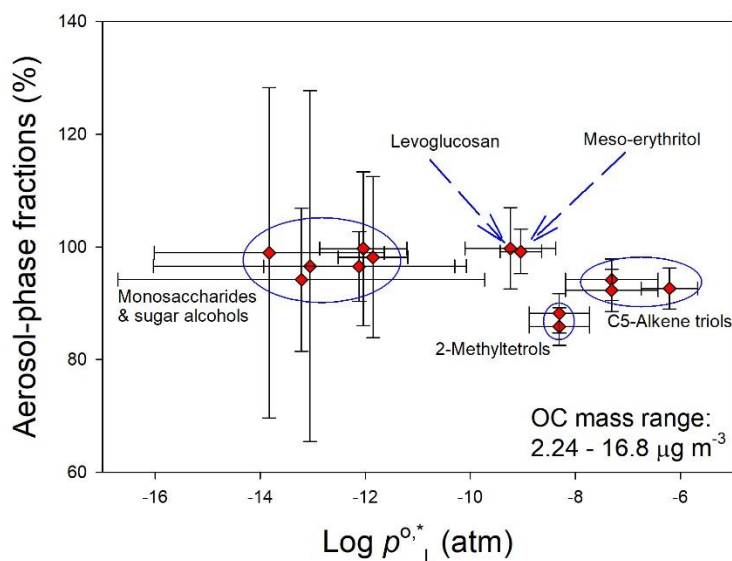

Figure 3. Average particle-phase fractions and log $p^{o,*}_L$ of individual polyol tracers. Whiskers represent uncertainties of *F*% and one standard deviation of log $p^{o,*}_L$ derived from different estimation tools.

Pages 17-18, lines 410-419

"In Figure 3, the average $F\%$ uncertainties (6.16–31.2%) of monosaccharides (e.g., fructose) and sugar alcohols (e.g., mannitol) were larger than those of isoprene SOA tracers and levoglucosan (3.33–7.24%) due to their low and variable recoveries (Table S2) and excessive breakthrough (Figure S2). However, the estimated uncertainties of $F\%$ for less volatile polyols ($p^{o,*}_L <$ ~10^{-10} atm) were not physically meaningful, as more than 95% of these compounds existed in the particle phase. Considering the uncertainties in $F\%$ and log $p^{o,*}_L$ and high average $F\%$ (> 85%) of target polyol tracers, a dependence of $F\%$ on the vapor pressure could not be determined, and the seasonality and day-night difference ($p > 0.05$) of $F\%$ were obscured."

12. Line 334: "their F% values did not show seasonality or day-night difference";

The range of particle phase fractions observed may not allow for such conclusions if the material is predominantly in the particle phase. Uncertainties in the measurements and temperature dependence of the vapor pressures may mask actual variations.

Response:

The original expression has been changed. See responses to *Comment 11* (Pages 17-18, lines 410-419).

13. Lines 339 – 340: "Thus, the changes in vapor pressures with the ambient temperature might not be the main factor driving gas-particle partitioning of polyol tracers in northern Nanjing."

What about variations in organic aerosol mass concentrations as additional influence?

Response:

Thanks. Xie et al. (2014) found that the gas-particle partitioning of 2-methyltetrols and levoglucosan in urban Denver were dependent on the variations in ambient temperature and absorbing organic matter (M_{OM}). So, the original expression was changed into

"Thus, the changes in vapor pressures with the ambient temperature and/or particulate OM loadings might not be the main factors driving gas-particle partitioning of polyol tracers in Nanjing." (Page 17, lines 408-410)

14. Line 360: The re-evaluation of the SV-TAG measurements by Isaacman-VanWertz et al. (2016) in the study by Pye et al. (2018) (see their Fig. 5) involving other models, considerations of vapor pressure adjustments and additional measurement comparisons, shows that higher and lower particle phase fractions were predicted, but that generally the agreement between models and observed F% were consistent across a selection of tracers and much better than the orders of magnitude differences reported in this manuscript.

Response:

When the dissolution of polyols in aerosol water was included, the agreement

between measurement-based and predicted partitioning coefficients of gas vs organic phases ($K_{p,OM}$) were improved substantially. However, the variability of gas-particle partitioning was poorly predicted. The study by Pye et al. (2018) was cited and discussed to explain the discrepancy between measurements and predictions. (Pages 19-20, lines 450-464)

"Similarly, the measured average $F\%$ of isoprene SOA tracers in southeastern US and central Amazonia were higher than predictions by assuming instantaneous equilibrium between the gas phase and particulate OM only, and the agreement was improved when parameterization of solubility was included for predictions (Isaacman-VanWertz et al., 2016). But none of these two studies could reasonably predict the temporal variability of $F\%$ or log $K^m_{p,OM}$. One possible explanation is that the activity coefficients of isoprene SOA tracers and levoglucosan deviate from unity (0.42–2.04; Pye et al., 2018) and vary with PM composition. Pye et al. (2018) re-analyzed the measurement data from Isaacman-VanWertz et al. (2016) using a thermodynamic equilibrium gas-particle partitioning model in two LLPS modes, which involved organic-inorganic interactions and estimations of activity coefficients as a function of liquid PM mixture composition. The resulting predictions captured both the average and diurnal variations of measured $F\%$ for polyol tracers, suggesting a necessity in obtaining time-resolved activity coefficients for the implementation of absorptive equilibrium partitioning model."

15. Lines 364 – 367: These statements are misleading and need to be rephrased. Henry's law partitioning is a form of absorptive partitioning (in contrast to adsorptive partitioning). In the case of SVOCs and LVOCs, the difference between vapor–liquid equilibrium and liquid-phase mixing described by using Raoult's law or Henry's law (when accounting for non-ideal mixing) is essentially a matter of choice of reference state (while for non-vapor gases only Henry's law can be applied).

The observed large differences between measurements and different predictions could be the result of a combination of issues and uncertainties associated with the measurements and the models used. If reactive uptake is considered to be the key difference between predictions and measurements, this should be clarified.

Response:

Thanks. In the revised manuscript, the absorptive partitioning of gaseous polyols to organic and aqueous phases in aerosols were clearly distinguished, and uncertainties of measurements and predictions and their influences on the calculation of partitioning coefficients were estimated.

Through the comparisons of measurement-based and precited $K_{p,OM}$ before and after the inclusion of polyols dissolution in aerosol water, we inferred that the aerosol liquid water is also an important absorbing phase of ambient polyol tracers in Nanjing. The large gaps of $K^m_{H,e}$ versus $K^t_{H,w}$ could be partly parameterized using the equation defining "salting-in" effects. However, the "salting-in" effect is a known phenomenon that is not likely linked with a specific physical or chemical mechanism. According to existing studies, reactive uptake, aqueous phase reactions, and chemical similarity between partitioning species and the absorbing phase might be responsible for increasing the partitioning of polyol tracers into the condensed phase. In the revised manuscript, we have re-organized and re-written most of the discussions on comparisons between measured and predicted partitioning coefficients. (Sections 3.4

and 3.5, Pages 18-23, lines 420-560).

Here are some discussions on mechanisms related to the gap between $K^m_{H,e}$ and $K^t_{H,w}$. (Pages 23-24, lines 534-560)

"However, the "salting-in" effect is a known phenomenon that is not likely linked with a specific physical or chemical mechanism. Quantum chemical calculation results indicated negative Gibbs free energy of water displacement for interactions between SO_4^{2-} and glyoxal monohydrate (Waxman et al., 2015). The net "salting-in" effect of 1-nitro-2-naphthol in NaF solution was interpreted by postulating hydrogen bonding (Almeida et al., 1983). A direct binding of cations to ether oxygens was proposed to be responsible for the increased solubility of water-soluble polymers (Sadeghi and Jahani, 2012). Due to the moderate correlations and negative intercepts in Figures 4 and S5, the gap between $K^t_{H,e}$ and $K^m_{H,w}$ cannot be closed by the "salting-in" effect alone. Shen et al. (2018) also obtained negative intercepts when plotting log $(K^t_{H,w}/K^m_{H,e})$ over $c_{sulfate}$ for glyoxal and methylglyoxal in ambient atmosphere, and attributed this to unknown gas-particle partitioning mechanisms. Evidences showing that the thermal degradation of less volatile oligomers and organosulfates can lead to an overestimation of 2-methyltetrols by 60–188% when using a conventional GC/EI-MS method (Cui et al., 2018). To fit the gas-particle distribution of 2-methyltetrols in southeastern US, 50% of particulate 2-methyltetrols was presumed to exist in chemical forms with much lower vapor pressures by Pye et al. (2018). So, the reactive uptake and aqueous phase chemistry could be explanations for the enhanced uptake of isoprene SOA tracers. Moreover, log $(K^t_{H,w}/K^m_{H,e})$ values of polyol tracers also negatively correlated with the aqueous-phase concentrations of WSOC (c_{WSOC}, Figure S6), but not NH_4^+ or NO_3^-. This dependence might be associated with the "like-dissolves-like" rule, or indicate the importance of aqueous-phase heterogeneous reactions (Hennigan et al., 2009; Volkamer et al., 2009). Although several studies have estimated Henry's law constants for a variety of polar organic compounds in pure water (e.g., polyols and polyacids; Compernolle and Müller, 2014a, b), more work is warranted to decrease the estimation uncertainty and explain their increased partitioning toward aerosol liquid water explicitly."

16. Lines 387 – 389: The statements on these lines seem to support the conclusion that absorptive partitioning may be applicable to describing the partitioning of these isoprene SOA tracers, but only if one uses the "appropriate" absorbing organic phase mass in the estimation of the measured Kp values (and given the uncertainty in the vapor pressures and activity coefficients, this seems to be reasonable). The phrasing could be improved to make that point.

Response:

Yes, the agreement between measurement-based and predicted $K_{p,OM}$ will be significantly improved when the "appropriate" absorbing organic phase is used.

To make it clear, we defined three partitioning cases in the revised manuscript. *Case 1* assumed that the particulate OM was the only absorbing material in aerosols based on the equilibrium absorptive partitioning theory. Solubility of polyol tracers in an aqueous phase was included in *Cases 2 and 3*, where water-soluble and water-insoluble OM partitioned into different liquid phases and a single OM phase, respectively. We found a much better agreement between measurement-based and precited $K_{p,OM}$ after considering polyols dissolution in aerosol liquid water, indicating

that aerosol liquid water is also an important absorbing phase of ambient polyols in Nanjing.

Pages 18-19, lines 421-450

"To understand if particulate OM is the only absorbing phase in aerosols for polyol tracers in Nanjing, the absorptive partitioning coefficients of gas vs. organic phases were calculated based on measurement results ($K^m_{p,OM}$) for predefined *Cases 1-3* and predicted theoretically ($K^t_{p,OM}$) using eq. 3 and vapor pressures listed in Table S4. In Table 1, $K^t_{p,OM}$ ranges of isoprene SOA tracers, levoglucosan, and meso-erythritol are within two orders of magnitude, while those of monosaccharides and mannitol are larger ($> 10^3$).When particulate OM was assumed as the only absorbing phase (*Case 1*), the average $K^m_{p,OM}$ of isoprene SOA tracers, levolgucosan, and meso-erythritol were more than 10 times greater than most of their $K^t_{p,OM}$ (Table 1), and this difference was not likely susceptible to measurement uncertainties. As shown in Table S5, the average relative uncertainties of measurement-based partitioning coefficients are all <50%, leading to an uncertainty of log $K^m_{p,OM}$ less than ± 0.30.. ……………………………………………

When solubility in aerosol liquid water was considered by defining a LLPS in ambient aerosols, and whenever WSOM and WIOM partitioned into separate (*Case 2*) or single (*Case 3*) phases, the average log $K^m_{p,OM}$ of the above mentioned compounds became much closer to or even lay within the range (levoglucosan) of log $K^t_{p,OM}$ (Table 1). These results indicated that the aerosol liquid water ($21.3 ± 24.2$ µg m^{-3}; Table S1) is also an important absorbing phase of ambient polyol tracers in Nanjing."

17. Lines 415 – 421: The finding that the intercept in Fig. 3 of the linear regression does not go through 0.0 indicates that there are substantial uncertainties, making this comparison far less convincing. The scatter in the data is large, also hinting at salting-in as an effect alone does not seem to be a good explanation of the deviations between predicted and measurement-derived Henry's law partitioning. The authors also mention this on lines 445 – 448. There may be other confounding factors that happen to correlate with sulfate concentration; leading to a spurious conclusion of a causal salting-in effect that is not strongly supported by the provided evidence. For example, the ratio of WIOC to WSOC organic material may correlate with sulfate concentrations since sulfate and ammonia amounts will affect and respond to aerosol pH, which may also correlate with RH and absolute ALWC (Pye et al., 2020). Did the authors consider this?

Furthermore, a salting-in of polyols by sulfate is a finding that would be contrary to other studies on liquid–liquid phase partitioning involving polyols and ammonium sulfate, e.g. see Table 1 of Marcolli and Krieger (2006). In the study by Marcolli and Krieger (2006), ammonium sulfate led to salting-out while ammonium nitrate was found to show a salting-in effect on polyols. However, the complexity of the samples from Nanjing, where perhaps acidity and other aerosol components affect uptake, may differ from those in laboratory experiments by Marcolli and Krieger. Please discuss your findings of potential reasons for the model–measurement discrepancies and sulfate influence also in comparison to findings on salting-in/out from those studies.

Response:

Although the "salting-in" effect has been known for a long time, it is poorly characterized at high salt concentrations and is not understood mechanistically. The

"salting-in" effect could be considered as a phenomenon that is not specifically linked with a physical or chemical mechanism. So, the equation defining "salting-in" effects was only used to parameterize the enhanced uptake of polyols in aerosol liquid water. In the revised manuscript, we provided some guesses on mechanisms related to the "salting-in" effect from previous work and other explanations for increased partitioning to the particle phase.

Pages 23-24, lines 534-560

"However, the "salting-in" effect is a known phenomenon that is not likely linked with a specific physical or chemical mechanism. Quantum chemical calculation results indicated negative Gibbs free energy of water displacement for interactions between SO_4^{2-} and glyoxal monohydrate (Waxman et al., 2015). The net "salting-in" effect of 1-nitro-2-naphthol in NaF solution was interpreted by postulating hydrogen bonding (Almeida et al., 1983). A direct binding of cations to ether oxygens was proposed to be responsible for the increased solubility of water-soluble polymers (Sadeghi and Jahani, 2012). Due to the moderate correlations and negative intercepts in Figures 4 and S5, the gap between $K^{t}_{H,e}$ and $K^{m}_{H,w}$ cannot be closed by the "salting-in" effect alone. Shen et al. (2018) also obtained negative intercepts when plotting log $(K^{t}_{H,w}/K^{m}_{H,e})$ over $c_{sulfate}$ for glyoxal and methylglyoxal in ambient atmosphere, and attributed this to unknown gas-particle partitioning mechanisms. Evidences showing that the thermal degradation of less volatile oligomers and organosulfates can lead to an overestimation of 2-methyltetrols by 60–188% when using a conventional GC/EI-MS method (Cui et al., 2018). To fit the gas-particle distribution of 2-methyltetrols in southeastern US, 50% of particulate 2-methyltetrols was presumed to exist in chemical forms with much lower vapor pressures by Pye et al. (2018). So, the reactive uptake and aqueous phase chemistry could be explanations for the enhanced uptake of isoprene SOA tracers. Moreover, log $(K^{t}_{H,w}/K^{m}_{H,e})$ values of polyol tracers also negatively correlated with the aqueous-phase concentrations of WSOC (c_{WSOC}, Figure S6), but not NH_4^+ or NO_3^-. This dependence might be associated with the "like-dissolves-like" rule, or indicate the importance of aqueous-phase heterogeneous reactions (Hennigan et al., 2009; Volkamer et al., 2009). Although several studies have estimated Henry's law constants for a variety of polar organic compounds in pure water (e.g., polyols and polyacids; Compernolle and Müller, 2014a, b), more work is warranted to decrease the estimation uncertainty and explain their increased partitioning toward aerosol liquid water explicitly."

As shown in the Figure below, concentrations of sulfate do not correlate with WIOC/WSOC ratios, RH, or ALWC in this work, so the condition raised in the comment was not considered.
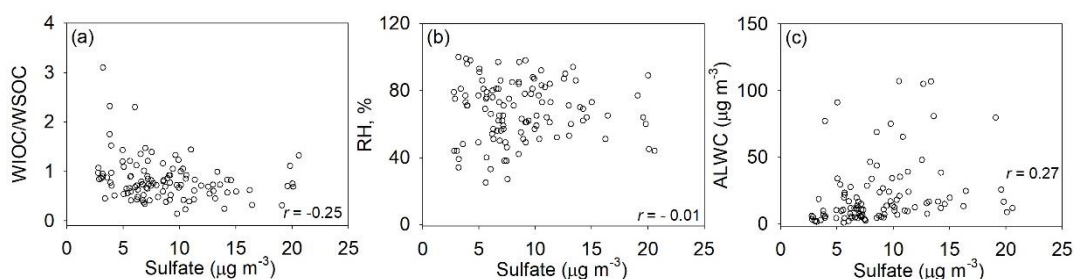
Marcolli and Krieger (2006) found that ammonium sulfate (AS) and NaCl are "salting-out" agent for alcohols with medium hydrophilicity, including glycerol, 1,4-butanediol, 1,2-hexanediol, and PEG400. But all the target polyols in this study are

highly water soluble, and there is no evidence showing that AS is salting out agent for any of the polyols studied in this work. A number of studies identified a close relationship between salt concentrations of aerosol water and enhanced uptake of very polar compounds (Setschenow 1889; Almeida et al., 1983; Kroll et al., 2005; Ip et al., 2009; Kampf et al., 2013; Shen et al., 2018). The particle-phase interactions of organic compounds, water, and inorganic ions were found to increase partitioning of isoprene SOA tracers and levoglucosan into the condensed phase (Pye et al., 2018). Since none of the polyol compounds in Marcolli and Krieger (2006) was studied in this work, the moderate dependence of increased uptake on sulfate concentrations is not contrary to their findings, and we did not compare the study results between these two studies.

In the revised manuscript, we re-organized section 3.5 (*Partitioning coefficients of gas versus aqueous phases*) and rewrote most part of it.

18. Lines 445 – 448: related to the previous comment, here the authors state that the large gap between KH,e and KH,w cannot be explained by salting-in by sulfate alone. This confirms my impression that the discussion about reasons of the substantial deviations is rather speculative. The presented analyses do not support a firm conclusion about absorptive or non-absorptive partitioning. Moreover, if the effective Henry's law coefficient obtained is due to reactive uptake and/or aqueous phase chemistry, such as oligomer formation, then enhanced particle-phase fractions would be a reasonable expectation. However, a key question would then be whether such chemistry would be reversible during the quantification of the filter material, such that an oligomerized species would appear as monomers, since otherwise it should not contribute to the parent species' particle phase amount. This reviewer would appreciate some discussion about this.

Response:

Reactive uptake is very likely contributing to increased partitioning of polyols into the particle phase. In the revised manuscript, we have clarified that the "salting-in" effect is a is a known phenomenon that is not specifically linked with a physical or chemical mechanism (Pages 23-24, lines 534-560, See responses to *Comments 15 and 17*).

The equation defining "salting-in" effects was only used to parameterize the enhanced uptake of polyols in aerosol liquid water (Pages 22-23, lines 517-533).

"As sulfate has been identified as the major factor influencing the salting effect of carbonyl species (Kroll et al., 2005; Ip et al., 2009), Figure 4 shows modified Setschenow plots for C5-alkene triols, 2-methyltetrols, and levoglucosan, where log ($K^t_{H,w}/K^m_{H,e}$) values were regressed to the molality of sulfate ion in aerosol liquid water ($c_{sulfate}$, mol kg^{-1} ALWC). The log ($K^t_{H,w}/K^m_{H,e}$) data increased faster when $c_{sulfate}$ approached 0, and deviated from their expected behavior with increased $c_{sulfate}$. Kampf et al. (2013) selected a threshold $c_{sulfate}$ of 12 mol kg^{-1} ALWC to illustrate the deviation for chamber experiments, and attributed it to elevated viscosity and slow particle-phase reactions at high $c_{sulfate}$. In Figure 4, negative correlations ($p < 0.01$) are observed at $c_{sulfate} < 12$ mol kg^{-1} ALWC, and Figure S5 exhibits significant negative correlations ($p < 0.01$) between log ($K^t_{H,w}/K^m_{H,e}$) and $c_{sulfate}$ for individual polyols even without excluding the deviations at high $c_{sulfate}$. The K_s values of polyol tracers from Figures 4 and S5 (-0.17 – -0.037 kg mol^{-1}) are in a similar range as that of glyoxal (-0.24 – -0.04 kg mol^{-1}; Kampf et al., 2013; Shen et al., 2018; Waxman et al., 2015). These results

indicated that the shifting of gas-particle equilibrium toward the condensed phase might be partly parameterized by the equation defining "salting-in" effects."

Moreover, we added some discussions about the influence of reactive uptake/aqueous chemistry on enhanced particle-phase concentrations. (Pages 23-24, lines 545-556)

"Evidences showing that the thermal degradation of less volatile oligomers and organosulfates can lead to an overestimation of 2-methyltetrols by 60–188% when using a conventional GC/EI-MS method (Cui et al., 2018). To fit the gas-particle distribution of 2-methyltetrols in southeastern US, 50% of particulate 2-methyltetrols was presumed to exist in chemical forms with much lower vapor pressures by Pye et al. (2018). So, the reactive uptake and aqueous phase chemistry could be explanations for the enhanced uptake of isoprene SOA tracers. Moreover, log ($K^t_{H,w}/K^m_{H,e}$) values of polyol tracers also negatively correlated with the aqueous-phase concentrations of WSOC (c_{WSOC}, Figure S6), but not NH_4^+ or NO_3^-. This dependence might be associated with the "like-dissolves-like" rule, or indicate the importance of aqueous-phase heterogeneous reactions (Hennigan et al., 2009; Volkamer et al., 2009)."

19. Table 1. Units of $K_{p,OM}$ should be provided; also state the temperature range for the values shown. Same for Table 2 and other such table in the Supplementary Information document.

Response:

Unites and temperatures were added in all related Tables as suggested (See responses to *Comment 7*).

20. Figure 2: Assuming a form of absorptive vapor–liquid equilibrium partitioning, the fraction in the particle phase of a semi-volatile organic will not only depend on the pure component vapor pressure but also on the aerosol mass concentration of the absorbing phase (and its composition). Therefore, it would make sense to state the aerosol mass concentration range that was used from the measurements. This would also allow for better comparison to other field measurements.

Response:

In this work, mass concentrations of OC were directly obtained from measurements, and were used for the calculation of $K_{p,OM}$. The concentration range of OC (2.24 – 16.8 µg m^{-3}) was added as suggested (now Figure 3, See responses to *Comment 11*).

Supplementary Information (SI):

21. Text S2: activity coefficients were assumed to be unity for all species in each sample. Is that a justified assumption? Consider that activity coefficients could be far from unity for compounds that are moderately polar (between the polarity of water and that of hydrophobic organics) used for characterizing the two particle phases in this work. This might contribute an order of magnitude of uncertainty for some compounds, but little

17

for others.

Response:

In this work, the organic phase in aerosols was assumed to behave as ideal solution, and the variability of activity coefficient as a function of PM composition was not considered. This should be one reason the variations of measurement-based $K_{p,OM}$ were poorly characterized in this work. Mean activity coefficients of isoprene SOA tracers and levoglucosan in organic-rich phases had a range of 0.42 to 2.04 based on AIOMFAC predictions (Pye et al., 2018), then assuming the activity coefficient to be unity will contribute an uncertainty far less than an order of magnitude.

We added some discussions to state the influence of variability in activity coefficients in the revised manuscript.

Pages 19-20, lines 450-464.

"Similarly, the measured average F% of isoprene SOA tracers in southeastern US and central Amazonia were higher than predictions by assuming instantaneous equilibrium between the gas phase and particulate OM only, and the agreement was improved when parameterization of solubility was included for predictions (Isaacman-VanWertz et al., 2016). But none of these two studies could reasonably predict the temporal variability of F% or log $K^m_{p,OM}$. One possible explanation is that the activity coefficients of isoprene SOA tracers and levoglucosan deviate from unity (0.42–2.04; Pye et al., 2018) and vary with PM composition. Pye et al. (2018) re-analyzed the measurement data from Isaacman-VanWertz et al. (2016) using a thermodynamic equilibrium gas-particle partitioning model in two LLPS modes, which involved organic-inorganic interactions and estimations of activity coefficients as a function of liquid PM mixture composition. The resulting predictions captured both the average and diurnal variations of measured F% for polyol tracers, suggesting a necessity in obtaining time-resolved activity coefficients for the implementation of absorptive equilibrium partitioning model."

22. Text S2, below Eq. (3): why is it the "subcooled" liquid vapor pressure? It would be sufficient to denote it as the liquid vapor pressure or liquid-state vapour pressure. Whether it is subcooled/supercooled at given temperature or just a "regular" liquid state does not matter.

Response:

The term "subcooled liquid vapor pressure" has been changed into "liquid-state vapor pressure".

23. Also, given the relatively large uncertainty associated with vapor pressure estimation methods (O'Meara et al., 2014), it may be advised to compare those values to predictions from other methods (e.g. using the UManSysProp online tools). Uncertainties in pure-component vapor pressures could contribute more than one order of magnitude of uncertainty to Kp estimates.

Response:

Thanks. Pure-compound vapor pressures were estimated using a variety estimation tools (EPI, Evaporation, SPARC, and SIMPOL; Table S4), and the resulting $K_{p,OM}$ predictions were compared with measurement-based values in Table 1 of the revised manuscript (See responses to *Comments 7*). Descriptions of the results and associated discussions were rewritten (Section 3.4).

Pages 18-19, lines 420-464

"To understand if particulate OM is the only absorbing phase in aerosols for polyol tracers in Nanjing, the absorptive partitioning coefficients of gas vs. organic phases were calculated based on measurement results ($K^m_{p,OM}$) for predefined *Cases 1-3* and predicted theoretically ($K^t_{p,OM}$) using eq. 3 and vapor pressures listed in Table S4. In Table 1, $K^t_{p,OM}$ ranges of isoprene SOA tracers, levoglucosan, and meso-erythritol are within two orders of magnitude, while those of monosaccharides and mannitol are larger ($> 10^3$). When particulate OM was assumed as the only absorbing phase (*Case 1*), the average $K^m_{p,OM}$ of isoprene SOA tracers, levolgucosan, and meso-erythritol were more than 10 times greater than most of their $K^t_{p,OM}$ (Table 1), and this difference was not likely susceptible to measurement uncertainties. As shown in Table S5, the average relative uncertainties of measurement-based partitioning coefficients are all <50%, leading to an uncertainty of log $K^m_{p,OM}$ less than $\pm$ 0.30. Comparable or even greater (up to 10^5) gap between $K^m_{p,OM}$ and $K^t_{p,OM}$ has been observed for carbonyls in a number of laboratory and field studies (Healy et al., 2008; Zhao et al., 2013; Shen et al., 2018), which could be ascribed to reactive uptake (e.g., hydration, oligomerization, and esterification) of organic gases onto condensed phase (Galloway et al., 2009). Oligomers, sulfate and nitrate esters of 2-methyltetrols can be formed in the aerosol phase (Surratt et al., 2010; Lin et al., 2014), and their decomposition and hydrolysis during filter analysis will lead to an overestimation of particle-phase concentrations (Lin et al., 2013; Cui et al., 2018). However, the occurrence of oligomers, sulfate or nitrate esters of levoglucosan was not ever reported in ambient aerosols, although it can be readily oxidized by •OH in the aqueous phase of atmospheric particles (Hennigan et al., 2010; Hoffmann et al., 2010).

When solubility in aerosol liquid water was considered by assuming a LLPS in ambient aerosols, and whenever WSOM and WIOM partitioned into separate (*Case 2*) or single (*Case 3*) liquid phases, the average log $K^m_{p,OM}$ of the above mentioned compounds became much closer to or even lay within the range (e.g., levoglucosan) of log $K^t_{p,OM}$ (Table 1). These results indicated that the aerosol liquid water (21.3 $\pm$ 24.2 µg m^{-3}; Table S1) is also an important absorbing phase of ambient polyol tracers in Nanjing. Similarly, the measured average F% of isoprene SOA tracers in southeastern US and central Amazonia were higher than predictions by assuming instantaneous equilibrium between the gas phase and particulate OM only, and the agreement was improved when parameterization of solubility was included for predictions (Isaacman-VanWertz et al., 2016). But none of these two studies could reasonably predict the temporal variability of F% or log $K^m_{p,OM}$. One possible explanation is that the activity coefficients of isoprene SOA tracers and levoglucosan deviate from unity (0.42–2.04; Pye et al., 2018) and vary with PM composition. Pye et al. (2018) re-analyzed the measurement data from Isaacman-VanWertz et al. (2016) using a thermodynamic equilibrium gas-particle partitioning model in two LLPS modes, which involved organic-inorganic interactions and estimations of activity coefficients as a function of liquid PM mixture composition. The resulting predictions captured both the average and diurnal variations of measured F% for polyol tracers, suggesting a necessity in obtaining time-resolved activity coefficients for the implementation of absorptive equilibrium partitioning model."

24. Figure S5: Please state the vapor pressure units and reference temperature used for the stated Log (p0L) values (one should not have to go back to the text to search for these).

Response:

The vapor pressure unit (atm) and reference temperature (25°C) were added in the figure caption of Figure S5 (now Figure S4).

"Figure S4. Temporal variations of gas-phase concentrations and particle-phase fractions ($F\%$) of polyol tracers. $p^{o,*}_L$: Liquid-state vapor pressure (atm, EPI estimates) at 25 °C."

References

Almeida, M. B., Alvarez, A. M., Miguel, E. M. D., and Hoyo, E. S. D.: Setchenow coefficients for naphthols by distribution method, Can. J. Chem., 61, 244-248, 10.1139/v83-043, 1983.

Cai, J., Zeng, X., Zhi, G., Gligorovski, S., Sheng, G., Yu, Z., Wang, X., and Peng, P.: Molecular composition and photochemical evolution of water-soluble organic carbon (WSOC) extracted from field biomass burning aerosols using high-resolution mass spectrometry, Atmos. Chem. Phys., 20, 6115-6128, 10.5194/acp-20-6115-2020, 2020.

Hilal, S. H., Ayyampalayam, S. N., and Carreira, L. A.: Air−liquid partition coefficient for a diverse set of organic compounds: Henry's law constant in water and hexadecane, Environ. Sci. Technol., 42, 9231-9236, 10.1021/es8005783, 2008.

Ip, H. S. S., Huang, X. H. H., and Yu, J. Z.: Effective Henry's law constants of glyoxal, glyoxylic acid, and glycolic acid, Geophys. Res. Lett., 36, L01802, https://doi.org/10.1029/2008GL036212, 2009.

Isaacman-VanWertz, G., Yee, L. D., Kreisberg, N. M., Wernis, R., Moss, J. A., Hering, S. V., de Sá, S. S., Martin, S. T., Alexander, M. L., Palm, B. B., Hu, W., Campuzano-Jost, P., Day, D. A., Jimenez, J. L., Riva, M., Surratt, J. D., Viegas, J., Manzi, A., Edgerton, E., Baumann, K., Souza, R., Artaxo, P., and Goldstein, A. H.: Ambient gas-particle partitioning of tracers for biogenic oxidation, Environ. Sci. Technol., 50, 9952-9962, 10.1021/acs.est.6b01674, 2016.

Kampf, C. J., Waxman, E. M., Slowik, J. G., Dommen, J., Pfaffenberger, L., Praplan, A. P., Prévôt, A. S. H., Baltensperger, U., Hoffmann, T., and Volkamer, R.: Effective Henry's law partitioning and the salting constant of glyoxal in aerosols containing sulfate, Environ. Sci. Technol., 47, 4236-4244, 10.1021/es400083d, 2013.

Kroll, J. H., Ng, N. L., Murphy, S. M., Varutbangkul, V., Flagan, R. C., and Seinfeld, J. H.: Chamber studies of secondary organic aerosol growth by reactive uptake of simple carbonyl compounds, J. Geophys. Res. Atmos., 110, D23207, https://doi.org/10.1029/2005JD006004, 2005.

Liang, C., Pankow, J. F., Odum, J. R., and Seinfeld, J. H.: Gas/particle partitioning of semivolatile organic compounds to model inorganic, organic, and ambient smog aerosols, Environ. Sci. Technol., 31, 3086-3092, 10.1021/es9702529, 1997.

Marcolli, C., and Krieger, U. K.: Phase changes during hygroscopic cycles of mixed organic/inorganic model systems of tropospheric aerosols, J. Phys. Chem. A, 110, 1881-1893, 10.1021/jp0556759, 2006.

Pankow, J. F., and Bidleman, T. F.: Interdependence of the slopes and intercepts from log-log correlations of measured gas-particle paritioning and vapor pressure—I. theory and analysis of available data, Atmos. Environ. Part A. General Topics, 26, 1071-1080, 10.1016/0960-1686(92)90039-n, 1992.

Pye, H. O. T., Zuend, A., Fry, J. L., Isaacman-VanWertz, G., Capps, S. L., Appel, K. W., Foroutan, H., Xu, L., Ng, N. L., and Goldstein, A. H.: Coupling of organic and inorganic aerosol systems and the effect on gas–particle partitioning in the southeastern US, Atmos. Chem. Phys., 18, 357-370, 10.5194/acp-18-357-2018, 2018.

Setschenow, J.: Über die Konstitution der Salzlösungen auf Grund ihres Verhaltens zu Kohlensäure, Z. Phys. Chem., 4U, 117-125, https://doi.org/10.1515/zpch-1889-0409, 1889.

Shen, H., Chen, Z., Li, H., Qian, X., Qin, X., and Shi, W.: Gas-particle partitioning of carbonyl compounds in the ambient atmosphere, Environ. Sci. Technol., 52, 10997-11006, 10.1021/acs.est.8b01882, 2018.

Taylor, N. F., Collins, D. R., Lowenthal, D. H., McCubbin, I. B., Hallar, A. G., Samburova, V., Zielinska, B., Kumar, N., and Mazzoleni, L. R.: Hygroscopic growth of water soluble organic carbon isolated from atmospheric aerosol collected at US national parks and Storm Peak Laboratory, Atmos. Chem. Phys., 17, 2555-2571, 10.5194/acp-17-2555-2017, 2017.

Zhao, Y., Kreisberg, N. M., Worton, D. R., Isaacman, G., Weber, R. J., Liu, S., Day, D. A., Russell, L. M., Markovic, M. Z., VandenBoer, T. C., Murphy, J. G., Hering, S. V., and Goldstein, A. H.: Insights into secondary organic aerosol formation mechanisms from measured gas/particle partitioning of specific organic tracer compounds, Environ. Sci. Technol., 47, 3781-3787, 10.1021/es304587x, 2013.

Gas-particle partitioning of polyol tracers <u>at a suburban site</u> in ~~the western Yangtze River Delta, China~~<u>Nanjing, east China: Increased partitioning to particles</u>~~: Absorptive or Henry's law partitioning?~~

Chao Qin[a], Yafeng Gou[b], Yuhang Wang[c], Yuhao Mao[b], Hong Liao[b], Qin'geng Wang[d], Mingjie Xie[b,*]

[a] Colleges of Resources and Environmental Sciences, Nanjing Agricultural University, Nanjing 210095, China

[b] Collaborative Innovation Center of Atmospheric Environment and Equipment Technology, Jiangsu Key Laboratory of Atmospheric Environment Monitoring and Pollution Control, School of Environmental Science and Engineering, Nanjing University of Information Science & Technology, 219 Ningliu Road, Nanjing 210044, China

[c] School of Earth and Atmospheric Sciences, Georgia Institute of Technology, Atlanta, GA 30332

[d] State Key Laboratory of Pollution Control and Resources Reuse, School of the Environment, Nanjing University, Nanjing 210023, China

*Corresponding to:

Mingjie Xie (mingjie.xie@nuist.edu.cn; mingjie.xie@colorado.edu);

Tel: +86-18851903788l; Fax: +86-25-58731051;

Mailing address: 219 Ningliu Road, Nanjing, Jiangsu, 210044, China

30

31

Abstract

Gas-particle partitioning of water-soluble organic compounds plays a significant role in ~~influencing~~ the formation ~~and source apportionment~~, transport, and lifetime of organic aerosols in the atmosphere, but is poorly characterized. In this work, gas- and particle-phase concentrations of isoprene oxidation products (C5-alkene triols and 2-methylterols), levoglucosan, and sugar polyols were measured simultaneously at a suburban site of the western Yangtze River Delta in east China. All target polyols were primarily distributed into the particle phase (85.9 ~~–~~ 99.8~~%),~~ %). Given the uncertainties in measurements and vapor pressure predictions, a dependence of ~~and their average~~ particle-phase fractions ~~were not strictly dependent~~ on vapor pressures cannot be determined. To explore the impact of aerosol liquid water on gas-particle partitioning of polyol tracers, three partitioning schemes (*Cases 1-3*) were proposed based on equilibriums of gas versus organic and aqueous phases in aerosols. If particulate organic matter (OM) is presumed as the only absorbing phase (*Case 1*), the measurement-based absorptive partitioning coefficients ($K^{m}_{p,OM}$) of ~~Moreover, the measurement-based partitioning coefficients ($K_{p,OM}$) of~~ isoprene oxidation products and levoglucosan were more than 10~~10^2 to 10^4 times~~ times ~~larger~~ greater than predicted values ($K^{t}_{p,OM}$)~~their predicted $K_{p,OM}$ based on the equilibrium absorptive partitioning model~~. The agreement between $K^{m}_{p,OM}$ and $K^{t}_{p,OM}$ was substantially improved when solubility in a separate aqueous phase was included, whenever water-soluble and water-insoluble OM partitioned into separate (*Case 2*) or single (*Case 3*) liquid phases, suggesting that the partitioning of polyol tracers into the aqueous phase in aerosols should not be ignored. ~~These are likely attributed to the hygroscopic~~

2

55 ~~properties of polyol tracers and high aerosol liquid water (ALW) concentrations (~20~~

56 ~~μg m^{-3}) of the study location.~~ The ~~Due to the large gaps (up to 10^7) between~~

57 measurement-based effective Henry's law coefficients ($K^m_{H,e}$) of polyol tracers were

58 orders of magnitude higher than ~~and~~ their predicted values in pure water ($K^t_{H,w}$)~~,~~.

59 Due to the moderate correlations between log ($K^m_{H,e}/K^t_{H,w}$) and molality of sulfate

60 ions, the gap between $K^m_{H,e}$ and $K^t_{H,w}$ of polyol tracers could not be fully

61 parameterized by the equation defining "salting-in" effects, and might be ascribed to

62 mechanisms of reactive uptake, aqueous phase reaction, "like-dissolves-like"

63 principle, etc. ~~the gas-particle partitioning of polyol tracers could not be depicted~~

64 ~~using Henry's law alone either. The regressions of log ($K_{H,w}/K_{H,e}$) versus molality of~~

65 ~~major water-soluble components in ALW indicated that sulfate ions ("salting-in~~

66 ~~effect") and water-soluble organic carbon can promote the partitioning of polyol~~

67 ~~tracers into the aqueous phase. These~~ These study results also partly reveals the

68 discrepancy between ~~results suggest a partitioning mechanism of enhanced aqueous~~

69 ~~phase uptake for polyol tracers, which partly reveals the discrepancy between~~

70 observation and modeling of ~~secondary~~ organic aerosols.

71

72

73

1 Introduction

75   The water-soluble organic carbon (WSOC) ~~documented for~~in ambient aerosols

76 can account for 20-80% of particulate organic matter (OM) based on carbon mass

77 (Saxena and Hildemann, 1996; Kondo et al., 2007). Fi~~l~~eld studies on the hygroscopic

78 growth and cloud condensation nucleus (CCN) activity of aerosol extracts indicated

79 that WSOC contributed significantly to aerosol hygroscopicity, and modified the

80 hydration behavior of inorganic species (e.g., sulfate, nitrate, and ammonium; Hallar

81 et al., 2013; Taylor et al., 2017). Thus, WSOC plays an important role in changing

82 radiative and cloud nucleating properties of atmospheric particles. Particulate WSOC

83 is a complex mixture of polar organic compounds containing oxygenated functional

84 groups (e.g., hydroxyl, carboxyl, and carbonyl groups), among which a list of organic

85 compounds with multiple hydroxyl (polyols) groups have been identified using gas

86 chromatography (GC)-mass spectrometry (GC-MS) and linked with specific emission

87 sources. For example, C5-alkene triols and 2-methyltetrols are isoprene oxidation

88 products (Claeys et al., 2004; Wang et al., 2005; Surratt et al., 2006); levoglucosan is

89 a typical pyrolysis product of cellulose (Simoneit et al., 1999); primary saccharides

90 (e.g., fructose and glucose) and saccharide polyols (e.g., arabitol and mannitol) are

91 commonly associated with soil microbiota and fungal spores, respectively (Simoneit

92 et al., 2004; Bauer et al., 2008).

93   To quantify the sources contributing to WSOC, concentrations of individual

94 organic tracers are often used as inputs for receptor-based modeling (Zhang et al.,

95 2009; Hu et al., 2010). Due to the influences of gas-particle partitioning on source

96 apportionment, Xie et al. (2013, 2014c) suggested the involvement of gas-phase

97 concentrations of organic makers through theoretical prediction or field measurements.

98 The equilibrium absorptive partitioning theory outlined by Pankow (1994a, b) and

99 laboratory measurements of secondary organic aerosol (SOA) yields (Odum et al.,

100 1996) have been widely applied to predict SOA formation in traditional modeling

101 studies (Heald et al., 2005; Volkamer et al., 2006; Hodzic et al., 2010). In addition to

4

absorptive partitioning to particulate OM after the formation of oxygenated organic compounds in gas phase, other formation pathways (e.g., reactive uptake) have been identified and are responsible for the large discrepancy between modeled and observed SOA loadings ~~The large discrepancy between modeled and observed SOA loadings might be partly explained by the fact that the newly generated SOA did not undergo gas phase oxidation followed by absorptive partitioning~~ (Jang et al., 2002; Kroll et al., 2005; Perraud et al., 2012). Unlike non-polar species ~~such as~~ (e.g., *n*-alkanes ~~and~~, polycyclic aromatic hydrocarbons ~~(PAHs)~~) and alkanoic acids that are well simulated (Simcik et al., 1998; Xie et al., 2014a; Yatavelli et al., 2014; Isaacman-VanWertz et al., 2016), ~~the absorptive partitioning model underestimated~~ particle-phase concentrations of carbonyls were underestimated by several orders of magnitude when particulate OM is presumed as the only absorbing phase in ideal condition (Healy et al., 2008; Kampf et al., 2013; Shen et al., 2018~~;~~). Zhao et al. (2013) observed a positive dependence of particle-phase pinonaldehyde on relative humidity (RH, %), and inferred that aerosol water ~~favored~~ played a role in the formation of pinonaldehyde in the atmosphere. However, ~~e~~very few studies have been performed on the measurement of gaseous polyols (Xie et al., 2014b; Isaacman-VanWertz et al., 2016), and their gas-particle partitioning were poorly understood.

Henry's law can ~~depict~~ describe the uptake of a compound into a liquid, highly dilute solution ~~in~~ (e.g., cloud droplets) in the atmosphere (Ip et al., 2009; Compernolle and Müller, 2014a). Aerosol water is also a major component of atmospheric particles, and accounts for 40% by volume at 50% RH in Europe (Tsyro, 2005). But the bulk aerosol solution is highly concentrated with inorganic ions and WSOC. An effective Henry's law coefficient ($K_{H,e}$, mol m^{-3} atm^{-1}) can be used to account for the measured

5

126 partitioning between the gas phase and aerosol liquid water (Volkamer et al., 2009).

127 Both laboratory and field studies observed enhanced $K_{H,e}$ ~~effective Henry's law~~

128 ~~coefficients (K^e_H, mol m^{-3} atm^{-1})~~ of carbonyl compounds with inorganic salt

129 concentrations (in mol kg^{-1} aerosol liquid water content, ALWC; Kampf et al., 2013;

130 Waxman et al., 2015; Shen et al., 2018). This ~~termed~~ "salting-in" effect (Setschenow,

131 1889) is not mechanistically understood, and might be linked with the hydrophilic

132 interactions (e.g., hydrogen bonding) between polar organic compounds and inorganic

133 ions leading to an increase of entropy or decrease of Gibbs free energy (Almeida et al.,

134 1983; Waxman et al., 2015). Polyol tracers are highly water-soluble and their gas-

135 particle partitioning is very likely driven by the aqueous phase containing substantial

136 ionic species in ambient aerosols. In the Southeastern US, the particle-phase fraction

137 ($F\%$) of WSOC is highly dependent on RH and ALWC (Hennigan et al., 2009).

138   In the present study, polyols related to specific emission sources in gaseous and

139 particle phases were measured concurrently in northern Nanjing, China. The sampling

140 and chemical analysis were performed in a similar manner as Xie et al. (2014b), while

141 an additional step was added prior to GC-MS analysis to clean the extracts of gaseous

142 samples. To explore the roles of aerosol liquid water on gas-particle partitioning of

143 polyol tracers, three modes (*Cases 1-3*) were proposed based on equilibriums between

144 gas and liquid aerosol phases, and the measurement-based and predicted partitioning

145 coefficients were compared across individual cases. ~~The absorptive and Henry's law~~

146 ~~partitioning coefficients of polyol tracers were calculated based on measurements and~~

147 ~~predicted theoretically for comparison. Finally, the effects of water-soluble inorganic~~

148 ~~ions and WSOC on the partitioning of atmospheric polyols were evaluated.~~ This work

149 ~~unveils~~ tends to explain the gas-particle partitioning of polyols at a suburban site in

150 eastern China, where the estimated average mass concentration of aerosol liquid water

151 is close to 20 µg m^{-3} (Yang et al., 2021). ~~The results will benefit future studies on~~

152 ~~modeling and source apportionment of organic aerosols.~~

153 **2 Methods**

154 *2.1 Field Sampling*

155 Details of the sampling information were provided in Yang et al. (2021). Briefly,

156 ambient air was sampled on the rooftop of a seven-story library building located in

157 Nanjing University of Information Science and Technology (NUIST 32.21 ^{o}N, 118.71

158 ^{o}E), a suburban site in the western Yangtze River Delta of east China. A medium

159 volume sampler (PM-PUF-300, Mingye Environmental, Gugangzhou, China)

160 equipped with a 2.5 µm cut impactor was configured to collect particulate matter with

161 aerodynamic diameter less than 2.5 µm (PM$_{2.5}$) and gaseous organic compounds at a

162 flow rate of 300 L min^{-1}. After the impactor, the sampled air flowed through a filter

163 pack containing two stacked pre-baked (550 ^{o}C, 4 h) quartz filters (20.3 cm $\times$ 12.6 cm,

164 Munktell Filter AB, Sweden) and a polyurethane foam (PUF, 65 mm diameter $\times$ 37.5

165 mm length) cartridge in series. The top quartz filter (Q_f) in the filter pack was loaded

166 with PM$_{2.5}$; gaseous organic compounds adsorbed on the backup quartz filter (Q_b) ~~was~~

167 <u>were</u> determined to evaluate sampling artifacts ~~("blow on" and "blow off" effects)~~;

168 and the PUF cartridge was used for the sampling of gaseous polyols. ~~Xie et al. (2014b)~~

169 ~~demonstrated that using bare PUF material could capture gaseous 2-methytetrols and~~

170 ~~levoglucosan with no excessive breakthrough (< 33%).~~ Filter and PUF samples were

171 collected every sixth day during daytime (8:00 AM – 7:00 PM) and night time (7:00

172 PM – 7:00 AM next day), respectively, from 09/28/2018 to 09/28/2019. Collection

173 efficiency of gaseous polyols were examined by performing breakthrough

7

174　experiments using two PUF plugs during nine sampling intervals. Prior to sampling,

175　PUF adsorbents were cleaned and dried in the same way as Xie et al. (2014b). Field

176　blank filter and PUF materials were collected every 10th sample for contamination

177　adjustment. Filter and PUF samples were sealed in prebaked aluminum foil and glass

178　jars, respectively, at – 20 °C until analysis.

179　*2.2 Chemical Analysis*

180　**Bulk speciation.** The accumulated $PM_{2.5}$ mass and bulk components including water

181　soluble ions (NH_4^+, SO_4^{2-}, NO_3^-, Ca^{2+}, Mg^{2+}, and K^+), organic (OC) and elemental

182　carbon (EC), and WSOC were measured for each filter sample. Their final

183　concentrations were determined by subtracting measurement results of Q_b from those

184　of Q_f. Concentrations of aerosol liquid water were predicted by ISORROPIA II model

185　~~involving~~ using ambient temperature, RH, and concentration data of NH_4^+, SO_4^{2-}, and

186　NO_3^- under the metastable state. The estimated water content contributed by

187　hygroscopic WSOC was relatively small (< 1 μg m^{-3}) and not accounted for in this

188　work (Text S1 of supplementary information). Table S1 lists averages and ranges of

189　ambient temperature, RH, measured $PM_{2.5}$ components, and predicted aerosol liquid

190　water from Yang et al. (2021).

191　**Polyols analysis.** Details of the analysis method for gaseous and particulate polyols

192　were provided in supplementary information (Text ~~S1~~S2). Briefly, 1/8 of each filter

193　sample was pre-spiked with deuterated internal standard and extracted ultrasonically

194　twice for 15 min in 10–15 mL of methanol and methylene chloride mixture (1:1, v/v).

195　After filtration, rotary evaporation, N_2 blown down to dryness, and reaction with 50

196　μL of N, O-bis(trimethylsilyl)trifluoroacetamide (BSTFA) containing 1%

197　trimethylchlorosilane (TMCS) and 10 μL of pyridine, the derivatives of polyols were

198 diluted to 400 μL using pure hexane for GC-MS analysis. Pre-spiked PUF samples

199 were Soxhlet extracted using a mixture of 225 mL of methylene chloride and 25 mL

200 of methanol, followed by the same procedures of filter sample pretreatment. Prior to

201 GC-MS analysis, 50 μL of pure water was added to precipitate PUF impurities from

202 the final extract. As shown in Figure S1e, all PUF residues are kept in aqueous phase

203 at the bottom of the vial, while the derivatives of polyol tracers are supposed to be

204 retained in the top clear hexane solution. An aliquot of 2 μL of the supernatant was

205 injected for GC-MS analysis under splitless mode, and an internal standard method

206 with a six-point calibration curve (0.05–5 ng μL^{-1}) was performed to quantify polyols

207 concentrations. In this work, isoprene SOA products, including three C5-alkene triols

208 (cis-2-methyl-1,3,4-trihydroxy-1-butene,   3-methyl-2,3,4-trihydroxy-1-butene,   and

209 trans-2-methyl-1,3,4-trihydroxy-1-butene; abbreviated as C5-alkene 1, 2, and 3) and

210 two 2-methyltetrols (2-methylthreitol and 2-methylerythritol), were quantified using

211 meso-erythritol; other polyols were determined using authentic standards.

212   Analytical recoveries of target polyols were obtained by adding known amounts

213 of standards to blank sampling materials (quartz filter and PUF), followed by

214 extraction and instrumental analysis identically as ambient samples. Method detection

215 limits (MDL) of individual species were estimated as three times the standard

216 deviation of their concentrations determined from six injections of the lowest

217 calibration standard. Table S2 lists recovery and MDL values of authentic standard

218 compounds. Concentrations of polyols in field blank samples were measured and

219 subtracted from air samples if necessary. To obtain appropriate gas-particle

220 distribution of polyol tracers, their field-blank corrected concentrations in filter and

221 PUF samples were adjusted by recoveries. Final concentrations of individual polyols

9

222 in Q_f, Q_b, and PUF samples are summarized in Table S3.

223 *2.3 Data analysis*

224 **Gas-particle separation and breakthrough calculation.** Polyol tracers detected in

225 Q_b samples are contributed by both gaseous adsorption ("positive artifact") and

226 particle-phase evaporation –from Q_f samples ("negative artifact"), while but their

227 relative contributions are unknown. Previous studies rarely considered the sampling

228 artifacts of particulate polyols. Xie et al. (2014b) adjusted particle- and gas-phase

229 concentrations of levoglucosan and 2-methyltetrol based on Q_b measurements in two

230 different ways. One assumed that Q_b values were completely attributed to gaseous

231 adsorption; the other presumed equal contributions from gaseous adsorption and Q_f

232 evaporation. However, negligible difference in gas-particle distribution was observed

233 due to the small Q_b values. In Table S3, concentrations of polyol tracers on Q_b are far

234 below those on Q_f, and it would be safe to presume equal positive and negative

235 artifacts. ThusIn this study, particle-phase concentrations of polyols in this study were

236 represented by Q_f values, and the gas phase was calculated as the sum of Q_b and PUF

237 measurements.

238   The sampling efficiency of target polyols were evaluated by collecting and

239 analyzing tandemly installed PUF plugs during nine sampling intervals. The

240 breakthrough of each polyol was calculated as

241 $B = \frac{[PUF]_{back}}{[PUF]_{front}+[PUF]_{backup}} \times 100\%$ (1)

242 where B is the breakthrough of gaseous sampling, and [PUF] represents the

243 concentration of specific compound in front or backup PUF sample. A value of 33%

244 was typically used to indicate excessive breakthrough (Peters et al., 2000; Ahrens et

245 al., 2011).

10

Calculations of partitioning coefficients. Here, we defined three partitioning cases to explore the influence of dissolution in aerosol liquid water on gas-particle partitioning of polyol tracers in the atmosphere. *Case 1* presumes instantaneous equilibrium between the gas phase and particulate OM based on the equilibrium absorptive partitioning theory. In this case, particulate OM is assumed to be the only absorbing phase and behave as an ideal solution. Then the absorptive gas-particle partitioning coefficients ($K_{p,OM}$, $m^3\,\mu g^{-1}$) were calculated from measurements ($K^m_{p,OM}$) and predicted theoretically ($K^t_{p,OM}$) as follows

$$K^m_{p,OM} = \frac{F/M_{OM}}{A} \qquad\qquad\qquad (2)$$

$$K^t_{p,OM} = \frac{RT}{10^6 \overline{MW}_{OM} \zeta_{OM} p^o_L} \qquad\qquad\qquad (3)$$

where M_{OM} denotes the mass concentration of absorptive organic matter (OM = OC × 1.6; Turpin and Lim, 2001); F ($ng\,m^{-3}$) and A ($ng\,m^{-3}$) are particulate and gaseous concentrations of individual polyols, respectively. In eq 3, R ($m^3\,atm\,K^{-1}\,mol^{-1}$) and T (K) are the ideal gas constant and ambient temperature; $\overline{MW}_{OM}$, average molecular weight of absorptive OM, is set at 200 g mol^{-1} for all samples (Barsanti and Pankow, 2004; Williams et al., 2010); ζ_{OM} denotes the mole fraction scale activity coefficient, and is presumed to be unity for all species in each sample; p^o_L (atm) is the vapor pressure of each pure compound, and is predicted with several estimation tools and adjusted for each sampling interval based on the average temperature (Text S3 and Table S4). ~~he calculations of measurement- and theory-based absorptive partitioning coefficients ($K^m_{p,OM}$ and $K^t_{p,OM}$, $m^3\,ug^{-1}$) were conducted identically as those in Xie et al. (2013, 2014a, b). The equations and parameters were detailed in supplementary information (Text S2)~~

11

269   Due to the influence of mixing state and water content in aerosols, several studies

270   modeled the gas-particle partitioning of oxygenated organic compounds by defining a

271   liquid-liquid phase separation (LLPS) in the aerosol (Zuend and Seinfeld, 2012; Pye

272   et al., 2018). The organic-inorganic interactions and changes of activity coefficients in

273   aqueous mixtures were fully considered as well. ~~As aerosol liquid water plays a~~

274   ~~significant role in the gas-particle partitioning of water-soluble organic compounds,~~ In

275   this study, we proposed ~~an~~ a simplified ~~equilibrium~~ LLPS partitioning mechanism

276   (*Case 2*) in Figure S~~2~~1. First, aerosol ~~liquid~~ water and ~~water~~ water-insoluble OM

277   (WIOM $= OM - WSOC \times 1.6$) exist in two separate liquid phases ~~(liquid-liquid phase~~

278   ~~separation)~~, and WSOC and inorganic ions are totally dissolved in the aqueous phase.

279   The distribution of polyol tracers between aqueous (F_W, ng m^{-3}) and WIOM (F_{WIOM},

280   ng m^{-3}) phases is simply depicted by their octanol-water partition coefficients (K_{OW})

281    $$K_{OW} = \frac{F_{WIOM}/V_{WSIOM}}{F_W/V_W} = \frac{c_{WIOM}}{c_W} \qquad (2\underline{4})$$

282   ~~W~~where V_{WIOM} and V_W are volumes (m^3) of WIOM and water in aerosols per cubic

283   meter air; $c_{\Theta WIOM}$ and c_W are solution concentrations (ng m^{-3}) of polyols

284   concentrations ~~(ng m^{-3} in solution)~~ in ~~WIOM~~ organic and aqueous phases; log K_{OW}

285   values of target polyols were ~~given~~ estimated using~~by~~ the Estimation Programs

286   Interface (EPI) Suite developed by the US Environmental Protection Agency and

287   Syracuse Research Corporation ~~in Table S3~~ (Table S4; US EPA, 2012). The density

288   of organic matter and water (ρ_w) in aerosols are set at 1.4 and 1.0 g cm^{-3}, respectively

289   (Isaacman-VanWertz et al., 2016; Taylor et al., 2017). ~~Due to the high water~~

290   ~~solubility of target polyols ($K_{OW} < 0.15$), more than 95% of their particle-phase~~

291   ~~concentrations were distributed into the aqueous phase.~~ Second, gas-phase polyol

292   tracers are in equilibrium with hydrophobic OM and the aqueous phase, respectively,

12

293 ~~following absorptive partitioning theory (eqs 1 and 2 in Text S2) and Henry's law (eq~~

294 ~~3)~~

295 $$K_{p,\text{WIOM}}^{\text{m}} = \frac{F_{\text{WIOM}}/M_{\text{WIOM}}}{A} \underline{\hspace{4cm}} \tag{5}$$

296 $$\underline{K_{\text{H,e}}^{\text{m}}}\cancel{K_{\text{H,e}}} = \frac{\frac{F_{\text{W}}\cancel{F}}{M_i}}{\frac{A}{M_i}\times R\times T\times\frac{c_{\text{ALW}}}{\rho_{\text{w}}}} = \frac{\rho_{\text{w}}\times F_{\text{W}}\cancel{F}}{A\times R\times T\times c_{\text{ALW}}} \tag{3\underline{6}}$$

297 where $K_{\text{H,e}}^{\text{m}}$ (mol m^{-3} atm^{-1}) is the measurement-based effective Henry's law

298 coefficient; $\underline{M_{\text{WIOM}} \text{ represents the mass concentration (µg m}^{-3}\text{) of WIOM;}}$ ~~F and A (ng~~

299 ~~m^{-3}) represent particle- and gas-phase concentrations of polyol tracers in ambient air;~~

300 M_i (g mol^{-1}) is the molecular weight of specific compound; ~~R (m^3 atm K^{-1} mol^{-1}) and T~~

301 ~~(K) are ideal gas constant and ambient temperature, respectively;~~ c_{ALW} (µg m^{-3}) is the

302 mass concentration of aerosol liquid water predicted using ISORROPIA II model~~; ρ_{w}~~

303 ~~(1 g cm^{-3}) is water density~~. $\underline{\textit{Case 3} \text{ is generally the same as } \textit{Case 2}, \text{ and the only}}$

304 $\underline{\text{difference is that water-soluble OM (WSOM) and WIOM exist in a single organic}}$

305 $\underline{\text{phase. Here total particulate OM was used instead of WIOM to assess the distribution}}$

306 $\underline{\text{of polyol tracers between aqueous and organic phases, and calculate partitioning}}$

307 $\underline{\text{coefficients of gas vs. particulate organic } (K_{\text{p,OM}}^{\text{m}}) \text{ and aqueous } (K_{\text{H,e}}^{\text{m}}) \text{ phases. Note}}$

308 $\underline{\text{that the polarity of particulate OM phase in } \textit{Case 3} \text{ was expected to increase, then}}$

309 $\underline{\text{using } K_{\text{OW}} \text{ to calculate the distribution of polyols between organic and aqueous phases}}$

310 $\underline{\text{might lead to underestimated } K_{\text{p,OM}}^{\text{m}} \text{ and overestimated } K_{\text{H,e}}^{\text{m}}.}$ ~~Due to the high water-~~

311 ~~solubility of target polyols ($K_{\text{OW}} < 0.15$), more than 95% of their particle-phase~~

312 ~~concentrations were distributed into the aqueous phase.~~ For comparison purposes, the

313 Henry's law coefficient in pure water at 25 °C ($K_{\text{H,w}}^{*}$) was ~~predicted~~ $\underline{\text{estimated}}$ ~~from~~

314 $\underline{\text{using}}$ EPI ~~suite~~ and SPARC (Hilal et al., 2008; http://archemcalc.com/sparc-web/calc),

315 $\underline{\text{respectively}}$ (Table ~~S3~~$\underline{\text{S4}}$), and was adjusted for each sampling interval due to the

13

316 changes in ambient temperature using van -'t Hoff equation (Text ~~S3~~S4).

317 ***Uncertainty estimation.*** To obtain the uncertainty associated with the calculation of $F\%$

318 and partitioning coefficients ($K^m_{p,OM}$ and $K^m_{H,e}$), measurement uncertainties of polyol

319 tracers in filter and PUF samples were estimated from their recoveries and

320 breakthrough for gaseous sampling. The root sum of squares (RSS) method was

321 applied to propagate uncertainties of gas and particle-phase concentrations for $F\%$,

322 $K^m_{p,OM}$, and $K^m_{H,e}$ calculations. Details of the uncertainty estimation and propagation

323 methods were provided in Text S5, and the average relative uncertainties were

324 summarized in Table S5.

325 **3 Results and discussion**

326 *3.1 Method evaluation*

327   In our previous study, PUF/XAD-4 resin/PUF and PUF/XAD-7 resin/PUF

328 adsorbent sandwiches were tested for sampling gaseous 2-methyltetrols and

329 levoglucosan (Xie et al., 2014b). The results of breakthrough experiments suggested

330 that both the two sandwiched composites had high sampling efficiency (close to

331 100%). Moreover, individual parts of the two types of composites (top PUF, middle

332 XAD-4/XAD-7 resin, and backup PUF) were analyzed for 7 samples, and target

333 compounds were only detected in top PUF. It is therefore suitable to collect gaseous

334 2-methylterols and levoglucosan using PUF materials only~~Thus, bare PUF material is~~

335 ~~suitable for sampling gaseous 2-methyltetrols and levoglucosan~~.

336   Although PUF materials were pre-cleaned prior to sampling, a few short-chain

337 polyurethanes or impurities could be dissolved during Soxhlet extraction of target

338 compounds using the mixture of methanol and methylene chloride. These substances

339 precipitated when sample extracts were concentrated (Figure S1a, b), and re-dissolved

14

340   in BSTFA:TMCS/pyridine and hexane after the derivatization step (Figure S1c, d). In

341   Xie et al. (2014b), an aliquot of 2 µL of the sample extract as shown in Figure S1d

342   was injected for GC-MS analysis. ~~Due to the fact that~~ Since the dissolved PUF

343   materials did not vaporize at ~300 °C, the GC inlet liner had to be changed for

344   cleaning every few samples. In this work, 50 µL of pure water was added to separate

345   PUF materials from polyol derivatives in hexane solution. As shown in Figure S1e, all

346   PUF residues were retained in the aqueous solution after ~~liquid-liquid~~ phase

347   separation. This pretreatment step was added for the analysis of gaseous samples to

348   save time for changing and cleaning GC inlet liners. However, the revised method did

349   not improve the recoveries of meso-erythritol and levoglucosan in PUF samples

350   (Table S2) compared to those in Xie et al. (2014b). This is because the dissolved PUF

351   materials should have an impact on the derivatization efficiency of polyol species, and

352   future work is warranted to remove dissolved PUF materials in sample extracts before

353   the derivatization step.

354   Measurement results of breakthrough samples and the resulting B values were

355   shown in Figure ~~S3~~S2. C5-alkene triols and 2-methyltetrols were mainly observed in

356   summertime, and levoglucosan was only detected in three pairs of breakthrough

357   samples. Their average B values (< 33%) indicated no excessive breakthrough (Figure

358   ~~S3a~~S2a-c), but were higher than those reported by Xie et al. (2014b). This might be

359   ascribed to the greater face velocity (1.5 cm s^{-1}) for sampling gaseous polyols than

360   that (0.61 cm s^{-1}) in our previous study. Due to the limit in sample number for

361   breakthrough tests and low detection rates, the dependence of breakthrough on

362   ambient temperature or OM loadings cannot be evaluated. The breakthrough of an

363   ideal sampling method is expected to be extremely low (e.g., <10%) and have no

15

364   dependence on ambient temperature, OM loadings, etc. Unlike fructose which had

365   low breakthrough (Figure S3dS2d), glucose and mannitol had comparable

366   concentrations between front and backup PUF samples for several breakthrough

367   experiments (Figure S3eS2e, f), indicating that PUF materials are not suitable for

368   sampling gaseous glucose and mannitol. Mannose and arabitol were not detected or

369   had BDL values for breakthrough samples, and their breakthrough was not provided.

370   In the current work, concentrations of polyol tracers in filter and PUF samples were

371   all reported, but the data of mannose, glucose, arabitol, and mannitol in PUF samples

372   should be treated with caution due to high breakthrough or the lack of valid

373   breakthrough results.

374   *3.2 General description of measurement results*

375   ~~Concentrations of individual polyols in Q_f, Q_b, and PUF samples are summarized~~

376   ~~in Table S4, and their t~~Total ambient concentrations (Q_f + Q_b + PUF) of individual

377   polyols are depicted using boxplots in Figure 1̶2. Figure S4 S3 presents temporal

378   variations of total and Q_f concentrations of individual polyols with daytime and night-

379   time measurements distinguished. In general, polyol tracers were predominantly

380   observed on Q_f with averages 1-3 orders of magnitude higher than those on Q_b and

381   PUF (Table S3). Levoglucosan had the highest average total concentration (66.1 $\pm$

382   71.1 ng m^{-3}), followed by fructose (15.0 $\pm$ 62.9 ng m^{-3}) and mannose (14.3 $\pm$ 31.3 ng

383   m^{-3}). C5-alkene triols and 2-methyltetrols are formed from isoprene epoxydiols

384   (IEPOX) under low NO$_X$ conditions (Surratt et al., 2010). All the five species on Q_b

385   were more frequently detected and had average concentrations 2-20 times higher than

386   those in PUF samples. While in Xie et al. (2014b), the sum of 2-methyltetrols in Q_b

387   and adsorbent samples were up to 2.7 times higher than those on Q_f in summer

16

388 Denver, so isoprene products are not similarly distributed between gas and aerosol

389 phases across different regions. Moreover, isoprene-derived polyols exhibited

390 prominent elevations in summer (Figure ~~S4a~~S3a-e), and their daytime concentrations

391 $(2.02 \pm 3.73 - 10.5 \pm 29.3$ ng m^{-3}) were only slightly higher than those during night-

392 time $(1.63 \pm 4.40 - 9.65 \pm 32.7$ ng m^{-3}). Previous field studies observed strong diurnal

393 variations of isoprene SOA tracers with peak concentrations from afternoon till

394 midnight (Fu and Kawamura, 2011; Isaacman-VanWertz et al., 2016). ~~Fu and~~

395 ~~Kawamura (2011) investigated diurnal variations of polar organic tracers at a forest~~

396 ~~site in summer by sampling aerosol particles every 4 h. They found that isoprene-~~

397 ~~derived SOA tracers maximized from later afternoon to early evening.~~ Although no

398 IEPOX will be generated from the oxidation of isoprene by •OH and HO$_2$• after

399 sunset, the formations of C5-alkene triols and 2-methyltetrols might continue until

400 pre-existing IEPOX is exhausted. In this work, neither the daytime (8:00 AM–7:00

401 PM) or night-time (7:00 AM–7:00 AM next day) sample covered the whole period

402 when isoprene SOA tracers had peak concentrations, and the strong diurnal variations

403 of C5-alkene triols and 2-methyltetrols were not captured. ~~This explains the~~

404 ~~insignificant ($p > 0.05$) day-night differences of C5-alkene triols and 2-methyltetrols~~

405 ~~in this work.~~

406   Levoglucosan was more frequently detected but far less concentrated in PUF than

407 in Q$_b$ samples. Its total concentrations were comparable to those in urban Denver

408 (average 65.3 ± 96.8 ng m^{-3}, range $2.48 - 478$ ng m^{-3}), where an average of ~20%

409 partitioned into the gas phase (Xie et al., 2014b). Due to the enhanced biomass

410 burning activities in cold periods for domestic heating at night, levoglucosan showed

411 a clear seasonal pattern (winter maxima and summer minima) and significant ($p =$

17

412   0.03) higher concentrations during night-time (Figure ~~S4f~~S3f). Sugars and sugar

413   alcohols are commonly linked with soil/dust resuspension and associated microbial

414   activities (Simoneit et al., 2004). They were frequently detected in Q_b samples with

415   comparable averages and ranges as those in PUF samples (Table ~~S4~~S3). Total

416   concentrations of fructose and glucose were strongly ($r = 0.98$) correlated peaking in

417   middle spring (April 2019, Figure ~~S4h~~S3h, j), when Ca^{2+} on Q_f also reached its

418   maxima of the year (Yang et al., 2021), indicating an influence from soil/dust

419   resuspension. Arabitol and mannitol had identical seasonal pattern ($r = 0.89$) with

420   elevated total concentrations from May to October (Figure ~~S4i~~S3i, m), which might

421   be attributed to ~~the~~ high levels of vegetation during growing seasons and autumn

422   decomposition ~~decomposing~~ (Burshtein et al., 2011). Multiple peaks of mannose

423   concentrations were observed from spring to autumn, suggesting a variety of

424   contributing sources (e.g., microbial activity, vegetation). Xylitol is likely derived

425   from biomass burning in northern Nanjing due to its strong correlation ($r = 0.89$) with

426   levoglucosan.

427   ***3.3 Gas- and particle-phase distributions ~~and absorptive partitioning coefficient~~***

428   ~~Q_b measurements were often used to assess positive sampling artifacts of~~

429 ~~particulate OC (Chow et al., 2010; Subramanian et al., 2004), but rarely for particle-~~

430 ~~phase organic markers. In this study~~As mentioned in sections 2.3, concentrations of

431   particulate polyols were obtained directly from Q_f measurements, and the gas phase

432   was calculated as the sum of Q_b and PUF values. Figure ~~S5~~ S4 shows the time series

433   of gas-phase concentrations and particle-phase fractions (F%) of individual polyol

434   tracers. The average F% values of measured species are ~~linearly regressed~~plotted

435   against the logarithms of their ~~subcooled~~ liquid-state vapor pressures at 25 ^{o}C ($p^{o,*}_L$)

436 in Figure ~~2~~3. Gas-phase C5-alkene triols and 2-methyltetrols had maximum

437 concentrations in summer and significant ($p < 0.05$) day-night variations (Figure S4),

438 while other polyols had extremely low concentrations in the gas phase with $F\%$

439 (average $\pm$ standard deviation) ranging from $94.2 \pm 8.02 - 99.8 \pm 1.21\%$. The

440 average $F\%$ values of 2-methyltetrols ($87.5 \pm 10.6\%$) and levoglucosan ($99.8 \pm 1.21\%$)

441 were greater than those in urban Denver (50–80%; Xie et al., 2014b), where the

442 average sampling temperature (12.5 ± 10.1 ºC) was much lower. Thus, the changes in

443 vapor pressures with the ambient temperature and/or particulate OM loadings might

444 not be the main factors driving gas-particle partitioning of polyol tracers in Nanjing.

445 In Figure 3, the average $F\%$ uncertainties (6.16–31.2%) of monosaccharides (e.g.,

446 fructose) and sugar alcohols (e.g., mannitol) were larger than those of isoprene SOA

447 tracers and levoglucosan (3.33–7.24%) due to their low and variable recoveries (Table

448 S2) and excessive breakthrough (Figure S2). However, the estimated uncertainties of

449 $F\%$ for less volatile polyols ($p^{\mathrm{o},*}_\mathrm{L} < \sim 10^{-10}$ atm) were not physically meaningful, as

450 more than 95% of these compounds existed in the particle phase. Considering the

451 uncertainties in $F\%$ and log $p^{\mathrm{o},*}_\mathrm{L}$ and high average $F\%$ ($> 85\%$) of target polyol

452 tracers, a dependence of $F\%$ on the vapor pressure could not be determined, and the

453 seasonality and day-night difference ($p > 0.05$) of $F\%$ were obscured.~~Unlike non-~~

454 ~~polar organic tracers (e.g., n-alkanes and PAHs), some polyols (e.g., 2-methyltetrols~~

455 ~~and levoglucosan) data did not follow the linear regression line of $F\%$ versus log $p^{\mathrm{o},*}_\mathrm{L}$.~~

456 ~~Although gas-phase C5-alkene triols and 2-methyltetrols were majorly observed in~~

457 ~~summer with significant ($p < 0.05$) day-night variations, their $F\%$ values did not show~~

458 ~~seasonality or day-night difference ($p = 0.18-0.73$). Other polyols had extremely low~~

459 ~~concentrations in the gas phase with average $F\%$ ranging from $94.2 \pm 8.02 - 99.8 \pm$~~

460 ~~1.21%. The average *F*% values of 2-methyltetrols (87.5 ± 10.6%) and levoglucosan~~

461 ~~(99.8 ± 1.21%) were greater than those in urban Denver (50–80%; Xie et al., 2014b),~~

462 ~~where the average sampling temperature (12.5 ± 10.1 °C) was much lower. Thus, the~~

463 ~~changes in vapor pressures with the ambient temperature might not be the main factor~~

464 ~~driving gas-particle partitioning of polyol tracers in northern Nanjing.~~

465 *__3.4 Partitioning coefficients of gas versus organic phases__*

466 To understand if particulate OM is the only absorbing phase in aerosols for

467 polyol tracers in Nanjing, the absorptive partitioning coefficients of gas vs. organic

468 phases were calculated based on measurement results ($K^{m}_{p,OM}$) for predefined *Cases*

469 *1-3* and predicted theoretically ($K^{t}_{p,OM}$) using eq. 3 and vapor pressures listed in Table

470 S4. In Table 1, $K^{t}_{p,OM}$ ranges of isoprene SOA tracers, levoglucosan, and meso-

471 erythritol are within two orders of magnitude, while those of monosaccharides and

472 mannitol are larger (> 10^{3}). ~~understand if traditional absorptive partitioning theory~~

473 ~~could be applied to predict the gas-particle partitioning of polyol tracers in northern~~

474 ~~Nanjing,~~ When particulate OM was assumed as the only absorbing phase (*Case 1*),

475 ~~Table 1 compares log $K^{m}_{p,OM}$ and log $K^{t}_{p,OM}$ of individual compounds. The~~ the

476 average $K^{m}_{p,OM}$ ~~values~~ of isoprene SOA tracers, levolgucosan, and meso-erythritol

477 were ~~10^{2} to 10^{3}~~more than 10 times ~~larger~~ greater than most of their ~~corresponding~~

478 $K^{t}_{p,OM}$ (Table 1), and this difference was not likely susceptible to measurement

479 uncertainties. As shown in Table S5, the average relative uncertainties of

480 measurement-based partitioning coefficients are all <50%, leading to an uncertainty

481 of log $K^{m}_{p,OM}$ less than ± 0.30. Comparable or even greater (up to 10^{5}) gap between

482 $K^{m}_{p,OM}$ and $K^{t}_{p,OM}$ has been observed for carbonyls in a number of laboratory and field

483 studies (Healy et al., 2008; Zhao et al., 2013; Shen et al., 2018), which could be

484 ascribed to reactive uptake (e.g., hydration, oligomerization, and esterification) of

485 organic gases onto condensed phase (Galloway et al., 2009). Oligomers, sulfate and

486 nitrate esters of 2-methyltetrols can be formed in the aerosol phase (Surratt et al.,

487 2010; Lin et al., 2014), and their decomposition and hydrolysis during filter analysis

488 will lead to an overestimation of particle-phase concentrations (Lin et al., 2013; Cui et

489 al., 2018). ~~but these products were not expected to dominate particle phase~~

490 ~~concentrations of 2-methyltetrols (Lin et al., 2013; Xie et al., 2014b).~~ However,

491 ~~Although levoglucosan can be readily oxidized by •OH in the aqueous phase of~~

492 ~~atmospheric particles (Hennigan et al., 2010; Hoffmann et al., 2010),~~ the occurrence

493 of ~~its~~ oligomers, sulfate or nitrate esters of levoglucosan was not ever reported in

494 ambient aerosols, ~~A~~although ~~levoglucosan~~ it can be readily oxidized by •OH in the

495 aqueous phase of atmospheric particles (Hennigan et al., 2010; Hoffmann et al.,

496 2010)~~,~~.

497 When solubility in aerosol liquid water was considered by assuming a LLPS in

498 ambient aerosols, and whenever WSOM and WIOM partitioned into separate (*Case 2*)

499 or single (*Case 3*) liquid phases, the average log $K^{m}_{p,OM}$ of the above mentioned

500 compounds became much closer to or even lay within the range (e.g., levoglucosan)

501 of log $K^{t}_{p,OM}$ (Table 1). These results indicated that the aerosol liquid water (21.3 ±

502 24.2 µg m^{-3}; Table S1) is also an important absorbing phase of ambient polyol tracers

503 in Nanjing. ~~Xie et al. (2014b) found that the gas-particle partitioning of 2-~~

504 ~~methyltetrols and levoglucosan in urban Denver were highly dependent on the~~

505 ~~variations in ambient temperature and absorbing organic matter (M$_{OM}$).~~ Similarly,

506 ~~While in southeastern US,~~ the ~~particle-phase fractions~~ measured average *F%* of

507 isoprene SOA tracers in southeastern US and central Amazonia were ~~generally~~ higher

508   than prediction~~s~~ by assuming instantaneous equilibrium between the gas phase and

509   particulate OM only, and the agreement was improved when parameterization of

510   solubility was included for predictions (Isaacman-VanWertz et al., 2016). But none of

511   these two studies could reasonably predict the temporal variability of $F\%$ or log

512    $K^{\mathrm{m}}_{\mathrm{p,OM}}$. One possible explanation is that the activity coefficients of isoprene SOA

513   tracers and levoglucosan deviate from unity (0.42–2.04; Pye et al., 2018) and vary

514   with PM composition. Pye et al. (2018) re-analyzed the measurement data from

515   Isaacman-VanWertz et al. (2016) using a thermodynamic equilibrium gas-particle

516   partitioning model in two LLPS modes, which involved organic-inorganic interactions

517   and estimations of activity coefficients as a function of liquid PM mixture

518   composition. The resulting predictions captured both the average and diurnal

519   variations of measured $F\%$ for polyol tracers, suggesting a necessity in obtaining

520   time-resolved activity coefficients for the implementation of absorptive equilibrium

521   partitioning model.

522   ~~based on absorptive partitioning model (Isaacman-VanWertz et al., 2016). This~~

523   ~~discrepancy might be related to the spatial heterogeneity of ALWC, which is expected~~

524   ~~to control the gas-particle partitioning of water-soluble organic matter in the Eastern~~

525   ~~US (Carlton and Turpin, 2013). In this study, the large difference between $K^{\mathrm{m}}_{\mathrm{p,OM}}$ and~~

526   ~~$K^{\mathrm{t}}_{\mathrm{p,OM}}$ indicated that some mechanisms other than absorptive partitioning (e.g.,~~

527   ~~Henry's law partitioning) should be involved to predict the gas-particle partitioning~~

528   ~~of polyol tracers in northern Nanjing, where the ambient particles contained~~

529   ~~substantial liquid water (21.3 ± 24.2 µg m^{-3}; Table S1).~~

530   Unlike isoprene SOA tracers and levoglucosan, the average $K^{\mathrm{t}}_{\mathrm{p,OM}}$ values of

531   monosaccharides (fructose, mannose, and glucose) and sugar alcohols (xylitol,

arabitol, and mannitol) were ~~up to 10^3 times~~<u>orders of magnitude</u> larger than their

$K^{\mathrm{m}}_{\mathrm{p,OM}}$ <u>for *Cases 2 and 3* </u>(Table 1). This is probably caused by the overestimation of

gas-phase concentrations of sugar polyols. The organic matter on Q_b is mainly

composed of volatile and semi-volatile organic compounds. If the concentrations of

organic compounds on Q_b were comparable or higher than those on Q_f, their Q_f values

should be dominated by ~~positive artifact~~<u>positive artifact</u>. As the vapor pressure

decreases, the evaporation loss from Q_f samples becomes non-negligible. Note that

the magnitude of negative artifacts is unknown and very difficult to assess, and the

vapor pressures of monosaccharides and sugar alcohols are ~~mostly <~~<u>far below</u> 10^{-10}

atm<u> (Table S4)</u>, their concentrations in Q_b and even PUF samples might contain more

contributions from negative artifacts than isoprene SOA tracers and levoglucosan.

~~Considering that~~<u>As</u> low-volatile sugar polyols had <u>lower and </u>less stable recoveries

(Table S2) and greater breakthrough (Figure ~~S3e~~<u>S2e</u>, f), caution is warranted in

analyzing their $K^{\mathrm{m}}_{\mathrm{p,OM}}$ values obtained in this study.

~~Figure S2 presumes that gas-phase polyols are in equilibrium with WIOM and the~~

~~aqueous phase, respectively. Then concentrations of WIOM [1.4 × (OC-WSOC)] was~~

~~used to adjust the calculation of absorptive partitioning coefficients ($K^{\mathrm{m}}_{\mathrm{p,WIOM}}$) based~~

~~on eq 1 in supplementary information. In comparison to log $K^{\mathrm{m}}_{\mathrm{p,OM}}$, the average log~~

~~$K^{\mathrm{m}}_{\mathrm{p,WIOM}}$ values of isoprene SOA tracers and levoglucosan were much closer to~~

~~average log $K^{\mathrm{t}}_{\mathrm{p,OM}}$ (Tables 1 and S5), supporting that the aerosol liquid water should~~

~~have significant impacts on gas-particle partitioning of polyol tracers.~~

3.~~4~~ <u>5</u> Partitioning coefficients of gas versus aqueous phases~~Effective Henry's law~~

~~coefficient~~

~~Table 2 lists the statistics of measurement-based log $K_{\mathrm{H,e}}$ and predicted log $K_{\mathrm{H,w}}$.~~

556 The predicted Henery's law coefficients in pure water ($K^t_{H,w}$, mol m^{-3} atm^{-1}) from EPI

557 and SPARC estimates differed by several orders of magnitude, but literature values of

558 isoprene SOA and levoglucosan were closer to EPI estimates (Table S4). If SPARC

559 $K^*_{H,w}$ values were used, the average log $K^m_{H,e}$ of most polyol tracers would be lower

560 than their average log $K^t_{H,w}$ (Table 2), indicating that the aqueous phase of ambient

561 aerosol is less hospital to polyol tracers than pure water. This is in conflict with the

562 fact that the interactions of organic compounds, water, and inorganic ions in aerosols

563 will increase the partitioning of highly oxygenated compounds (O:C ≥ 0.6; e.g.,

564 isoprene SOA tracers and levoglucosan) into the particle phase (Pye et al., 2018).

565 Several studies identified a close relationship between salt concentrations of aerosol

566 water and enhanced uptake of very polar compounds (Almeida et al., 1983; Kroll et

567 al., 2005; Ip et al., 2009; Kampf et al., 2013; Shen et al., 2018). Thus, log $K^t_{H,w}$ values

568 of EPI estimates were used for further data analysis.

569 In Table 2, ~~T~~the ~~average~~ ~~$K^t_{H,w}$~~$K_{H,w}$ values of isoprene SOA tracers, levoglucosan,

570 and meso-erythritols based on EPI estimations were ~~2–6 orders of magnitude~~10^2 to 10^6

571 lower than their corresponding ~~average~~ ~~$K^m_{H,e}$~~$K_{H,e}$~~,~~. Log $K^m_{H,e}$ values of *Cases 2* and *3*

572 had ignorable difference and were not presented separately. ~~indicating that the~~

573 ~~ambient atmosphere in northern Nanjing favored the condensation of these polyols.~~

574 Other polyol compounds exhibited less difference between log ~~$K^m_{H,e}$~~$K_{H,e}$ and log

575 ~~$K^t_{H,w}$~~$K_{H,w}$, which was very likely caused by the overestimation of their gas-phase

576 concentrations. The average $K^m_{H,e}$ values of polyol tracers (10^{13}–10^{15} mol m^{-3} atm^{-1}) in

577 this study were several orders of magnitude larger than those of carbonyls derived

578 from ambient measurements (10^{10}–10^{12} mol m^{-3} atm^{-1}; Shen et al., 2018) and chamber

579 simulations (~10^{11} mol m^{-3} atm^{-1}; Kroll et al., 2005; Volkamer et al., 2006; Galloway

24

et al., 2009). This is because low molecular weight carbonyls (e.g., glyoxal) are much more volatile ($p^{\text{o,*}}_{\text{L}} > 10^{-2}$ atm) than our target polyols (Table S4). According to existing studies, the minimum concentrations of gas-phase glyoxal and methylglyoxal in Chinese cities (~0.1 µg m^{-3}) are magnitudes higher than the averages of polyol tracers in this work, while their particle-phase concentrations are of the same magnitude (Shen et al., 2018; Liu et al., 2020).

A number of previous studies observed enhanced $K_{\text{H,e}}$ of carbonyls with salt concentrations in aqueous solution (Ip et al., 2009; Kampf et al., 2013; Waxman et al., 2015; Shen et al., 2018), and described this "salting-in" effect using

$$\text{Log}\left(\frac{K_{\text{H,w}}}{K_{\text{H,e}}}\right) = K_{\text{s}} c_{\text{salt}} \qquad (47)$$

where K_{s} (kg mol^{-1}) is the salting constant, and c_{salt} is the aqueous-phase concentration of salt in mol kg^{-1} ALWC. This equation is originally defined in Setschenow (1889) by plotting log ($K_{\text{H,w}}/K_{\text{H,e}}$) versus the total salt concentration (mol L^{-1}).

As sulfate has been identified as the major factor influencing the salting effect of carbonyl species (Kroll et al., 2005; Ip et al., 2009), Figure ~~3~~ 4 shows modified Setschenow plots for C5-alkene triols, 2-methyltetrols, and levoglucosan, where log ($K^{\text{t}}_{\text{H,w}}/K^{\text{m}}_{\text{H,e}}$) values were regressed to the molality of sulfate ion in aerosol liquid water (c_{sulfate}, mol kg^{-1} ALWC). ~~However, t~~The log ($K^{\text{t}}_{\text{H,w}}/K^{\text{m}}_{\text{H,e}}$)~~($K_{\text{H,w}}/K_{\text{H,e}}$)~~ data increased faster when c_{sulfate} approached 0, and deviated from their expected behavior with ~~in the modified Setschenow plot~~ increased c_{sulfate}. Kampf et al. (2013) selected a threshold c_{sulfate} of 12 mol kg^{-1} ALWC to illustrate the deviation for chamber experiments, and attributed it to elevated viscosity and slow particle-phase reactions at high c_{sulfate}. ~~at c_{sulfate} > 12 mol kg^{-1} ALWC, which was also observed for glyoxal (Kampf et al., 2013). This might be because the ambient particles did not undergo~~

25

604 ~~liquid-liquid phase separation at $c_{sulfate} >$ 12 mol kg^{-1} ALWC, when the average RH~~

605 ~~(51.5 ± 15.4%) was lower than the lowest deliquescence RH (61.8%) of major~~

606 ~~inorganic salts (e.g., NH$_4$NO$_3$, (NH$_4$)$_2$SO$_4$) in ambient aerosols (Seinfeld and Pandis,~~

607 ~~2016), and the corresponding average concentration of aerosol liquid water was only~~

608 ~~5.31 ± 4.05 μg m^{-3}.~~ In Figure ~~3~~4, negative correlations ($p <$ 0.01) are observed at

609 $c_{sulfate} <$ 12 mol kg^{-1} ALWC~~,~~, and Figure S5 exhibits significant negative correlations

610 ($p <$ 0.01) between log ($K^t_{H,w}/K^m_{H,e}$) and $c_{sulfate}$ for individual polyols even without

611 excluding the deviations at high $c_{sulfate}$. The K_s values of polyol tracers from Figures 4

612 and S5 (-0.17 – -0.037 kg mol^{-1}) are in a similar range as that of glyoxal (-0.24 – -0.04

613 kg mol^{-1}; Kampf et al., 2013; Shen et al., 2018; Waxman et al., 2015). These results

614 indicated that the shifting of gas-particle equilibrium toward the condensed phase

615 might be partly parameterized by the equation defining "salting-in" effects.

616 ~~and the K_s values range from -0.17 to -0.15 kg mol^{-1}. Figure S6 shows the~~

617 ~~regressions between log ($K_{H,w}/K_{H,e}$) of individual polyols and $c_{sulfate}$ without~~

618 ~~considering the deviations at high $c_{sulfate}$, and nearly all species exhibit significant~~

619 ~~negative correlations ($p <$ 0.01). These results indicated the "salting in" effects for~~

620 ~~polyol tracers in northern Nanjing, and to our knowledge the present study is the first~~

621 ~~to calculate their $K_{H,e}$ and K_s. Although several studies have estimated Henry's law~~

622 ~~constants for a variety of polar organic compounds in pure water (e.g., polyols and~~

623 ~~polyacids; Compernolle and Müller, 2014a, b), salting effects should be considered in~~

624 ~~describing their gas-particle partitioning in the ambient atmosphere.~~

625 ~~The average $K_{H,e}$ values of polyol tracers (10^{13}–10^{15} mol m^{-3} atm^{-1}) in this study~~

626 ~~were several orders of magnitude larger than those of carbonyls derived from ambient~~

627 ~~measurements (10^{10}–10^{12} mol m^{-3} atm^{-1}; Shen et al., 2018) and chamber simulations~~

628 ~~(~10^{11} mol m^{-3} atm^{-1}; Kroll et al., 2005; Volkamer et al., 2006; Galloway et al., 2009).~~

629 ~~This is because low molecular weight carbonyls (e.g., glyoxal) are much more volatile~~

630 ~~($p^{\circ,*}{}_L$ > 10^{-2} atm) than our target polyols (Table S3). According to existing studies, the~~

631 ~~minimum concentrations of gas-phase glyoxal and methylglyoxal in Chinese cities~~

632 ~~(~0.1 µg m^{-3}; Liu et al., 2020) are magnitudes higher than the averages of polyol~~

633 ~~tracers in this work, while their particle phase concentrations are of the same~~

634 ~~magnitude. The K_s values of polyol tracers from Figures 3 and S5 (-0.17 – 0.037 kg~~

635 ~~mol^{-1}) are in a similar range as that of glyoxal (-0.24 – 0.04 kg mol^{-1}; Kampf et al.,~~

636 ~~2013; Shen et al., 2018; Waxman et al., 2015), indicating that the uptake of different~~

637 ~~water-soluble organic compounds might be enhanced by sulfate in a similar manner.~~

638 ~~However, the mechanisms of "salting-in" effects are not fully understood. Kampf et al.~~

639 ~~(2013) inferred that the enhanced uptake of glyoxal was accompanied by chemical~~

640 ~~reactions in the aqueous phase (e.g., hydration and oligomerization), and the~~

641 ~~interactions between SO$_4^{2-}$ and glyoxal monohydrate had negative Gibbs free energy~~

642 ~~of water displacement (Waxman et al., 2015). The net "salting-in" effect of 1-nitro-2-~~

643 ~~naphthol in NaF solution was interpreted by postulating hydrogen bonding (Almeida~~

644 ~~et al., 1983). A direct binding of cations to ether oxygens was proposed to be~~

645 ~~responsible for the increased solubility of water-soluble polymers (Sadeghi and Jahani,~~

646 ~~2012).~~

647 ~~Due to the complexity of PM composition~~However, the "salting-in" effect is a

648 known phenomenon that is not likely linked with a specific physical or chemical

649 mechanism. Quantum chemical calculation results indicated negative Gibbs free

650 energy of water displacement for interactions between SO$_4^{2-}$ and glyoxal monohydrate

651 (Waxman et al., 2015). The net "salting-in" effect of 1-nitro-2-naphthol in NaF

652 solution was interpreted by postulating hydrogen bonding (Almeida et al., 1983). A

653 direct binding of cations to ether oxygens was proposed to be responsible for the

654 increased solubility of water-soluble polymers (Sadeghi and Jahani, 2012). Due to the

655 moderate correlations and negative intercepts in Figures 4 and S5, the large gap

656 between $K^t_{H,e}$ and $K^m_{H,w}$ cannot be closed by the "salting-in" effect alone. which is

657 supported by the Shen et al. (2018) also obtained negative intercepts when plotting

658 log $(K^t_{H,w}/K^m_{H,e})$ over $c_{sulfate}$ for glyoxal and methylglyoxal in ambient atmosphere,

659 and attributed this to unknown gas-particle partitioning mechanisms. Evidences

660 showing that the thermal degradation of less volatile oligomers and organosulfates can

661 lead to an overestimation of 2-methyltetrols by 60–188% when using a conventional

662 GC/EI-MS method (Cui et al., 2018). To fit the gas-particle distribution of 2-

663 methyltetrols in southeastern US, 50% of particulate 2-methyltetrols was presumed to

664 exist in chemical forms with much lower vapor pressures by Pye et al. (2018). So, the

665 reactive uptake and aqueous phase chemistry could be explanations for the enhanced

666 uptake of isoprene SOA tracers. Moreover, negative intercepts of linear regressions

667 in Figure 3. As shown in Figures S7, log $(K^t_{H,w}/K^m_{H,e})$$(K_{H,w}/K_{H,e})$ values of polyol

668 tracers also negatively correlated with the aqueous-phase concentrations of WSOC

669 (c_{WSOC}, Figure S6), but not NH_4^+ or NO_3^-. given that the plots are more scattered at

670 high c_{WSOC}. This dependence might be partly explained usingassociated with the

671 "like-dissolves-like" rule, orand indicate the importance of aqueous-phase

672 heterogeneous reactions chemistry in the particle phase (Hennigan et al., 2009;

673 Volkamer et al., 2009). No significant correlation was observed between log

674 $(K_{H,w}/K_{H,e})$ and NH_4^+ or NO_3^- concentrations. Although several studies have estimated

675 Henry's law constants for a variety of polar organic compounds in pure water (e.g.,

676 polyols and polyacids; Compernolle and Müller, 2014a, b), more work is warranted to

677 decrease the estimation uncertainty and explain their increased partitioning toward

678 aerosol liquid water explicitly. ~~Therefore, the bulk WSOC and sulfate ion should play~~

679 ~~important roles during the condensation of gas-phase polyols, and further research is~~

680 ~~warranted to explicitly explain these effects.~~

681 **4 Implications and Conclusions** ~~and implications~~

682   In this work, concentrations of gas- and particle-phase polyol tracers were

683 measured simultaneously in northern Nanjing. The temporal variations of individual

684 compounds were dominated by their particle-phase concentrations. ~~Because receptor-~~

685 ~~based models identify and quantify aerosol sources based on inter-sample variability,~~

686 Then gas-particle partitioning of polyol tracers should have little influence on source

687 apportionment ~~barely using~~ based on particle-phase data ~~in northern~~ Nanjing. ~~When it~~

688 ~~comes to other places (e.g., western US) where the concentration of aerosol liquid~~

689 ~~water is extremely low, the influence of gas-particle partitioning will still be a concern.~~

690 An improved agreement between measurement-based and predicted $K_{p,OM}$ of polyol

691 tracers was observed when the solubility in aerosol liquid water was considered,

692 indicating that the aqueous solution in aerosols is also an important absorbing phase.

693 ~~Similar to southeastern US, the ambient atmosphere in northern Nanjing also favored~~

694 ~~the condensation of polyol tracers, which was ascribed to the significant ALWC in~~

695 ~~these locations. T~~The large gaps of $K^m_{H,e}$ versus $K^t_{H,w}$ ~~measured versus predicted $K_{p,OM}$~~

696 ~~and K_H implied~~ could be partly parameterized using the equation defining "salting-in"

697 effects. According to existing studies, ~~that the gas-particle partitioning of polyol~~

698 ~~tracers could not be depicted using equilibrium absorptive partitioning model or~~

699 ~~Henry's law alone.~~ In addition to the "salting-in" effect primarily due to the sulfate

700 ~~ions, other aerosol components like bulk WSOC~~reactive uptake, aqueous phase

701 reactions, and chemical similarity between partitioning species and the absorbing

702 phase~~-~~ might ~~also~~ be responsible for increasing the partitioning of polyol tracers into

703 the condensed phase. So, the results of this study have important implications on the

704 prediction of gas-particle partitioning of water-soluble organics, and further studies

705 are required to explain their enhanced aqueous-phase uptake mechanistically. Due to

706 the hygroscopic properties of highly oxidized organic aerosols, ~~the proposed scheme~~

707 ~~for gas particle partitioning of polyol tracers~~this study also partly reveals the

708 discrepancy between modeled and observed SOA in previous studies. However,

709 several ~~pre-~~assumptions (e.g., ~~liquid-liquid phase separation~~LLPS) were made for ~~the~~

710 proposed gas-particle partitioning scheme~~s~~ in this work, more laboratory research is

711 needed to understand the mixing state of inorganic salts, organic components, and

712 aerosol liquid water in atmospheric particles.

713

714 *Data availability*

715 Data used in the writing of this paper is available at the Harvard Dataverse

716 (https://doi.org/10.7910/DVN/U3IGQR, Qin et al., 2021)

717

718 *Author contributions*

719 MX designed the research. CQ and YG performed the sampling and chemical analysis.

720 CQ, YM, and MX analyzed the data. CQ and MX wrote the paper with significant

721 contributions from YW, HL, and QW.

722

723 *Competing interests*

30

724   The authors declare that they have no conflict of interest.

725

730

731   **References**

732   Ahrens, L., Shoeib, M., Harner, T., Lane, D. A., Guo, R., and Reiner, E. J.: Comparison of annular
733   diffusion denuder and high volume air samplers for measuring per- and polyfluoroalkyl
734   substances in the atmosphere, Anal. Chem., 83, 9622-9628, 10.1021/ac202414w, 2011.

735   Almeida, M. B., Alvarez, A. M., Miguel, E. M. D., and Hoyo, E. S. D.: Setchenow coefficients for
736   naphthols by distribution method, Can. J. Chem., 61, 244-248, 10.1139/v83-043, 1983.

737   Barsanti, K. C., and Pankow, J. F.: Thermodynamics of the formation of atmospheric organic
738   particulate matter by accretion reactions—Part 1: aldehydes and ketones, Atmos. Environ., 38,
739   4371-4382, 10.1016/j.atmosenv.2004.03.035, 2004.

740   Bauer, H., Claeys, M., Vermeylen, R., Schueller, E., Weinke, G., Berger, A., and Puxbaum, H.:
741   Arabitol and mannitol as tracers for the quantification of airborne fungal spores, Atmos. Environ.,
742   42, 588-593, https://doi.org/10.1016/j.atmosenv.2007.10.013, 2008.

743   Burshtein, N., Lang-Yona, N., and Rudich, Y.: Ergosterol, arabitol and mannitol as tracers for biogenic
744   aerosols in the eastern Mediterranean, Atmos. Chem. Phys., 11, 829-839, 10.5194/acp-11-829-
745   2011, 2011.

746   Carlton, A. G., and Turpin, B. J.: Particle partitioning potential of organic compounds is highest in the
747   Eastern US and driven by anthropogenic water, Atmos. Chem. Phys., 13, 10203-10214,
748   10.5194/acp-13-10203-2013, 2013.

749   Chow, J. C., Watson, J. G., Chen, L. W. A., Rice, J., and Frank, N. H.: Quantification of PM2.5 organic
750   carbon sampling artifacts in US networks, Atmos. Chem. Phys., 10, 5223-5239, 10.5194/acp-10-
751   5223-2010, 2010.

752   Claeys, M., Graham, B., Vas, G., Wang, W., Vermeylen, R., Pashynska, V., Cafmeyer, J., Guyon, P.,
753   Andreae, M. O., Artaxo, P., and Maenhaut, W.: Formation of secondary organic aerosols through
754   photooxidation of isoprene, Science, 303, 1173-1176, 10.1126/science.1092805, 2004.

755   Compernolle, S., and Müller, J. F.: Henry's law constants of polyols, Atmos. Chem. Phys., 14, 12815-
756   12837, 10.5194/acp-14-12815-2014, 2014a.

757   Compernolle, S., and Müller, J. F.: Henry's law constants of diacids and hydroxy polyacids:
758   recommended values, Atmos. Chem. Phys., 14, 2699-2712, 10.5194/acp-14-2699-2014, 2014b.

759   Cui, T., Zeng, Z., dos Santos, E. O., Zhang, Z., Chen, Y., Zhang, Y., Rose, C. A., Budisulistiorini, S. H.,
760   Collins, L. B., Bodnar, W. M., de Souza, R. A. F., Martin, S. T., Machado, C. M. D., Turpin, B. J.,
761   Gold, A., Ault, A. P., and Surratt, J. D.: Development of a hydrophilic interaction liquid
762   chromatography (HILIC) method for the chemical characterization of water-soluble isoprene
763   epoxydiol (IEPOX)-derived secondary organic aerosol, Environmental Science: Environ. Sci.:
764   Process. Impacts, 20, 1524-1536, 10.1039/C8EM00308D, 2018.

765   Fu, P., and Kawamura, K.: Diurnal variations of polar organic tracers in summer forest aerosols: A case
766   study of a Quercus and Picea mixed forest in Hokkaido, Japan, Geochem. J., 45, 297-308,
767   10.2343/geochemj.1.0123, 2011.

768   Galloway, M. M., Chhabra, P. S., Chan, A. W. H., Surratt, J. D., Flagan, R. C., Seinfeld, J. H., and
769   Keutsch, F. N.: Glyoxal uptake on ammonium sulphate seed aerosol: reaction products and
770   reversibility of uptake under dark and irradiated conditions, Atmos. Chem. Phys., 9, 3331-3345,

771   10.5194/acp-9-3331-2009, 2009.

772 Hallar, A. G., Lowenthal, D. H., Clegg, S. L., Samburova, V., Taylor, N., Mazzoleni, L. R., Zielinska,
773   B. K., Kristensen, T. B., Chirokova, G., McCubbin, I. B., Dodson, C., and Collins, D.: Chemical
774   and hygroscopic properties of aerosol organics at Storm Peak Laboratory, J. Geophys. Res.
775   Atmos., 118, 4767-4779, https://doi.org/10.1002/jgrd.50373, 2013.

776 Heald, C. L., Jacob, D. J., Park, R. J., Russell, L. M., Huebert, B. J., Seinfeld, J. H., Liao, H., and
777   Weber, R. J.: A large organic aerosol source in the free troposphere missing from current models,
778   Geophys. Res. Lett., 32, L18809, https://doi.org/10.1029/2005GL023831, 2005.

779 Healy, R. M., Wenger, J. C., Metzger, A., Duplissy, J., Kalberer, M., and Dommen, J.: Gas/particle
780   partitioning of carbonyls in the photooxidation of isoprene and 1,3,5-trimethylbenzene, Atmos.
781   Chem. Phys., 8, 3215-3230, 10.5194/acp-8-3215-2008, 2008.

782 Hennigan, C. J., Bergin, M. H., Russell, A. G., Nenes, A., and Weber, R. J.: Gas/particle partitioning of
783   water-soluble organic aerosol in Atlanta, Atmos. Chem. Phys., 9, 3613-3628, 10.5194/acp-9-
784   3613-2009, 2009.

785 Hennigan, C. J., Sullivan, A. P., Collett Jr, J. L., and Robinson, A. L.: Levoglucosan stability in
786   biomass burning particles exposed to hydroxyl radicals, Geophys. Res. Lett., 37, L09806,
787   https://doi.org/10.1029/2010GL043088, 2010.

788 Hilal, S. H., Ayyampalayam, S. N., and Carreira, L. A.: Air−liquid partition coefficient for a diverse set
789   of organic compounds: Henry's Law constant in water and hexadecane, Environ. Sci. Technol.,
790   42, 9231-9236, 10.1021/es8005783, 2008.

791 Hodzic, A., Jimenez, J. L., Madronich, S., Canagaratna, M. R., DeCarlo, P. F., Kleinman, L., and Fast,
792   J.: Modeling organic aerosols in a megacity: potential contribution of semi-volatile and
793   intermediate volatility primary organic compounds to secondary organic aerosol formation,
794   Atmos. Chem. Phys., 10, 5491-5514, 10.5194/acp-10-5491-2010, 2010.

795 Hoffmann, D., Tilgner, A., Iinuma, Y., and Herrmann, H.: Atmospheric stability of levoglucosan: A
796   detailed laboratory and modeling study, Environ. Sci. Technol., 44, 694-699, 10.1021/es902476f,
797   2010.

798 Hu, D., Bian, Q., Lau, A. K. H., and Yu, J. Z.: Source apportioning of primary and secondary organic
799   carbon in summer PM2.5 in Hong Kong using positive matrix factorization of secondary and
800   primary organic tracer data, J. Geophys. Res. Atmos., 115, D16204,
801   https://doi.org/10.1029/2009JD012498, 2010.

802 Ip, H. S. S., Huang, X. H. H., and Yu, J. Z.: Effective Henry's law constants of glyoxal, glyoxylic acid,
803   and glycolic acid, Geophys. Res. Lett., 36, L01802, https://doi.org/10.1029/2008GL036212, 2009.

804 Isaacman-VanWertz, G., Yee, L. D., Kreisberg, N. M., Wernis, R., Moss, J. A., Hering, S. V., de Sá, S.
805   S., Martin, S. T., Alexander, M. L., Palm, B. B., Hu, W., Campuzano-Jost, P., Day, D. A.,
806   Jimenez, J. L., Riva, M., Surratt, J. D., Viegas, J., Manzi, A., Edgerton, E., Baumann, K., Souza,
807   R., Artaxo, P., and Goldstein, A. H.: Ambient gas-particle partitioning of tracers for biogenic
808   oxidation, Environ. Sci. Technol., 50, 9952-9962, 10.1021/acs.est.6b01674, 2016.

809 Jang, M., Czoschke, N. M., Lee, S., and Kamens, R. M.: Heterogeneous atmospheric aerosol
810   production by acid-catalyzed particle-phase reactions, Science, 298, 814,
811   10.1126/science.1075798, 2002.

812 Kampf, C. J., Waxman, E. M., Slowik, J. G., Dommen, J., Pfaffenberger, L., Praplan, A. P., Prévôt, A.
813   S. H., Baltensperger, U., Hoffmann, T., and Volkamer, R.: Effective Henry's law partitioning and
814   the salting constant of glyoxal in aerosols containing sulfate, Environ. Sci. Technol., 47, 4236-
815   4244, 10.1021/es400083d, 2013.

816 Kondo, Y., Miyazaki, Y., Takegawa, N., Miyakawa, T., Weber, R. J., Jimenez, J. L., Zhang, Q., and
817   Worsnop, D. R.: Oxygenated and water-soluble organic aerosols in Tokyo, J. Geophys. Res.
818   Atmos., 112, D01203, 10.1029/2006jd007056, 2007.

819 Kroll, J. H., Ng, N. L., Murphy, S. M., Varutbangkul, V., Flagan, R. C., and Seinfeld, J. H.: Chamber
820   studies of secondary organic aerosol growth by reactive uptake of simple carbonyl compounds, J.
821   Geophys. Res. Atmos., 110, D23207, https://doi.org/10.1029/2005JD006004, 2005.

822 Lin, Y.-H., Budisulistiorini, S. H., Chu, K., Siejack, R. A., Zhang, H., Riva, M., Zhang, Z., Gold, A.,
823   Kautzman, K. E., and Surratt, J. D.: Light-absorbing oligomer formation in secondary organic
824   aerosol from reactive uptake of isoprene epoxydiols, Environ. Sci. Technol., 48, 12012-12021,
825   10.1021/es503142b, 2014.

826 Lin, Y. H., Knipping, E. M., Edgerton, E. S., Shaw, S. L., and Surratt, J. D.: Investigating the
827   influences of SO2 and NH3 levels on isoprene-derived secondary organic aerosol formation using
828   conditional sampling approaches, Atmos. Chem. Phys., 13, 8457-8470, 10.5194/acp-13-8457-

829   2013, 2013.

830 Liu, J., Li, X., Li, D., Xu, R., Gao, Y., Chen, S., Liu, Y., Zhao, G., Wang, H., Wang, H., Lou, S., Chen,
831   M., Hu, J., Lu, K., Wu, Z., Hu, M., Zeng, L., and Zhang, Y.: Observations of glyoxal and
832   methylglyoxal in a suburban area of the Yangtze River Delta, China, Atmos. Environ., 238,
833   117727, https://doi.org/10.1016/j.atmosenv.2020.117727, 2020.

834 Odum, J. R., Hoffmann, T., Bowman, F., Collins, D., Flagan, R. C., and Seinfeld, J. H.: Gas/particle
835   partitioning and secondary organic aerosol yields, Environ. Sci. Technol., 30, 2580-2585,
836   10.1021/es950943+, 1996.

837 Pankow, J. F.: An absorption model of the gas/aerosol partitioning involved in the formation of
838   secondary organic aerosol, Atmos. Environ., 28, 189-193, 10.1016/1352-2310(94)90094-9, 1994a.

839 Pankow, J. F.: An absorption model of gas/particle partitioning of organic compounds in the
840   atmosphere, Atmos. Environ., 28, 185-188, 10.1016/1352-2310(94)90093-0, 1994b.

841 Perraud, V., Bruns, E. A., Ezell, M. J., Johnson, S. N., Yu, Y., Alexander, M. L., Zelenyuk, A., Imre,
842   D., Chang, W. L., Dabdub, D., Pankow, J. F., and Finlayson-Pitts, B. J.: Nonequilibrium
843   atmospheric secondary organic aerosol formation and growth, Proc. Natl. Acad. Sci. U.S.A., 109,
844   2836-2841, 10.1073/pnas.1119909109, 2012.

845 Peters, A. J., Lane, D. A., Gundel, L. A., Northcott, G. L., and Jones, K. C.: A comparison of high
846   volume and diffusion denuder samplers for measuring semivolatile organic compounds in the
847   atmosphere, Environ. Sci. Technol., 34, 5001-5006, 10.1021/es000056t, 2000.

848 Pye, H. O. T., Zuend, A., Fry, J. L., Isaacman-VanWertz, G., Capps, S. L., Appel, K. W., Foroutan, H.,
849   Xu, L., Ng, N. L., and Goldstein, A. H.: Coupling of organic and inorganic aerosol systems and
850   the effect on gas–particle partitioning in the southeastern US, Atmos. Chem. Phys., 18, 357-370,
851   10.5194/acp-18-357-2018, 2018.

852 Qin, C., Gou, Y., Wang, Y., Mao, Y., Liao, H., Wang, Q. g., and Xie, M.: Replication Data for: Gas-
853   particle partitioning of polyol tracers in the western Yangtze River Delta, China, in, V1 ed.,
854   Harvard Dataverse, https://doi.org/10.7910/DVN/U3IGQR, 2021.

855 Sadeghi, R., and Jahani, F.: Salting-in and salting-out of water-soluble polymers in aqueous salt
856   solutions, J. Phys. Chem. B, 116, 5234-5241, 10.1021/jp300665b, 2012.

857 Saxena, P., and Hildemann, L.: Water-soluble organics in atmospheric particles: A critical review of
858   the literature and application of thermodynamics to identify candidate compounds, J. Atmos.
859   Chem., 24, 57-109, 10.1007/bf00053823, 1996.

860 Seinfeld, J. H., and Pandis, S. N.: Atmospheric chemistry and physics: from air pollution to climate
861   change, John Wiley & Sons, 2016.

862 Setschenow, J.: Über die Konstitution der Salzlösungen auf Grund ihres Verhaltens zu Kohlensäure, Z.
863   Phys. Chem., 4U, 117-125, https://doi.org/10.1515/zpch-1889-0409, 1889.

864 Shen, H., Chen, Z., Li, H., Qian, X., Qin, X., and Shi, W.: Gas-particle partitioning of carbonyl
865   compounds in the ambient atmosphere, Environ. Sci. Technol., 52, 10997-11006,
866   10.1021/acs.est.8b01882, 2018.

867 Simcik, M. F., Franz, T. P., Zhang, H., and Eisenreich, S. J.: Gas-particle partitioning of PCBs and
868   PAHs in the Chicago urban and adjacent coastal atmosphere: States of equilibrium, Environ. Sci.
869   Technol., 32, 251-257, 10.1021/es970557n, 1998.

870 Simoneit, B. R. T., Schauer, J. J., Nolte, C. G., Oros, D. R., Elias, V. O., Fraser, M. P., Rogge, W. F.,
871   and Cass, G. R.: Levoglucosan, a tracer for cellulose in biomass burning and atmospheric
872   particles, Atmos. Environ., 33, 173-182, http://dx.doi.org/10.1016/S1352-2310(98)00145-9, 1999.

873 Simoneit, B. R. T., Elias, V. O., Kobayashi, M., Kawamura, K., Rushdi, A. I., Medeiros, P. M., Rogge,
874   W. F., and Didyk, B. M.: Sugars dominant water-soluble organic compounds in soils and
875   characterization as tracers in atmospheric particulate matter, Environ. Sci. Technol., 38, 5939-
876   5949, 10.1021/es0403099, 2004.

877 Subramanian, R., Khlystov, A. Y., Cabada, J. C., and Robinson, A. L.: Positive and negative artifacts in
878   particulate organic carbon measurements with denuded and undenuded sampler configurations
879   special issue of aerosol science and technology on findings from the fine particulate matter
880   supersites program, Aerosol Sci. Tech., 38, 27-48, 10.1080/02786820390229354, 2004.

881 Surratt, J. D., Murphy, S. M., Kroll, J. H., Ng, N. L., Hildebrandt, L., Sorooshian, A., Szmigielski, R.,
882   Vermeylen, R., Maenhaut, W., Claeys, M., Flagan, R. C., and Seinfeld, J. H.: Chemical
883   composition of secondary organic aerosol formed from the photooxidation of isoprene, J. Phys.
884   Chem. A, 110, 9665-9690, 10.1021/jp061734m, 2006.

885 Surratt, J. D., Chan, A. W. H., Eddingsaas, N. C., Chan, M., Loza, C. L., Kwan, A. J., Hersey, S. P.,
886   Flagan, R. C., Wennberg, P. O., and Seinfeld, J. H.: Reactive intermediates revealed in secondary

887   organic aerosol formation from isoprene, Proc. Natl. Acad. Sci. U.S.A., 107, 6640-6645,
888   10.1073/pnas.0911114107, 2010.
889 Taylor, N. F., Collins, D. R., Lowenthal, D. H., McCubbin, I. B., Hallar, A. G., Samburova, V.,
890   Zielinska, B., Kumar, N., and Mazzoleni, L. R.: Hygroscopic growth of water soluble organic
891   carbon isolated from atmospheric aerosol collected at US national parks and Storm Peak
892   Laboratory, Atmos. Chem. Phys., 17, 2555-2571, 10.5194/acp-17-2555-2017, 2017.
893 Tsyro, S. G.: To what extent can aerosol water explain the discrepancy between model calculated and
894   gravimetric PM10 and PM2.5?, Atmos. Chem. Phys., 5, 515-532, 10.5194/acp-5-515-2005, 2005.
895 Turpin, B. J., and Lim, H.-J.: Species contributions to PM2.5 mass concentrations: Revisiting common
896   assumptions for estimating organic mass, Aerosol Sci. Technol., 35, 602-610,
897   10.1080/027868201193445, 2001.
898 US EPA: Estimation Program Interface (EPI) Suite. Version v4.11, 2012. United States Environmental
899   Protection Agency, Washington, DC, USA. https://www.epa.gov/tsca-screening-tools/download-
900   epi-suitetm-estimation-program-interface-v411
901 Volkamer, R., Jimenez, J. L., San Martini, F., Dzepina, K., Zhang, Q., Salcedo, D., Molina, L. T.,
902   Worsnop, D. R., and Molina, M. J.: Secondary organic aerosol formation from anthropogenic air
903   pollution: Rapid and higher than expected, Geophys. Res. Lett., 33, L17811,
904   https://doi.org/10.1029/2006GL026899, 2006.
905 Volkamer, R., Ziemann, P. J., and Molina, M. J.: Secondary Organic Aerosol Formation from
906   Acetylene (C2H2): seed effect on SOA yields due to organic photochemistry in the aerosol
907   aqueous phase, Atmos. Chem. Phys., 9, 1907-1928, 10.5194/acp-9-1907-2009, 2009.
908 Wang, W., Kourtchev, I., Graham, B., Cafmeyer, J., Maenhaut, W., and Claeys, M.: Characterization
909   of oxygenated derivatives of isoprene related to 2-methyltetrols in Amazonian aerosols using
910   trimethylsilylation and gas chromatography/ion trap mass spectrometry, Rapid Commun. Mass
911   Spectrom., 19, 1343-1351, https://doi.org/10.1002/rcm.1940, 2005.
912 Waxman, E. M., Elm, J., Kurtén, T., Mikkelsen, K. V., Ziemann, P. J., and Volkamer, R.: Glyoxal and
913   methylglyoxal Setschenow salting constants in sulfate, nitrate, and chloride solutions:
914   Measurements and Gibbs energies, Environ. Sci. Technol., 49, 11500-11508,
915   10.1021/acs.est.5b02782, 2015.
916 Williams, B. J., Goldstein, A. H., Kreisberg, N. M., and Hering, S. V.: In situ measurements of
917   gas/particle-phase transitions for atmospheric semivolatile organic compounds, Proc. Natl. Acad.
918   Sci. U.S.A., 107, 6676-6681, 10.1073/pnas.0911858107, 2010.
919 Xie, M., Barsanti, K. C., Hannigan, M. P., Dutton, S. J., and Vedal, S.: Positive matrix factorization of
920   PM2.5 - eliminating the effects of gas/particle partitioning of semivolatile organic compounds,
921   Atmos. Chem. Phys., 13, 7381-7393, 10.5194/acp-13-7381-2013, 2013.
922 Xie, M., Hannigan, M. P., and Barsanti, K. C.: Gas/particle partitioning of n-alkanes, PAHs and
923   oxygenated PAHs in urban Denver, Atmos. Environ., 95, 355-362,
924   http://dx.doi.org/10.1016/j.atmosenv.2014.06.056, 2014a.
925 Xie, M., Hannigan, M. P., and Barsanti, K. C.: Gas/particle partitioning of 2-methyltetrols and
926   levoglucosan at an urban site in Denver, Environ. Sci. Technol., 48, 2835-2842,
927   10.1021/es405356n, 2014b.
928 Xie, M., Hannigan, M. P., and Barsanti, K. C.: Impact of gas/particle partitioning of semivolatile
929   organic compounds on source apportionment with positive matrix factorization, Environ. Sci.
930   Technol., 48, 9053-9060, 10.1021/es5022262, 2014c.
931 Yang, L., Shang, Y., Hannigan, M. P., Zhu, R., Wang, Q. g., Qin, C., and Xie, M.: Collocated
932   speciation of PM2.5 using tandem quartz filters in northern nanjing, China: Sampling artifacts and
933   measurement uncertainty, Atmos. Environ., 246, 118066,
934   https://doi.org/10.1016/j.atmosenv.2020.118066, 2021.
935 Yatavelli, R. L. N., Stark, H., Thompson, S. L., Kimmel, J. R., Cubison, M. J., Day, D. A.,
936   Campuzano-Jost, P., Palm, B. B., Hodzic, A., Thornton, J. A., Jayne, J. T., Worsnop, D. R., and
937   Jimenez, J. L.: Semicontinuous measurements of gas–particle partitioning of organic acids in a
938   ponderosa pine forest using a MOVI-HRToF-CIMS, Atmos. Chem. Phys., 14, 1527-1546,
939   10.5194/acp-14-1527-2014, 2014.
940 Zhang, Y., Sheesley, R. J., Schauer, J. J., Lewandowski, M., Jaoui, M., Offenberg, J. H., Kleindienst, T.
941   E., and Edney, E. O.: Source apportionment of primary and secondary organic aerosols using
942   positive matrix factorization (PMF) of molecular markers, Atmos. Environ., 43, 5567-5574,
943   https://doi.org/10.1016/j.atmosenv.2009.02.047, 2009.
944 Zhao, Y., Kreisberg, N. M., Worton, D. R., Isaacman, G., Weber, R. J., Liu, S., Day, D. A., Russell, L.

945   M., Markovic, M. Z., VandenBoer, T. C., Murphy, J. G., Hering, S. V., and Goldstein, A. H.:
946   Insights into secondary organic aerosol formation mechanisms from measured gas/particle
947   partitioning of specific organic tracer compounds, Environ. Sci. Technol., 47, 3781-3787,
948   10.1021/es304587x, 2013.
949   Zuend, A., and Seinfeld, J. H.: Modeling the gas-particle partitioning of secondary organic aerosol: the
950   importance of liquid-liquid phase separation, Atmos. Chem. Phys., 12, 3857-3882, 10.5194/acp-
951   12-3857-2012, 2012.
952

Table 1. Comparisons of measurement-based log $K_{p,OM}$ (m³ μg⁻¹) at three proposed cases and predicted values.

Species	No. of obs.	Log $K^m_{p,OM}$ [a]			Log $K^t_{p,OM}$ [b]			
		Case 1	Case 2	Case 3	EPI	EVAPORATION	SPARC	SIMPOL
Isoprene SOA tracers								
C5-alkene triol 1	53	0.33 ± 0.71	-0.79 ± 0.86	-0.82 ± 0.85	-3.09	-2.84	-1.19	-2.88
C5-alkene triol 2	63	0.15 ± 0.55	-1.02 ± 0.74	-1.05 ± 0.73	-3.62	-3.67	-4.14	-2.85
C5-alkene triol 3	83	0.35 ± 0.68	-0.83 ± 0.86	-0.86 ± 0.85	-2.90	-2.65	-1.00	-2.69
2-Methylthreitol	101	-0.12 ± 0.48	-2.09 ± 0.71	-2.09 ± 0.70	-1.87	-1.30	-1.18	-0.47
2-Methylerythritol	95	-0.011 ± 0.58	-1.96 ± 0.71	-1.96 ± 0.71	-1.90	-1.34	-1.22	-0.50
Biomass burning tracer								
Levoglucosan	65	2.23 ± 0.72	0.63 ± 0.90	0.62 ± 0.90	-0.04	-0.81	1.04	-0.76
Sugars ang sugar alcohols								
Meso-erythritol	31	0.87 ± 0.53	-1.43 ± 0.60	-1.43 ± 0.60	-0.65	-1.21	-0.45	
Fructose	85	0.65 ± 0.73	-1.20 ± 0.83	-1.20 ± 0.89	1.17	2.76	6.94	
Mannose	74	0.62 ± 0.71	-2.12 ± 0.95	-2.12 ± 0.95	1.28	2.13	4.77	
Glucose	88	0.42 ± 0.67	-2.77 ± 0.93	-2.77 ± 0.93	0.34	3.75	7.32	
Xylitol	22	0.24 ± 0.54	-2.61 ± 0.72	-2.61 ± 0.72	3.37	2.34	3.57	
Arabitol	30	1.46 ± 0.89	-1.35 ± 1.24	-1.35 ± 1.24	3.25	1.67	2.90	
Manitol	65	1.08 ± 0.63	-2.24 ± 0.95	-2.24 ± 0.95	2.33	4.16	6.68	

[a] Average ± standard deviation; [b] temperature range: -4~36 °C.

Table 1. Statistics for measured and predicted log $K_{p,OM}$ of individual polyol tracers.

Species	No. of obs.	Log $K^m_{p,OM}$			Log $K^t_{p,OM}$		
		Median	Average	Range	Median	Average	Range
Isoprene SOA tracers							
C5-alkene triol 1	53	0.47	0.33 ± 0.71	-1.30 – 2.61	-3.23	-3.09 ± 0.44	-3.70 – -1.63
C5-alkene triol 2	63	0.19	0.15 ± 0.55	-1.02 – 2.26	-3.70	-3.62 ± 0.37	-4.24 – -2.67
C5-alkene triol 3	83	0.38	0.35 ± 0.68	-1.86 – 2.25	-3.01	-2.90 ± 0.48	-3.70 – -1.63
2-Methylthreitol	101	-0.13	-0.12 ± 0.48	-1.15 – 0.92	-1.90	-1.87 ± 0.52	-2.81 – -0.62
2-Methylerythritol	95	-0.089	-0.011 ± 0.58	-1.09 – 2.06	-1.91	-1.90 ± 0.51	-2.81 – -0.62
Biomass burning tracer							
Levoglucosan	65	2.34	2.23 ± 0.72	-0.11 – 3.36	-0.12	-0.038 ± 0.59	-1.00 – 1.29
Sugars ang sugar alcohols							
Meso-erythritol	31	0.84	0.87 ± 0.53	-0.47 – 1.81	-0.80	-0.65 ± 0.48	-1.35 – 0.69
Fructose	85	0.55	0.65 ± 0.73	-0.96 – 3.01	1.14	1.17 ± 0.62	0.015 – 2.72
Mannose	74	0.57	0.62 ± 0.71	-0.94 – 2.81	1.23	1.28 ± 0.66	0.18 – 2.81
Glucose	88	0.41	0.42 ± 0.67	-1.08 – 1.92	0.31	0.34 ± 0.65	-0.75 – 1.92
Xylitol	22	0.35	0.24 ± 0.54	-1.23 – 0.97	3.43	3.37 ± 0.57	2.11 – 4.39
Arabitol	30	1.40	1.46 ± 0.89	-0.19 – 4.20	3.15	3.25 ± 0.77	2.05 – 4.81
Manitol	65	1.06	1.08 ± 0.63	-0.35 – 2.53	2.31	2.33 ± 0.70	1.15 – 3.98

Table 2. Comparisons of measurement-based log $K_{H,e}$ (mol m^{-3} atm^{-1}) and predicted log $K_{H,w}$ of individual polyol tracers.

Species	No. of obs.	Log $K^m_{H,e}$ (Cases 2)[a]			Log $K_{H,w}$[b]	
		Median	Average	Range	EPI	SPARC
Isoprene SOA tracers						
C5-alkene triol 1	53	14.0	13.9 ± 0.86	11.5 – 16.4	7.22	11.7
C5-alkene triol 2	63	13.7	13.6 ± 0.73	11.2 – 16.1	7.34	7.66
C5-alkene triol 3	83	13.9	13.8 ± 0.85	10.6 – 16.1	7.43	11.9
2-Methylthreitol	101	13.4	13.3 ± 0.70	10.9 – 14.8	10.0	14.1
2-Methylerythritol	95	13.5	13.5 ± 0.71	11.6 – 15.6	9.95	14.1
Biomass burning tracer						
Levoglucosan	65	15.7	15.7 ± 0.90	13.2 – 17.3	13.4	16.1
Sugars ang sugar alcohols						
Meso-erythritol	31	14.5	14.4 ± 0.60	12.8 – 15.6	9.65	13.8
Fructose	85	14.2	14.1 ± 0.89	11.9 – 16.5	14.7	19.9
Mannose	74	14.0	14.1 ± 0.94	12.1 – 16.8	10.9	18.8
Glucose	88	13.9	13.9 ± 0.93	11.3 – 16.3	14.7	20.9
Xylitol	22	13.8	13.7 ± 0.72	12.6 – 15.0	12.1	18.1
Arabitol	30	15.1	15.0 ± 1.23	13.0 – 18.2	11.3	17.4
Mannitol	65	14.6	14.5 ± 0.94	12.1 – 16.4	12.9	20.8

[a] Log $K^m_{H,e}$ values of _Case 3_ had ignorable difference, and were not exhibited separately; [b] temperature range: -4~36 ºC

~~Table 2. Statistics for log $K_{H,e}$ and log $K_{H,w}$ of individual polyol tracers.~~

~~species~~	~~No. of obs.~~	~~Log $K_{H,e}$~~			~~Log $K_{H,w}$~~		
		~~Median~~	~~Average~~	~~Range~~	~~Median~~	~~Average~~	~~Range~~

Isoprene SOA tracers							
C5-alkene triol 1	53	14.0	13.9 ± 0.86	11.5 – 16.4	7.06	7.22 ± 0.50	6.53 – 8.87
C5-alkene triol 2	63	13.7	13.6 ± 0.73	11.2 – 16.1	7.24	7.34 ± 0.45	6.60 – 8.49
C5-alkene triol 3	83	13.9	13.8 ± 0.85	10.6 – 16.1	7.31	7.43 ± 0.55	6.53 – 8.87
2-Methylthreitol	101	13.4	13.3 ± 0.70	10.9 – 14.8	9.96	10.0 ± 0.80	8.55 – 11.9
2-Methylerythritol	95	13.5	13.5 ± 0.71	11.6 – 15.6	9.93	9.95 ± 0.79	8.55 – 11.9
Biomass burning tracer							
Levoglucosan	65	15.7	15.7 ± 0.90	13.2 – 17.3	13.3	13.4 ± 0.56	12.4 – 14.6
Sugars ang sugar alcohols							
Meso-erythritol	31	14.5	14.4 ± 0.60	12.8 – 15.6	9.44	9.65 ± 0.66	8.68 – 11.5
Fructose	85	14.2	14.1 ± 0.89	11.9 – 16.5	14.6	14.7 ± 0.84	13.1 – 16.8
Mannose	74	14.0	14.1 ± 0.94	12.1 – 16.8	10.9	10.9 ± 0.88	9.46 – 13.0
Glucose	88	13.9	13.9 ± 0.93	11.3 – 16.3	14.6	14.7 ± 0.85	13.2 – 16.8
Xylitol	22	13.8	13.7 ± 0.72	12.6 – 15.0	12.1	12.1 ± 0.62	10.7 – 13.2
Arabitol	30	15.1	15.0 ± 1.23	13.0 – 18.2	11.2	11.4 ± 0.83	10.0 – 13.0
Mannitol	65	14.6	14.5 ± 0.94	12.1 – 16.4	12.9	12.9 ± 1.15	11.0 – 15.6

953 <u>Figure 1</u>

954
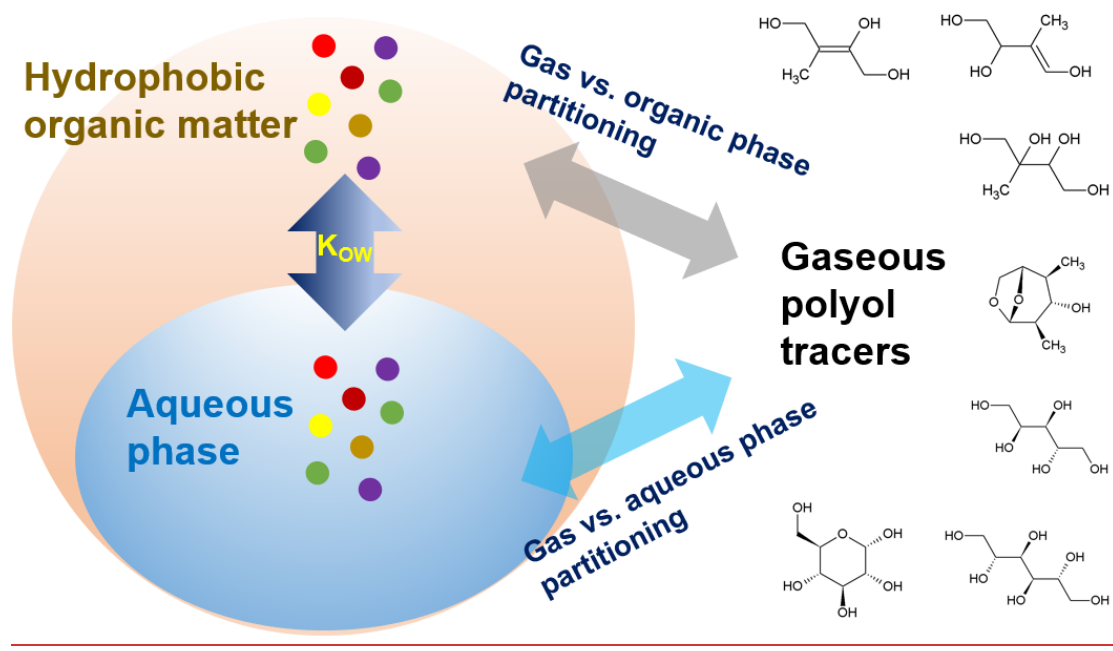
955

956

957 Figure 1. Proposed scheme for gas-particle partitioning of polyol tracers.
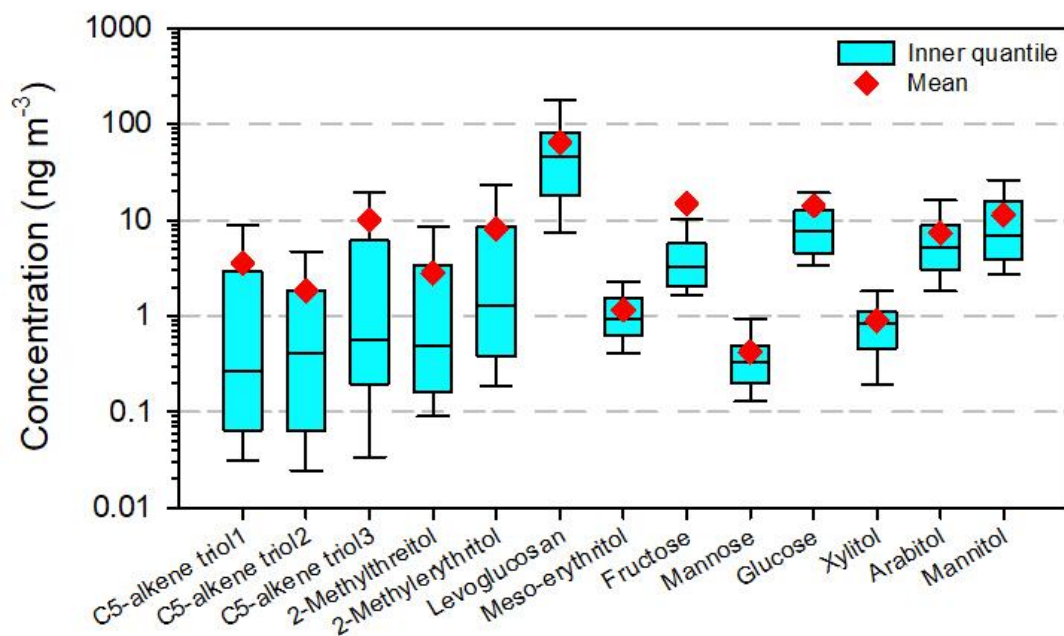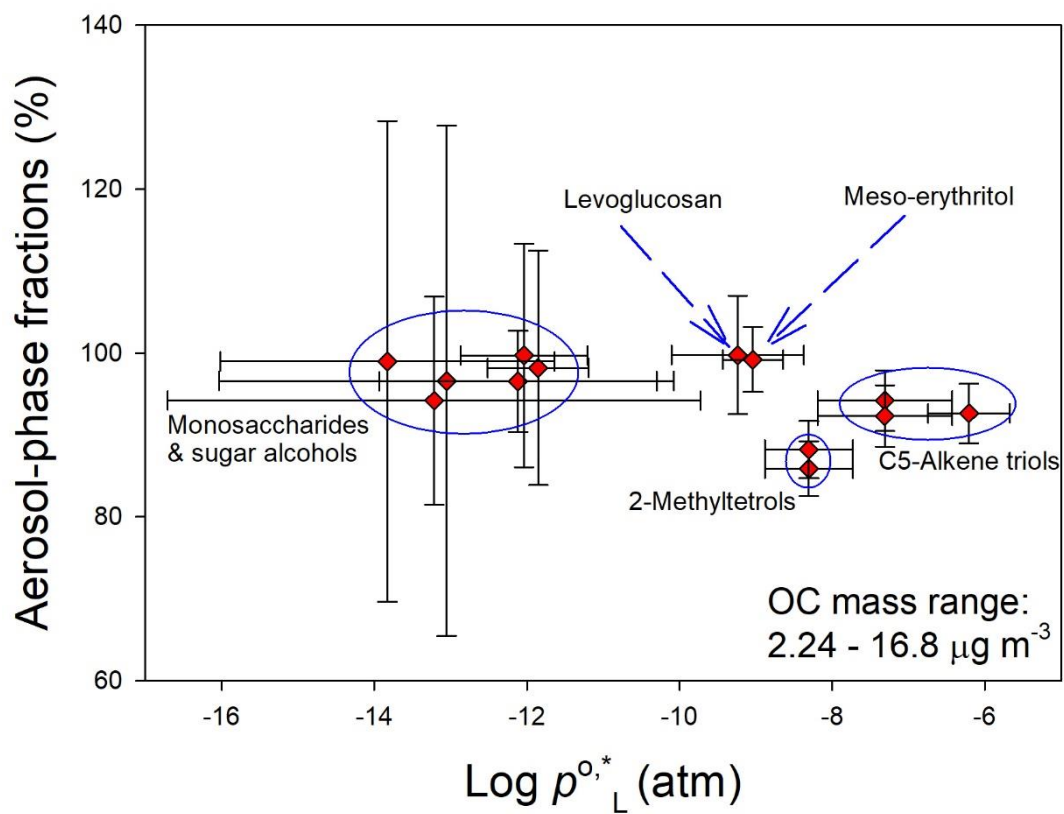
958

39

Figure 12

Figure 12. Total concentrations of individual polyols (Q_f + Q_b + PUF) in the ambient atmosphere of northern Nanjing. The boxes depict the median (dark line), inner quantile range (box), 10th and 90th percentiles (whiskers), and the mean (red diamond).
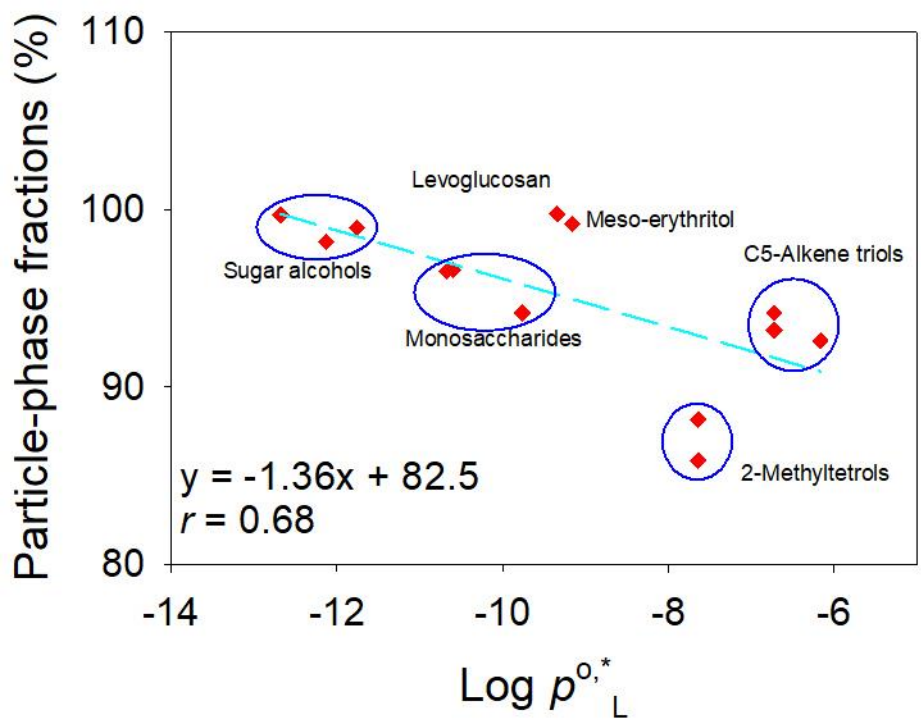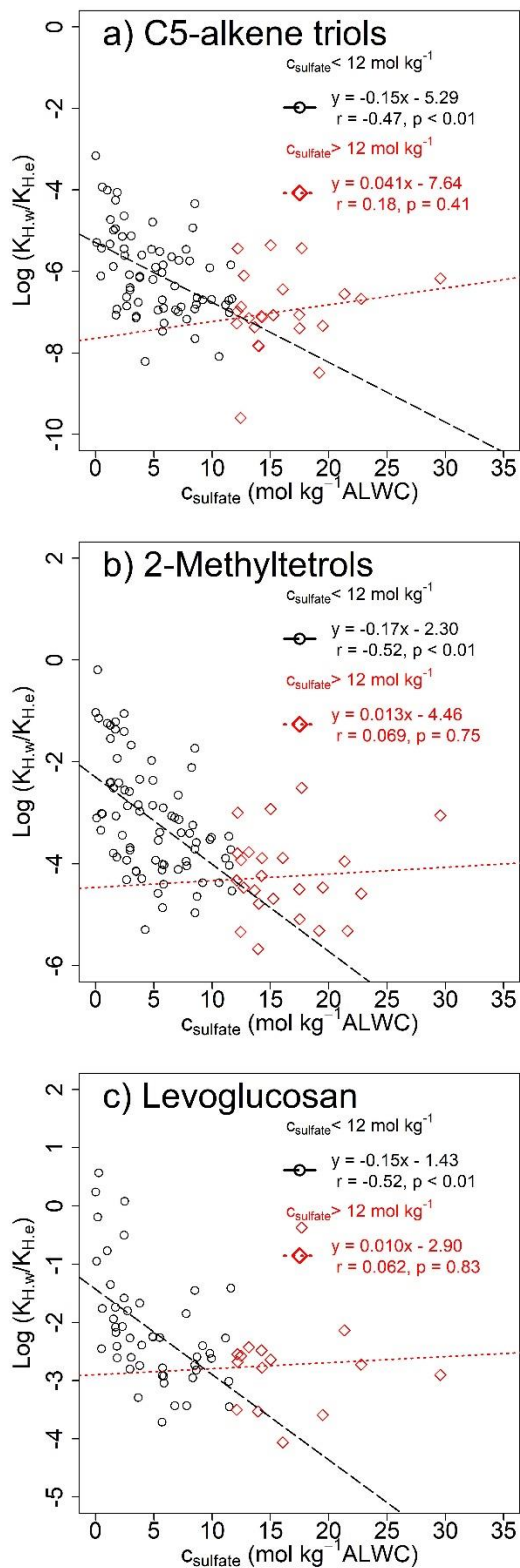
Figure 23

Figure description (axis labels and annotations):

Y-axis: Aerosol-phase fractions (%), ranging 60 to 140

X-axis: Log $p^{o,*}_L$ (atm), ranging -16 to -6

Annotations on plot:
- Levoglucosan
- Meso-erythritol
- Monosaccharides & sugar alcohols
- 2-Methyltetrols
- C5-Alkene triols
- OC mass range: 2.24 - 16.8 μg m^{-3}

Figure 23. Average particle-phase fractions and log $p^{o,*}_L$ of individual polyol tracers. Whiskers represent uncertainties of $F\%$ and one standard deviation of log $p^{o,*}_L$ derived from different estimation tools.

Linear relationship between average aerosol-phase fractions and log $p^{o,*}_L$ of polyol tracers.
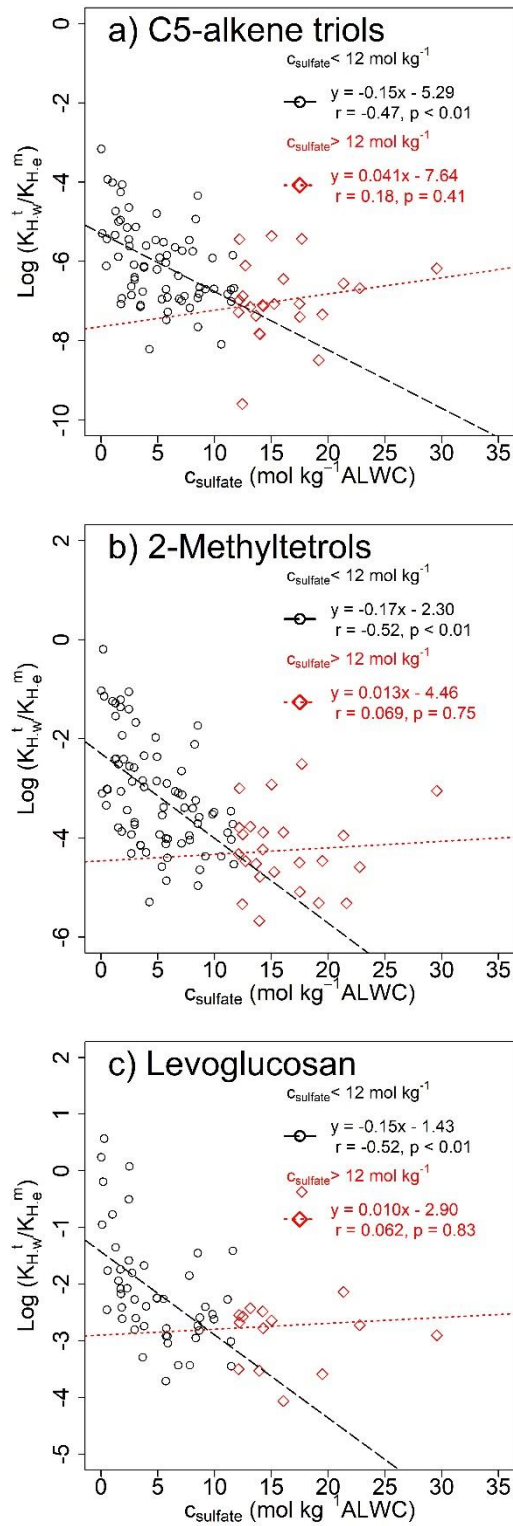
Figure 34

Figure 34. Modified Setschenow plots of log ($K^{t}_{H,w}/K^{m}_{H,e}$) vs. versus $c_{sulfate}$ for (a) C5-alkene triols, (b) 2-methyltetrols, and (c) levoglucosan.